DETERMINATION OF PLATINUM, PALLADIUM AND RHODIUM, IN AQUEOUS MEDIA BY MEANS OF REVERSED PHASE-HIGH PERFORMANCE LIQUID CHROMATOGRAPHY (RP-HPLC) AFTER COMPLEXATION WITH *N,N*-dialkyl-*N'*-acylthioureas

A thesis submitted to

DEPARTMENT OF CHEMISTRY
UNIVERSITY OF CAPE TOWN

in fulfilment of the requirements for the degree of

MASTER OF SCIENCE

by

Nare Alpheus Mautjana

September, 2000

ACKNOWLEDGEMENTS

- I give many thanks to AECI Limited for financial support throughout my studies in University of Cape Town.

- I would also like to thank my supervisor, Professor K.R. Koch, for the guidance and teaching.

- I thank Dr Susan Bourne for the crystallography work.

- I give a special word of gratitude to my mentor, Dr Kuku Voyi of CSIR, for the initial encouragement and her continued support.

- I thank UCT's PGM research team for the inputs which helped the course of my study. Thanks, particularly, to Jörn Miller for support in the lab and proof reading this work, Claire Lawrence for her valuable comments, as well as Sunny Wu for the discussions.

- Thanks also to Dr Michael Schwarzer (of Technical University of München) for friendly exchange of ideas during his post-doctoral research in 1998.

- A sincere thank you to my wife, Kgadi, who has been encouraging and supportive throughout.

---o0o---

Abstract

Relatively hydrophilic *cis*-[Pt(L^n-*S,O*)$_2$], *cis*-[Pd(L^n-*S,O*)$_2$] and *fac*-[Rh(L^n-*S,O*)$_3$] complexes, where HL^n is *N,N*-dimethyl- (HL^1), *N*-pyrrolidyl- (HL^2) and *N*-piperidyl-*N'*-(2,2-dimethylpropanoyl)thiourea (HL^3), have been prepared. These ligands and complexes were fully characterized using nuclear magnetic resonance spectroscopy (NMR), ultraviolet spectroscopy (UV) and other conventional means. The crystal structure of *fac*-Rh[L^2-*(S,O)*]$_3$ complex was determined by x-ray diffraction.

The complexes were successfully separated using conventional Reversed Phase-High Performance Liquid Chromatography (RP-HPLC) and a UV detector. A simple method of complexation of platinum(II) and palladium(II) in acidic, aqueous samples was developed. This method involves the mixing of excess ligand (HL^n) in acetonitrile with aqueous solutions containing traces of platinum(II) and palladium(II) at room temperature followed by salt-induced phase separation prior to RP-HPLC analysis. In the case of rhodium(III), however, complexation was extremely slow and it has not been possible to include this metal in the complexation procedure for platinum(II) and palladium(II).

As a way of verifying that platinum(II), palladium(II) and rhodium(III) in aqueous media are quantitatively complexed at trace concentrations, these metals were also pre-concentrated on a commercially available C18-modified silica disk as complexes of *N,N*-di(2-hydroxyethyl)-*N'*-benzoylthiourea and were then determined from dried disks by Laser Ablation-Inductively Coupled Plasma Mass Spectrometry (LA-ICP MS). Calibration graphs were extended down into the $\mu g.dm^{-3}$ or ppb concentration levels.

---o0o---

Table of contents

--o0o--

1.

Introduction

1.1. General introduction

N,N-dialkyl-*N'*-acylthioureas (Figure 1.1) were first prepared in 1873 by K Neucki[1]. A convenient, general method of synthesis was established sixty one years later, in 1934, by Douglass and Dains[2]. Some additional modifications to the method of Douglass and Dains[3] have lead to improved yields and a better understanding of the factors governing the synthesis of *N,N*-dialkyl-*N'*-acylthioureas. In many cases now, these molecules can be prepared readily and in high yields from simple, inexpensive reagents.

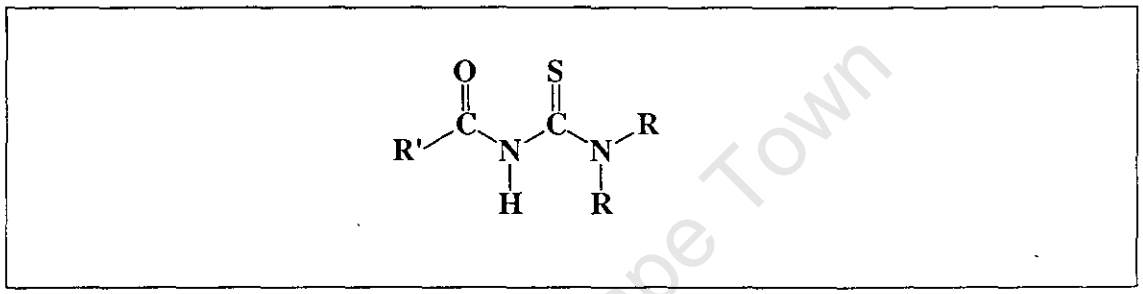

Figure 1.1: A general structure of *N,N*-dialkyl-*N'*-acylthioureas.

A wide variety of derivatives of *N,N*-dialkyl-*N'*-acylthioureas with interesting properties can be easily made by varying the R'- and R-groups. The co-ordination chemistry of *N,N*-dialkyl-*N'*-acylthioureas to some precious metals has been studied extensively[4,5,6]. Several practical applications can be envisaged, which include trace analysis and recovery of precious metals from complex matrices such as precious metal refinery waste solutions (also called post-process effluents). Trace analysis of platinum group metals namely ruthenium, rhodium, palladium, osmium, iridium and platinum is particularly difficult in these matrices. In this work, focus was placed on developing a reversed phase high performance liquid chromatographic (RP-HPLC) method for the determination of platinum, palladium and rhodium in aqueous media, after complexation with a suitable *N,N*-dialkyl-*N'*-acylthiourea.

Unrecovered platinum group metals (PGMs) can represent a significant loss in revenue to refiners which, due to the unavailability of sufficiently sensitive analytical methods, can be difficult to determine. In view of the high market prices of some prevalent PGMs - see Figure 1.2 - it has become worthwhile for mining companies to

evaluate the loss represented by one or two years' accumulation of PGM traces. In order to achieve this objective, selective analytical procedures should be developed. Based on accurate analytical measurements of these traces, an assessment of the viability of establishing second stage recovery technology can be made. Several post-process metal recovery technologies which include selective adsorption and differential precipitation have been proposed[8]. Selective adsorption could employ polymeric resins. Alternatively, porous media such as a packing of sand grains coated with a selectively adsorbing substance could be used. Differential precipitation can involve enforced formation of a desired salt for example a sulfide or carbonate precipitate, and has been described as effective for industrial effluent purification. The resultant sludges are then subjected to pyrometallurgy, which involves thermal techniques or hydrometallurgy, which uses leaching techniques, in order to recycle recovered metals.

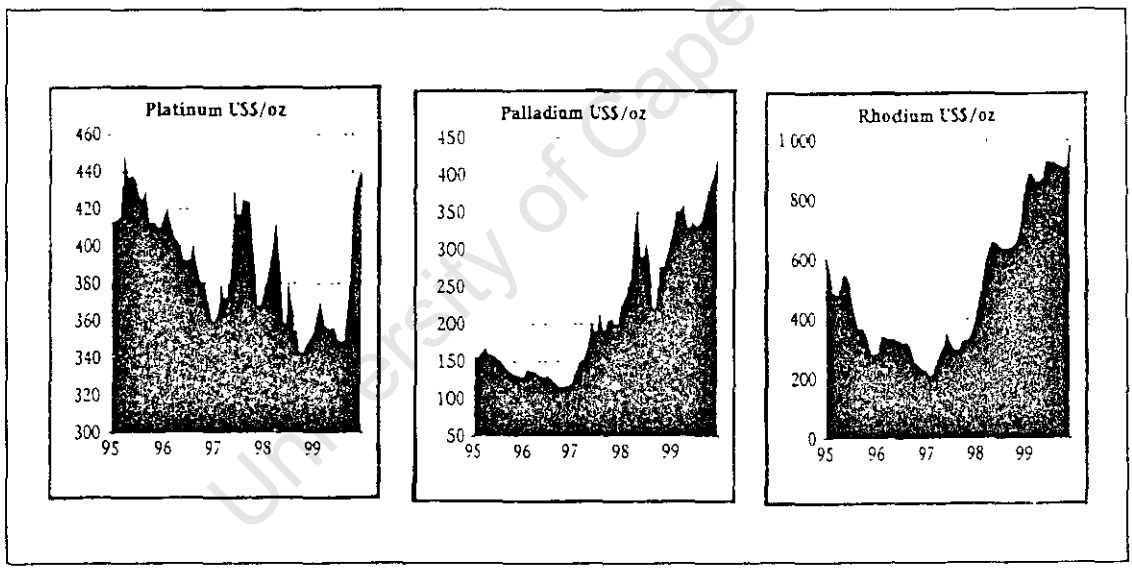

Figure 1.2: Market prices of pure PGMs (US $ per Oz) over the period: 1995-2000[7].

The processing of PGMs from ores is a highly complex process and generally includes their conversion into water soluble chloro species which facilitate their separation[9,10]. PGMs therefore exist as dissolved, charged species such as $PdCl_4^{2-}$ and $PtCl_6^{2-}$ in process solutions. An example of a separation process flow sheet is shown in Figure 1.3.

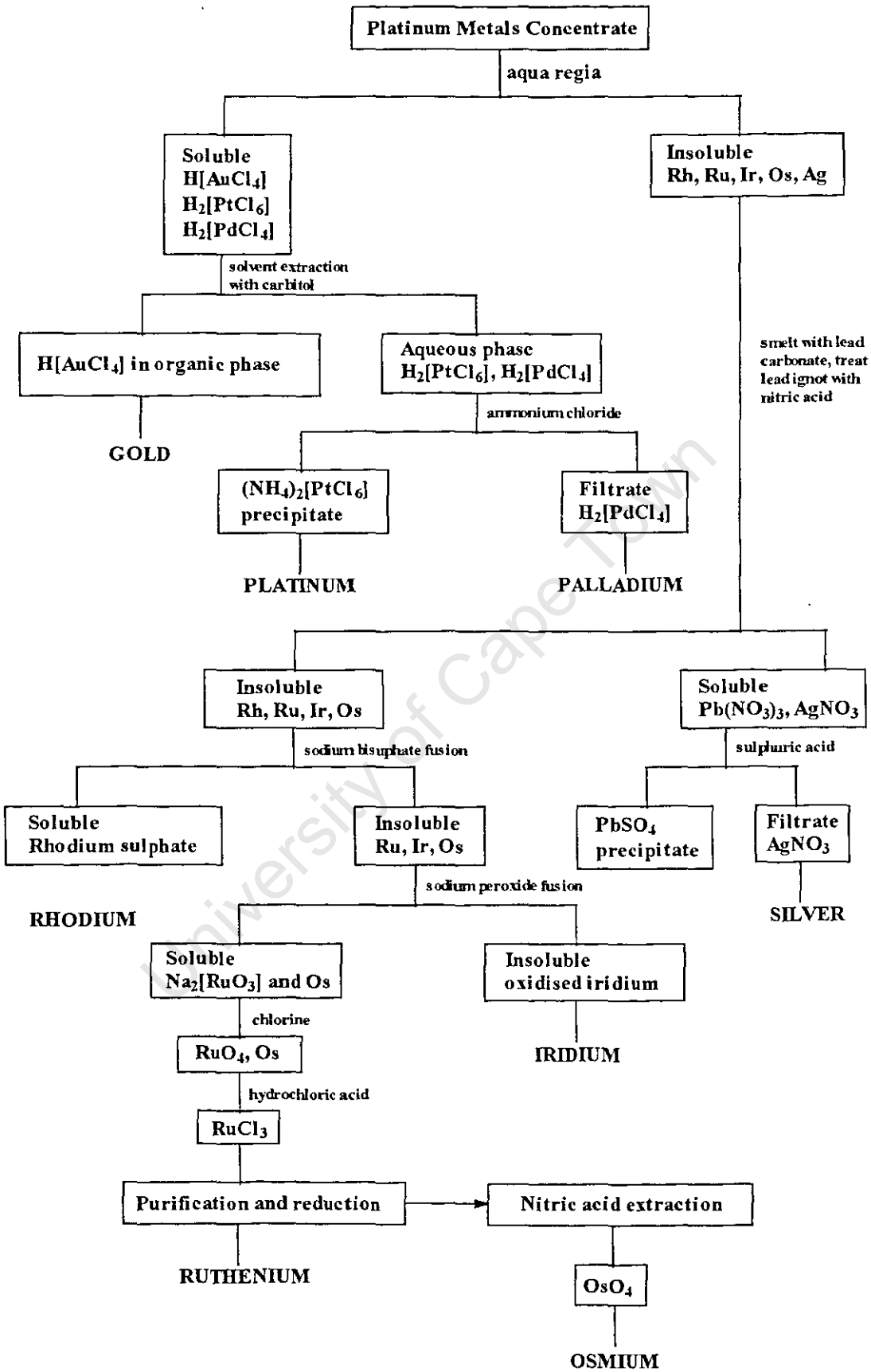

Figure 1.3: An example of process flow sheet for the separation of platinum group metals[10].

After recovery of pure metals, traces of these soluble species remain in the post-process effluents which, for environmental reasons, are contained in impermeable plastic-lined dams[11]. Accidental leaks of these dams, although extremely rare, may introduce small amounts of water soluble PGMs species into the environment. It is possible, by virtue of their solublity in water, that these species may be absorbed by crops, fruit-bearing plants and other vegetation edible to livestock. Sensitive analytical methods are again required in such incidents to aid in pollution control.

In this context, analytical procedures for traces of PGMs in solution could be adapted to other areas in which PGMs are involved in low concentrations. It has been expressed, for example[12-15], that the reported undesirable side effects which follow treatment of tumours with the anti-tumour drug, *cis*-$[PtCl_2(NH_3)_2]$, commonly known as cisplatin, could be easier to control if sensitive and reliable analytical methods were available to readily measure the amount of platinum in patients' blood.

1.2. Challenges

The challenges in the trace analysis of platinum group metals are formidable. Problems encountered, invariably arise from the complex chemical behaviour of these metals. It is well known that these metals exist in more than one oxidation states[16] and in aqueous media they may form many different species[17]. The problems caused by a multiplicity of PGM species during treatment of process effluents and samples of geological origin, are compounded by the presence of other transition metals namely iron, cobalt, nickel, copper and other elements[15] which occur naturally in the ores containing platinum group metals.

With the exception of palladium, PGMs are somewhat inert to ligand substitution[16,17]. Therefore, not many *in-situ* or on-line methods of chemical derivatization, for pre-concentration or better detection in various analytical determinations, are suitable. The chemical transformation of PGMs often require long reaction times, high temperatures, high reagent concentrations and even catalysts. These reactions are characterised by slow and complicated kinetics.

The metals in the groups: Pt and Pd, Ir and Rh, Os and Ru, resemble each other in their solution and coordination chemistry[17]. This resemblance leads to the formation of compounds of very similar properties.

Certain of the platinum group metals also have the tendency for hydrolysis and the formation of polynuclear complexes[17]. The hydroxy species of PGMs are insoluble in neutral and basic media, usually pH > 5, and precipitate out of solution on formation. Notwithstanding the complexities of the chemistry involved, some breakthroughs have been reported in the analysis of these metals at trace levels[15,18].

1.3. Analytical techniques for the determination of platinum group metals

Among the highly sensitive methods for the determination of platinum group metals at low concentrations are cathodic stripping voltametry and neutron activation analysis. Cathodic stripping voltametry is reported to be highly sensitive (for determinations of platinum) but is negatively affected by traces of organic substances in the solution[18]. In this method a formazone complex of platinum is formed *in situ* and gets adsorbed onto a hanging mercury-dropping electrode. The formazone complex serves as a catalyst for the reduction of protons producing molecular hydrogen. The reduction current associated with this reaction is related to the concentration of platinum. Neutron activation analysis[19,20] requires a nuclear reactor. A sample is irradiated by thermal neutrons and the radioactivity induced is measured. This technique is clearly not suitable for most routine analysis. However, it is described as extremely sensitive[21] and useful in the certification of reference samples[22].

The most popular technique for the determination of platinum group metals in all matrices, is atomic spectrometry. Both absorption and emission spectrometry have become extremely well developed[23,24]. In some cases, atomic spectrometers are coupled with mass spectrometers for enhanced detection and in other cases with separation techniques such as ion exchangers[25-29] to eliminate the matrix elements which cause spectral interference. Some creative approaches in using atomic spectrometry include adsorption of the metal complexes onto a solid phase followed

by laser, spark or arc ablation of the adsorbed complex molecules[30]. In other applications, on-line pre-concentration columns have been used with success. On-line pre-concentration is more popular and practical in the determination of palladium[31,32]. The column is reversibly loaded with a complexing agent which traps the metal ions by forming complexes during passage of the aqueous metal ion solution The complexes are then eluted with an appropriate solvent such as ethanol, and are then introduced into the graphite furnace or flame atomic spectrometer. The potential of atomic spectrometry for trace analysis of PGMs prompted us to make a study of the application of laser ablation inductively coupled plasma mass spectrometer (LA-ICP MS) for the determination of platinum, palladium and rhodium after their preconcentration as *N,N*-di-(2-hydroxyethyl)-*N'*-benzoylthiourea complexes. This preliminary study is described in detail in chapter 4.

Other potential analytical methods are those based on separation. These include ion-exchange chromatography (IC) and high performance liquid chromatography (HPLC). Ion-exchange chromatography methods are relatively well established and can separate platinum group metals from base metals[15,33,34]. These methods are largely designed for the anionic complexes of platinum group metals e.g. $PtCl_6^{2-}$, $PdCl_4^{2-}$, which are separated by anion exchange resins, commonly quaternary-amine functionalised polystyrene. A shortfall of IC is the low sensitivity of conductivity detection as compared to spectrophotometric detection using ultra-violet (UV) or visible light absorption. In this regard, HPLC promises to be a better choice. HPLC is, to some extent, a more versatile technique in that detectors of varying sensitivities and selectivities can be coupled to it. Although some researchers have used the normal phase mode with success[33,35-38], difficulties arise in many cases due to its incompatibility with the aqueous media in which metal ions are found.

1.4. The application of HPLC to metal analysis

The development of analytical high performance liquid chromatography (HPLC) instruments dates back to the 1960s. In the first ten to twenty years of its development, HPLC was considered only suitable for the separation and quantitative analysis of those mixtures whose components were insufficiently volatile or thermally

unstable for gas chromatography. It has become clear, however, that owing to the method's ruggedness, simplicity, variable detection methods and modes of operation, many other types of mixtures can be analyzed using this technique. Mixtures of transition metals remain a difficult case, however, especially at trace concentrations. For the analyses of metals, the most suitable mode of HPLC, it appears, would be reversed phase HPLC since it is compatible with the aqueous media in which the metal ions are usually found One of the most challenging aspects of these analyses is the quantitative derivatization of metal ions into complex species suitable for chromatographic determination.

Most uncharged metal complexes are often more soluble in organic solvents and have properties that are similar to free ligands. The kinetically stable complexes can be separated and analysed by HPLC as several researchers have shown[39-41]. The application of HPLC in these analyses requires creative incorporation of metal complexation steps in the final method. As part of a review of the advancements made in the application of HPLC to metal analysis, Robards and Starr[34] compiled a list of those ligands whose transition metal complexes in general were found to show good chromatographic behaviour. Complexes that were found suitable to chromatography were described as those whose stability does not arise mainly from the crystal field stabilisation energy of the metal but, rather, from the ligand structure. Some ligands have more than one binding sites or atoms which can donate an electron pair. These ligands (known as *bidentate, tridentate*, and so on) can, by forming a ring, hold the metal by two or more of its binding sites thereby forming kinetically stable complexes that are well suited to chromatography. Other ligands form single ionic and/or covalent bonds with the metal. Stability of the complexes formed by these ligands arises mainly from the crystal field stabilisation energy of the metal. Complexes of this type tend to not meet the requirements for chromatography.

HPLC methods are categorised in four different modes[20,42,43], based on the mechanisms of separation involved:

i) **Normal phase** separates neutral, non-polar to slightly polar compounds, which are soluble in water-immiscible organic solvents (also used as eluents) such as alkanes and chloroform. The compounds are separated on basis of

their varying retention by the stationary phase of the column due to interaction with the polar stationary phase, commonly silica gel. The (slightly) polar compounds are retarded more than the non-polar and elute more slowly.

ii) **Reversed phase HPLC** separates uncharged, polar to non-polar compounds which are soluble in water and water-miscible organic solvents such as methanol, or acetonitrile. The basis of separation is a distribution of the compounds between the relatively polar mobile and non-polar stationary phases such that the polar compounds essentially stay in the mobile phase and traverse the column rapidly while the non-polar compounds interact more with the non-polar stationary phase and are thus retarded. The stationary phase is commonly octadecyl silane, which is silica that has n-$C_{18}H_{38}$ chemically bonded to it, thus coating the particle surface to form a hydrophobic layer.

iii) **Ion-pair Chromatography** is most suitable for separation of ionic substances A positive ion pair reagent such as tertrabutyl-ammoniumchloride, $[(C_4H_9)_4N]^+Cl^-$, or a negative ion pair reagent such as hexyl-sodiumsulfonate, $C_6H_{13}SO_3^-Na^+$, is added to the mobile phase and by means of its hydrophobic butyl or hexyl group, is attached to the stationary phase (e.g. octadecyl silica). The charged end of the ion pair reagent provides interactive sites for the dissociated ions of the analyte. Separation takes place according to ion exchange principles whereby ions which have stronger affinity to the ion pair reagent are eluted last.

iv) **Gel permeation / size exclusion** separates large molecules, generally with molecular mass greater than 2000 $g.mol^{-1}$. These are separated on the basis of their size. Analyte molecules pass through porous solids that are generally inert and have known pore size distribution. The smaller molecules enter into the pores of the stationary phase and take long paths through the column while larger molecules cannot enter the pores (and are said to be excluded), and take the shortest distance. As a result large molecules are eluted first and smaller molecules last.

Reversed phase chromatography is generally perceived as being more versatile and its methods more rugged. While the solubility of many compounds is limited in water-organic solvent mixtures (used as mobile phase), this is not a practical limitation to using reversed phase HPLC as only small amounts of sample are introduced (typically 5 - 20μl) In addition, there is a great potential to detect much smaller concentrations of the metals when they are analysed as their complex derivatives. This is because ligands can be chosen to produce intense signals (to the chosen methods of detection). Strongly fluorescent or UV absorbing chromophores could be attached to the ligands to enhance sensitivity of the complex molecules.

Several reports on the analysis of platinum group metals as complexes of various compounds, by reversed phase HPLC, have been published[44-52] (Table 1 1.). In general, the methodology begins with complexation of the metal by the chosen ligand, which is achieved in various ways, either by means of pre- or post-column derivatization, on-line complexation, ligand exchange techniques or separate complexation.

Table 1.1. Ligands used in the analysis of PGMs by RP-HPLC.

Ligand	Metals	Reference
i) 1-(2-pyridylazo)-2-naphthol	Pd^{II}, Pt^{II}, Rh^{III}	44
ii) Diethyldithiocarbamate	Pd^{II}, Pt^{II}, Rh^{III}	45, 46
iii) Acetylacetone	- Co^{II}, Pd^{II}, Rh^{III},Ir^{III} - Co^{II}, Be^{II}, Rh^{III}, Cr^{III} Pd^{II}, Pt^{II}, Ru^{III} - Rh^{III}, Ir^{III}, Pd^{II}, Pt^{II}	47
iv) 2-(6-methyl-2-benzothiazolyl) -5-diethylaminophenol	Ir^{IV}, Pt^{II}, Ni^{II}, Ru^{III}, Os^{IV}, Co^{II}	48,49
v) 4-(5-nitro-2-pyridylazo) resorcinol	Pd^{II}, Rh^{III}, Ru^{III}, Pt^{II}	50
vi) 4-(2-thiazolylazo) resaceto-phenone oxime	Ru^{III}, Os^{IV}, Pd^{II}	51
vii) 2-(2-thiazolylazo)-5-diethyl-aminophenol	Pt^{II}, Ir^{IV}, Ru^{III}, Rh^{III}, Os^{IV}	52

Mueller and Lovett[46] included a novel salt-induced phase separation of the organic and aqueous phases in their method. An acetonitrile solution of diethyldithiocarbamate was added to an aqueous PGM sample. Once complexation had taken place, separation of the acetonitrile and water phases was induced by adding a saturated solution of sodium chloride to the mixture. In addition to pre-concentrating the diethyldithiocarbamate complexes, phase separation prevents contact of matrix ions and other charged species with the analytical column since these remain in the polar, aqueous layer and only the organic phase is analysed.

Properties of metal complexes suitable for separation by RP-HPLC have been defined by Alimarin *et al*[44] as those which:

i) are uncharged,
ii) are coordinatively saturated,
iii) have definite stoichiometry,
iv) are soluble in water-miscible organic solvents such as CH_3CN and CH_3OH.

In addition, it should be noted that:

i) Charged species tend to form strong electrostatic bonds with the residual silanol groups of the stationary phase thereby compromising the separation properties of the column. Such a column is described as "poisoned". Although a few salvage methods have been suggested[34], poisoning is not always reversible.
ii) Buffer agents tend to co-ordinate onto vacant sites around the metal center. This co-ordination may result in new species and thus the appearance of additional peaks or cause the peaks to split.
iii) Metal complexes that are likely to aggregate are not suitable for analysis by HPLC as they may result in excessively broad peaks and in addition, do not give a consistent signal.
iv) Precipitation during HPLC analysis may result in poor reproducibility of peak areas and ultimately, blockage of tubing and the analytical column.

It is also essential that the resultant metal complexes have suitable properties for the method of detection being used such as having a chromophore in the case of UV detection. Platinum(II), palladium(II) and rhodium(III) complexes of *N,N*-dialkyl-*N'*-acylthioureas were found to meet the RP-HPLC analysis criteria, and thus became the focus of attention for this study.

1.5. Complexation of PGMs with acylthioureas

N,N-dialkyl-*N'*-acylthioureas show extraordinary selectivity towards PGMs in acidic media. The pH conditions under which *N,N*-diethyl-*N'*-pyrenoylthiourea and *N*-methyl-*N*-(9-methylanthracene)-*N'*-benzoylthiourea complexes of PGMs and commonly associated metals form, were investigated by Schuster and Unterreitmaier[53,54]. From the representation of their results (Figure 1.4) it can be seen that at pH's below 3, all PGMs form complexes exclusively. The pH controlled selectivity of acylthiourea complex formation creates good opportunities for pre-concentration and selective extraction of PGMs.

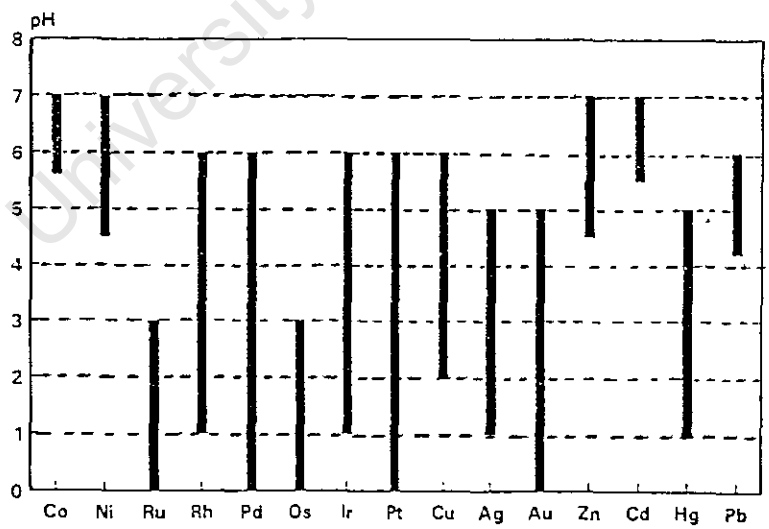

Figure 1.4: The pH ranges (indicated by the bars) within which the *N,N*-diethyl-*N'*-pyrenoylthiourea complexes of PGMs and other, commonly associated transition metals were formed[53].

N,N-dialkyl-*N'*-acylthioureas favour bidentate *(S,O)* mode of coordination. These ligands yield 1:2 (metal-to-ligand) complexes which are predominantly *cis* and square planar, with divalent d^8 metal ions[55]. The co-ordination to trivalent metal ions such as Rh(III) results in 1:3 (metal-to-ligand) complexes. Analysis of *tris*-[*N*-pyrrolidyl-*N'*-(2,2-dimethylpropanoyl)thioureato]rhodium(III) prepared in the present work, by x-ray diffraction, showed the complex to be the octahedral, *facial* isomer (see Figure 2.13).

Studies of molecular structures of *N,N*-dialkyl-*N'*-acylthiourea complexes by nuclear magnetic resonance spectroscopy (^{1}H and ^{195}Pt NMR) have shown evidence of some subtle differences[56]. Exploitation of these differences for analytical determinations remains a difficult challenge and requires innovation and creativity.

The chromatographic separation of neutral acylthiourea complexes of PGMs has previously been investigated by normal phase HPLC[57] and by high performance thin layer chromatography (HPTLC)[53,54]. In the case of normal phase HPLC, with chloroform as part of the mobile phase, these complexes were found to decompose on the column. The decomposition was thought to be induced by the acidic nature of silica, the stationary phase. According to this hypothesis, one or both co-ordinated ligands become protonated by the silanol groups of the silica particles during partitioning of the complex molecules as they travel through the column. The chelate rings open, resulting in charged complex species. Some of the complex molecules remain intact and emerge from the column. Thus additional peaks were observed.

In reversed phase HPLC, the stationary phase, also a silica material, is chemically modified with bonded normal hydrocarbon chains (usually C_{18} in length) which form a non-polar layer over the surface of the silica particles. Additionally, the pH of the mobile phase which is always a mixture of water and an organic solvent, can be controlled by means of a suitable buffer agent. These are more suitable conditions for analytes that can be protonated such as the *N,N*-dialkyl-*N'*-acylthiourea complexes of PGMs.

These complexes exhibit intense UV absorption spectra, which could be arising from the presence of π-electron systems in the coordination rings or metal to ligand charge

transfer absorption. It is therefore possible to detect these complexes by a UV detector.

1.6. Objectives of this work

This project was aimed at producing a practical reversed phase HPLC method with which to accomplish the determination of platinum, palladium and rhodium at trace levels in aqueous media using *N,N*-dialkyl-*N'*-acylthioureas as complexing agents Furthermore, it was a purpose of this project to demonstrate that reversed phase HPLC can be used to determine unrecovered PGM traces in the refinery waste effluents.

Some preliminary tests in the laboratory have shown that *N,N*-dialkyl-*N'*-(2,2-dimethylpropanoyl)thioureas generally have greater solubility in water than *N,N*-dialkyl-*N'*-benzoylthioureas including *N,N*-di(2-hydroxyethyl)-*N'*-benzoylthiourea, despite the hydrophilicity of the 2-hydroxyethyl groups. Three derivatives of 2,2-dimethylpropanoylthiourea (given below) were, therefore, selected as ligands for study in this project.

An outline of the approach taken is as follows:

i) Synthesis and characterisation of suitable hydrophilic ligands namely,

- *N,N*-dimethyl-*N'*-(2,2-dimethylpropanoyl)thiourea,

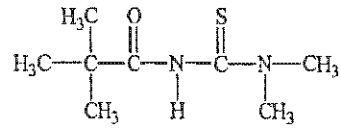

- *N*-pyrrolidyl-*N'*-(2,2-dimethylpropanoyl)thiourea,

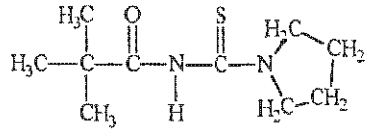

- *N*-piperidyl-*N'*-(2,2-dimethylpropanoyl)thiourea,

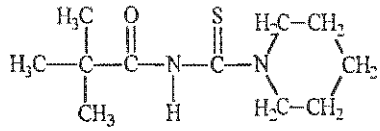

and their corresponding platinum(II), palladium(II) and rhodium(III) complexes

ii) Development of HPLC methodology, which entails:
- Sample preparation
- Chromatographic separation
- quantitative determination of platinum, palladium and rhodium (present as a mixture) in the aqueous sample.

iii) Laser Ablation - Inductively Coupled Plasma Mass Spectrometry (LA-ICP MS) study.

2.

Synthesis and characterisation of ligands and Pt(II), Pd(II), Rh(III), Ni(II) and Cu(II) complexes

2.1. Synthesis

2.1.1. Ligands

N,N-dialkyl-*N'*-acylthioureas were prepared according to the method of Douglass and Dains[2] in which a secondary amine is reacted with acyl isothiocyanate (Figure 2.1).

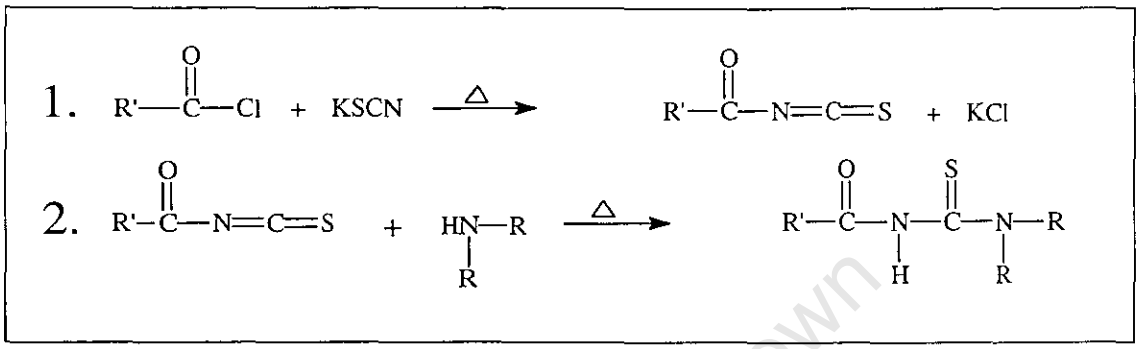

Figure 2.1: Reaction scheme for the synthesis of *N,N*-dialkyl-*N'*-acylthioureas.

The above reactions were carried out in dry acetone. With heating under reflux the acyl chloride reacts easily with potassium thiocyanate to give acyl isothiocyanate and potassium chloride which forms as a precipitate. The reaction mixture was cooled down to room temperature after 30 minutes. The solution of secondary amine was added to the cool mixture in the same flask. Heating under reflux was resumed and the reaction allowed 30 minutes whereby the *N,N*-dialkyl-*N'*-acylthiourea was produced. Experimental details are found in section 2.5.

A necessary precaution when carrying out this synthesis is to exclude moisture, since acyl chloride is readily hydrolysed, thereby forming carboxylic acid. Hence the reaction was carried out under dry nitrogen. It should also be noted that a side reaction which results in the formation of an amide as shown in figure 2.2 is possible, where the nucleophilic attack by the nitrogen atom of the secondary amine takes place at the carbonyl carbon instead of the thiocarbonyl carbon. However, bulky R'-groups such as 2,2-dimethylpropanone protects the carbonyl carbon from nucleophilic attack by steric hindrance, and were found to reduce the extent of amide formation significantly[3]. Electron-releasing groups such as a phenyl ring are believed to reduce the electrophilicity of the carbonyl carbon, and as a result are able to hinder amide side-product formation as well[3].

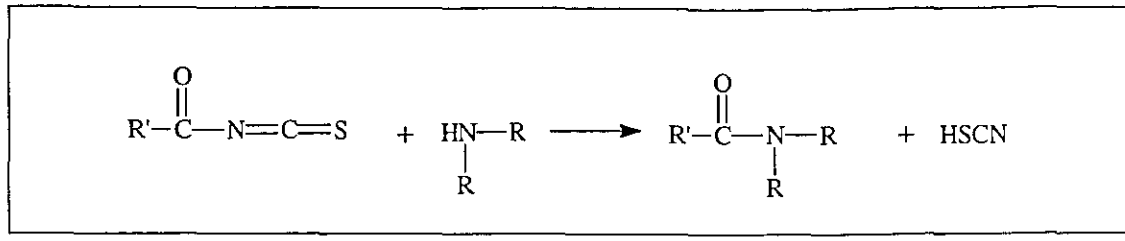

Figure 2.2: A competing nucleophilic attack at the carbonyl carbon results in the formation of an amide[3].

In this work, three compounds were synthesized, which together with their respective starting reagents are shown in Table 2.1.

Table 2.1. *N,N*-dialkyl-*N'*-(2,2-dimethylpropanoyl)thioureas synthesized and their starting reagents.

Compound	Starting reagents
1. 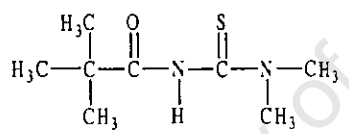	KSCN ; 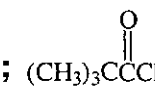 ; 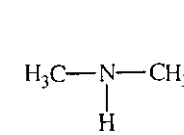
2. 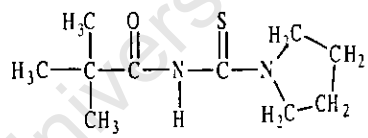	KSCN ; 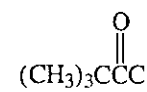 ; 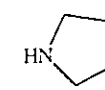
3. 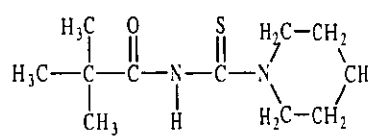	KSCN ; 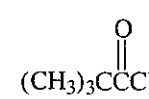 ; 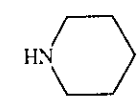

2.1.2. Pt(II) / Pd(II) complexes

A general reaction for the synthesis of *N,N*-dialkyl-*N'*-acylthiourea complexes of platinum(II) and palladium(II) is given in Figure 2.3 below.

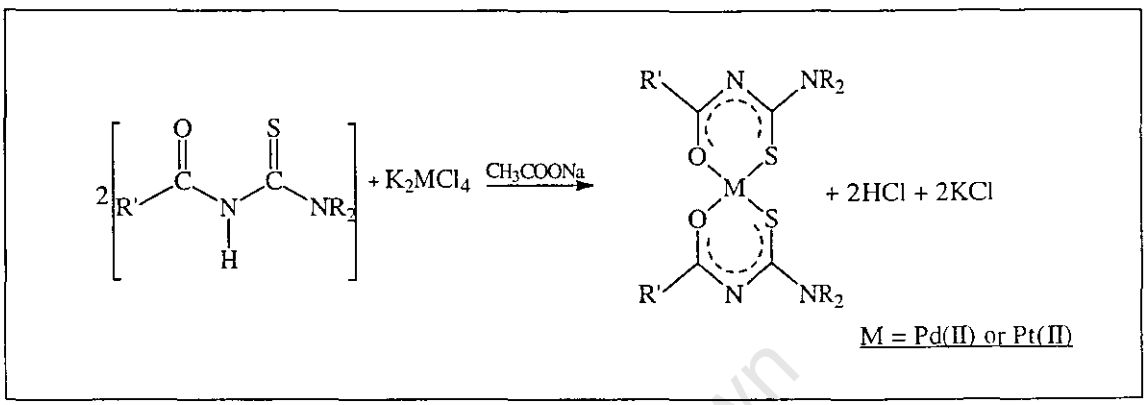

Figure 2.3. Synthesis of *N,N*-dialkyl-*N'*-acylthiourea complexes of platinum(II) or palladium(II).

Reaction of *N,N*-dialkyl-*N'*-acylthiourea (HL) with MCl_4^{2-} (M = Pt^{II}, Pd^{II} or Ni^{II}), yield exclusively *cis*-[M(L-*S,O*)$_2$] type of complexes with divalent d^8 metals[55] without metal-containing side products. This, and the selective coordination of these ligands towards soft metals[58] in acid solutions makes *N,N*-dialkyl-*N'*-acylthioureas well suited for quantitative determination of platinum group metals by HPLC. The formation of [M(L-*S,O*)$_2$] results in the loss of the dissociable N-H proton. It is on this account that a base is added to facilitate the reaction. The *N*-monoalkyl-*N'*-acylthiourea analogues (H_2L) lead to a mixture of *cis*-[M(H_2L-*S*)$_2X_2$] and *trans*-[M(H_2L-*S*)$_2X_2$] isomers, where X = Cl, Br or I[55,59,60]. In a study of a similar type of complex namely *bis*-[*N*-benzoyl-*N'*-propylthiourea]dichloroplatinum(II), Bourne and Koch[59] found the ^{1}H and ^{195}Pt NMR evidence that proved the presence of a *trans-bis*-[*N*-benzoyl-*N'*-propylthiourea]dichloroplatinum(II) isomer in a 1:2.3 ratio relative to the *cis* isomer.

2.1.3. Rh(III) complexes

N,N-dialkyl-*N'*-acylthiourea complexes of rhodium(II) are formed according to the reaction shown in Figure 2.4.

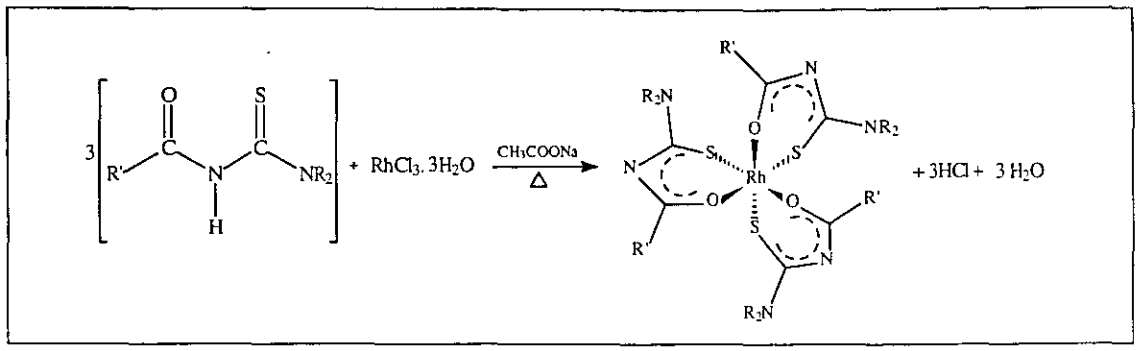

Figure 2.4: Synthesis of *N,N*-dialkyl-*N'*-acylthiourea complexes of rhodium(III).

The synthesis of *tris*[*N,N*-dimethyl-*N'*-(2,2-dimethylpropanoyl)thioureato]-rhodium(III) in 50/50 (%v/v) acetonitrile/water, in the presence of sodium acetate, was not successful. In spite of stirring at room temperature for 48 hours, the colour of the solution did not change and a precipitate did not form. However, on heating under reflux at 80°C, a black sticky substance formed in the mixture. Solvent extraction of the solution with chloroform isolated a black waxy solid. The ^{1}H and ^{13}C NMR spectra of this substance contained many resonance peaks and could not be assigned (figures 2.5 and 2.6). On investigating the C^{13} NMR spectrum (Figure 2.6), it appears that *meridinal tris*[*N,N*-dimethyl-*N'*-(2,2-dimethylpropanoyl)thioureato]rhodium(III) is formed. The carbonyl, thiocarbonyl, methyl and quarternary carbons of the coordinated ligands have slightly different resonance frequencies giving rise to sets of three resonance peaks for each carbon. Furthermore, the product seems to be a mixture of compounds because it did not melt completely within a specific range of temperature. This prevented determination of its elemental composition by combustion analysis. *Tris*[*N*-pyrrolidyl-*N'*-(2,2-dimethylpropanoyl)thioureato]-rhodium(III) and *tris*[*N*-piperidyl-*N'*-(2,2-dimethylpropanoyl)thioureato]rhodium(III) were, however, successfully synthesised and isolated.

2.1.4. Ni(II)/Cu(II) complexes

N-pyrrolidyl-*N'*-(2,2-dimethylpropanoyl)thiourea complexes of nickel(II) and copper(II), were also prepared. The elemental analysis results and melting points of these two complexes indicate comparable purity as the platinum(II) and palladium(II) complexes (section 2.5). The *bis*-[*N*-pyrrolidyl-*N'*-(2,2-dimethylpropanoyl)thioureato]nickel(II) complex was analysed by ^{13}C and ^{1}H NMR. The ^{13}C NMR spectrum was fully assigned (Appendix I) and the ^{1}H NMR was

characteristic of the *bis*, square planar, *cis* coordinated acylthiourea complexes which are deceptively simple (Appendix II). However, the copper(II) complex did not produce any NMR spectrum, due to the paramagnetism of copper(II).

2.2. NMR spectroscopy

The ^{1}H NMR spectra of *N*-pyrrolidyl-*N'*-(2,2-dimethylpropanoyl)thiourea complexes of platinum(II), palladium(II) and rhodium(III) are deceptively simple (Figures 2.7 and 2.12), presumably because of symmetry in these molecules. As a result, we focused more on the ^{13}C NMR which was relatively more informative. What does emerge from the ^{1}H NMR spectra, however, is that the methylene, N-$(CH_2)_2$-, protons of the alkyl substituents are magnetically inequivalent, as evidenced by two sets of ^{1}H-^{1}H couplings. This inequivalence which is also observed in the ^{13}C NMR has been attributed to the restricted rotation about the C(2)-N(3) bond (due to the partial double bond character) in a study of similar complexes[61](see annotation of atoms in page 25).

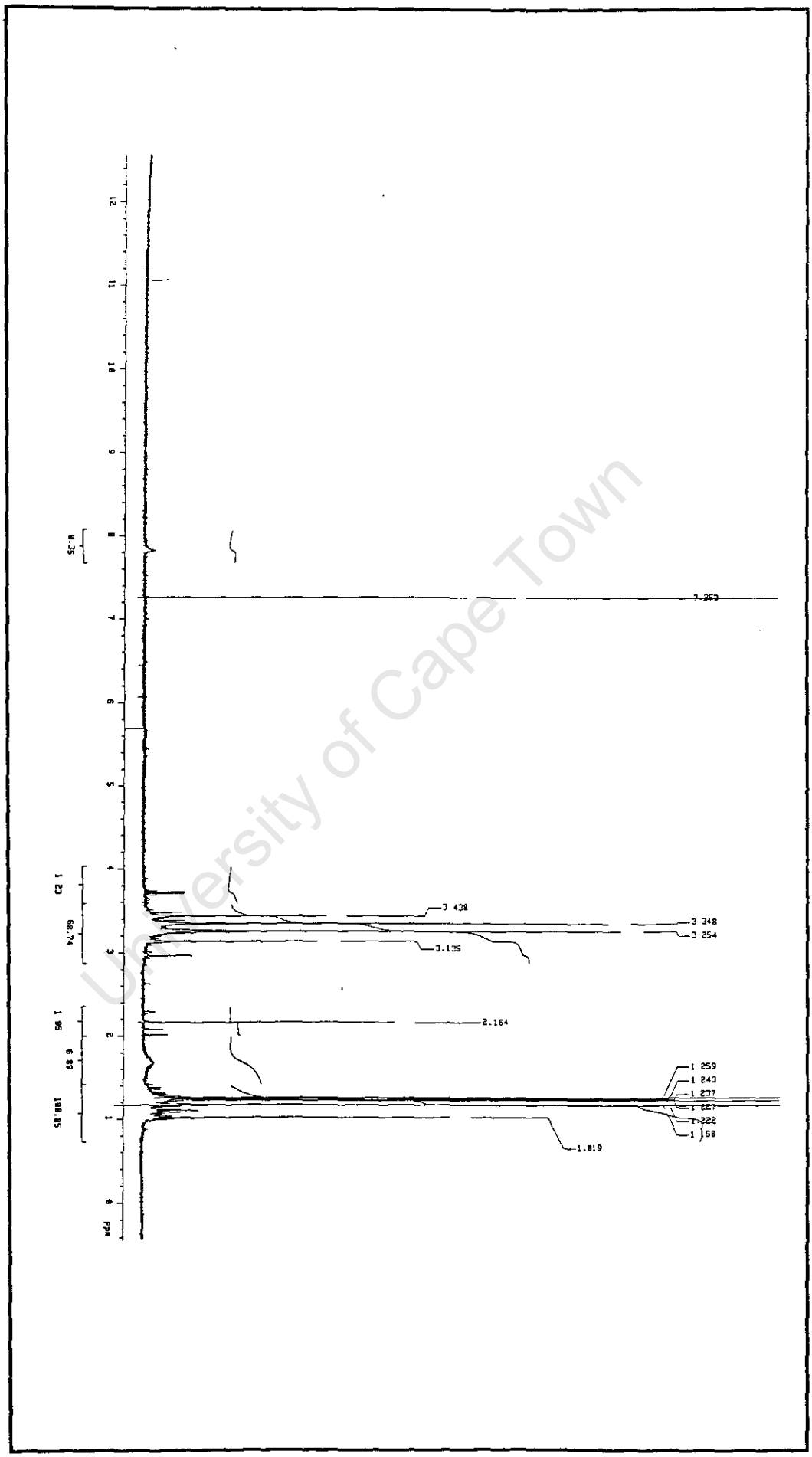

Figure 2.5: A ^{1}H NMR spectrum of the product obtained in the attempted synthesis of *tris*-[*N*,*N*-dimethyl-*N'*-(2,2-dimethylpropanoyl)-thioureato]rhodium(III).

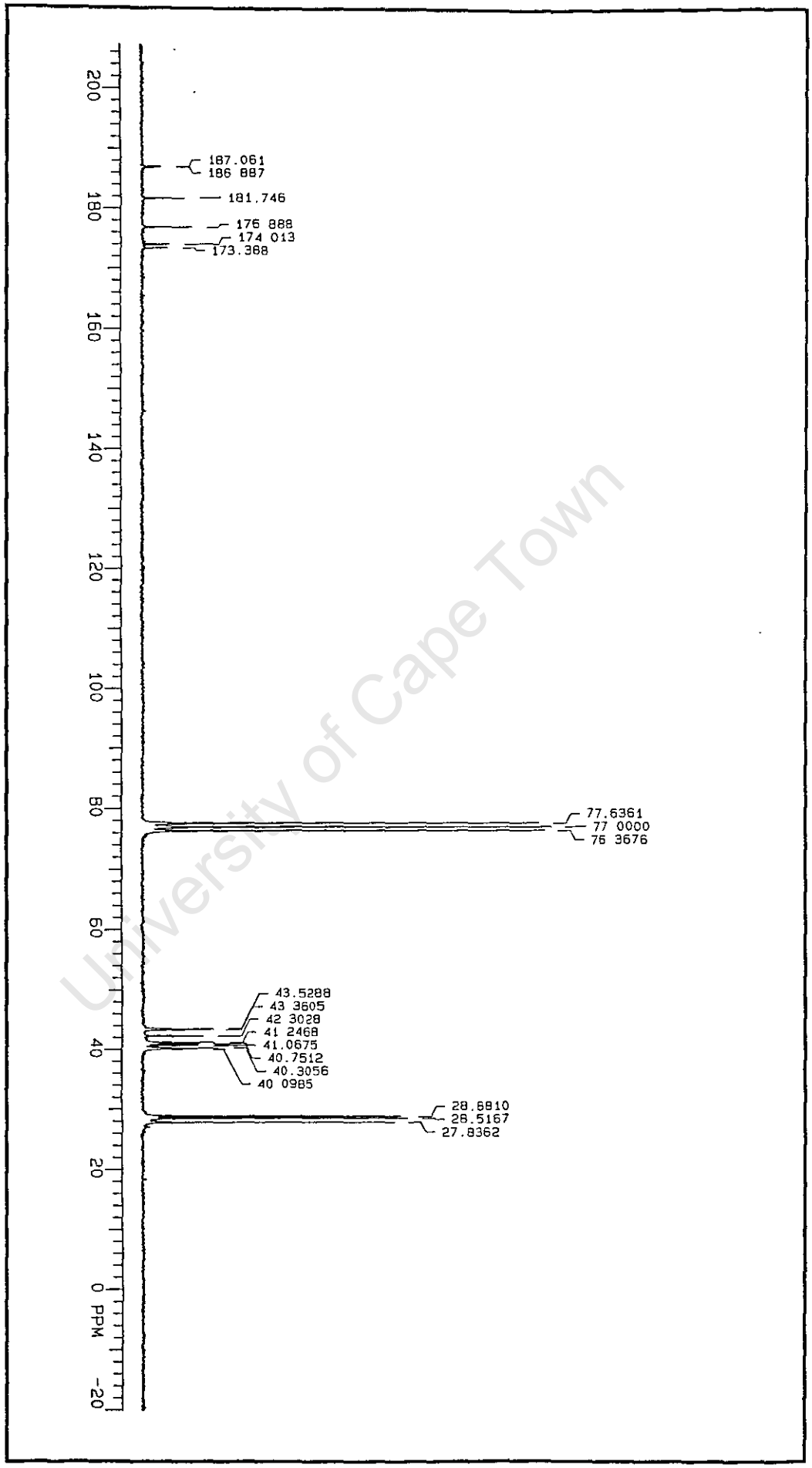

Figure 2.6: A ^{13}C NMR spectrum of the product obtained in the attempted synthesis of *tris*-[*N,N*-dimethyl-*N'*-(2,2-dimethylpropanoyl)-thiourcato]rhodium(III).

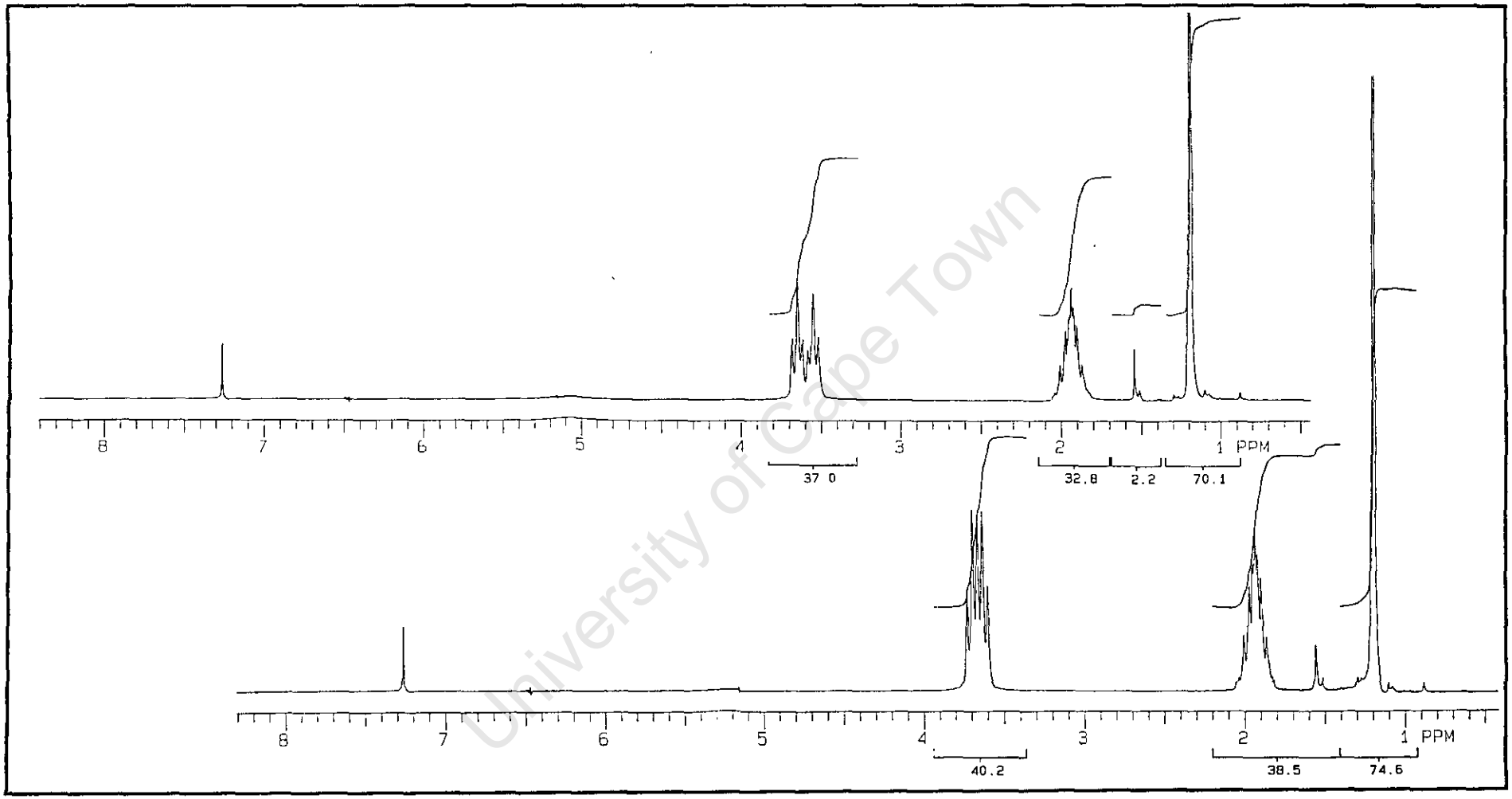

Figure 2.7: The ^{1}H NMR spectra of the *N*-pyrrolidyl-*N'*-(2,2-dimethylpropanoyl)thiourea complexes of platinum(II) - top, and palladium(II) - bottom.

The chemical shifts of the ligands and their respective platinum(II), palladium(II) and rhodium(III) complexes, obtained in the ^{13}C NMR are shown in Table 2.2. Key to shorthand notation used in Table 2.2 is given below:

HL^1 =

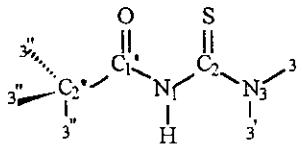

HL^2 =

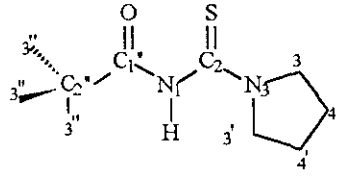

HL^3 =

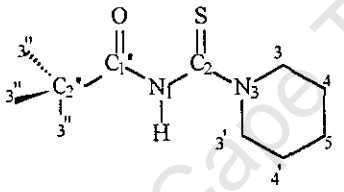

The carbons marked (3) and (3'), (4) and (4'), produced adjacent resonance peaks as a result of the restricted rotation about the C(2)-N(3) bond[61]. These peaks were assigned collectively. While the quartenary carbon, C(2), and C(5) of the piperidyl ring were easily assigned, the assignment of carbonyl and thiocarbonyl carbons, C(1) and C(2), were confirmed by fully ^1H coupled ^{13}C NMR. The carbonyl carbon couples with the (nine) methyl protons of the 2,2-dimethylpropanoyl group in its proximity giving rise to a multiplet while the thiocarbonyl carbon couples with the (four) methylene protons of the *N*-cycloalkyl subtituent on the other hand, producing a pentet (figure 2.8). A study by Koch and Matoetoe[61] in which ^{13}C isotope-enriched KSCN was used to synthesise *N,N*-dibutyl-*N'*-benzoylthiourea used in preparation of platinum(II) and palladium(II) complexes, provided additional guidance in distinguishing between the carbonyl carbon and the thiocarbonyl carbon peaks.

Table 2.2. Chemical shift data and assignments of free *N,N*-dialkyl-*N'*-acylthiourea carbons as well as those of their PGM complexes. (key to notation used is given in page 25).

Compound	Chemical shifts / ppm						
	C3''	C2''	C3, C3'	C4, C4'	C5	C(S)	C(O)
HL^1	27.04	39.61	44.15/42.90	-	-	180.32	174.36
cis-[Pt(L^1-*S,O*)$_2$]	28.22	42.26	41.51/40.42	-	-	167.83	183 26
cis-[Pd(L^1-*S,O*)$_2$]	28.57	41.90	41.76/40.61	-	-	171.93	185.58
HL^2	27.16	39.62	54.43/52.52	26.16/24.59	-	176.66	174.38
cis-[Pt(L^2-*S,O*)$_2$]	28.36	42.12	50.22/49.99	25.29/24.71	-	164.31	182.92
cis-[Pd(L^2-*S,O*)$_2$]	28.57	41.76	50.37/50.30	25.43/24.77	-	168 38	185 20
fac-[Rh(L^2-*S,O*)$_3$]	28.89	42.41	51.16/49.75	25.67/25.00	-	170.91	186.47
HL^3	27.06	39.64	52.87/52.87	26.01/25.19	23.83	178.49	174 08
cis-[Pt(L^3-*S,O*)$_2$]	28.27	42.22	47.97/50.35	24.49/25.79	25.79	166.60	183.59
cis-[Pd(L^3-*S,O*)$_2$	28.54	41.87	50.82/48.24	26 04/25.87	24.54	170.64	185.93
fac-[Rh(L^3-*S,O*)$_3$]	28.52	42.12	47.61/49.61	25.87/25.87	24.60	172.85	186.77

Long range ^{195}Pt–^{13}C couplings for the platinum(II) complexes, over 2, 3 and 4 bonds, were observed as satellites about certain ^{13}C resonance peaks (Figure 2.9). The coupling constants are given in Table 2.3. These couplings are between the same atoms as observed by Koch and Matoetoe[61]. Although other coupling constants differ significantly, the ^2J (^{195}Pt-C_2) appears to remain between 44 and 47Hz for all complexes studied in this work as well as previously[61].

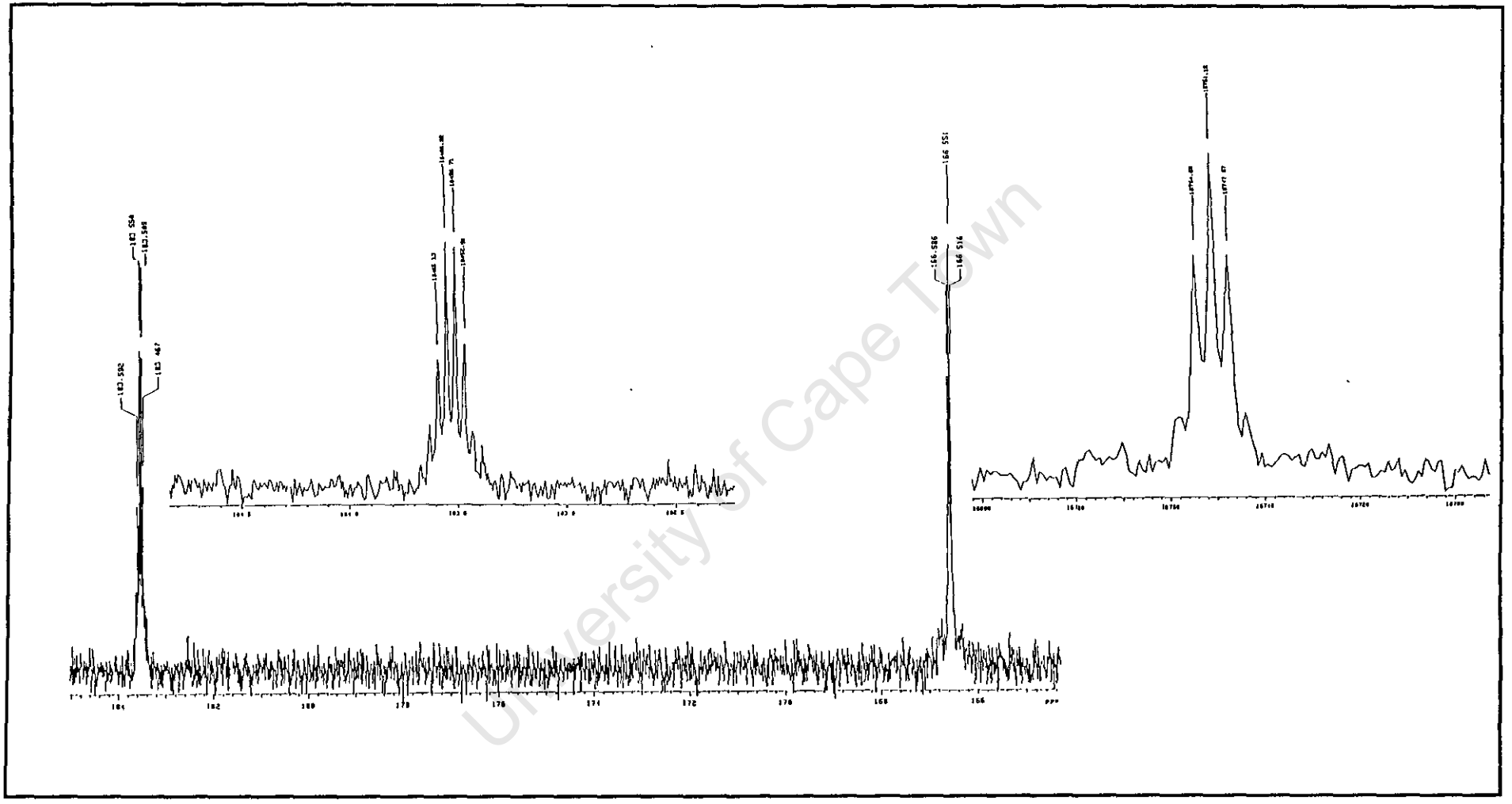

Figure 2.8: Multiplet and pentet couplings of carbonyl and thiocarbonyl carbons in a fully (^{1}H) coupled ^{13}C NMR spectrum of *bis*-[*N*-piperidyl-*N'*-(2,2-dimethylpropanoyl)thiourcato]platinum(II).

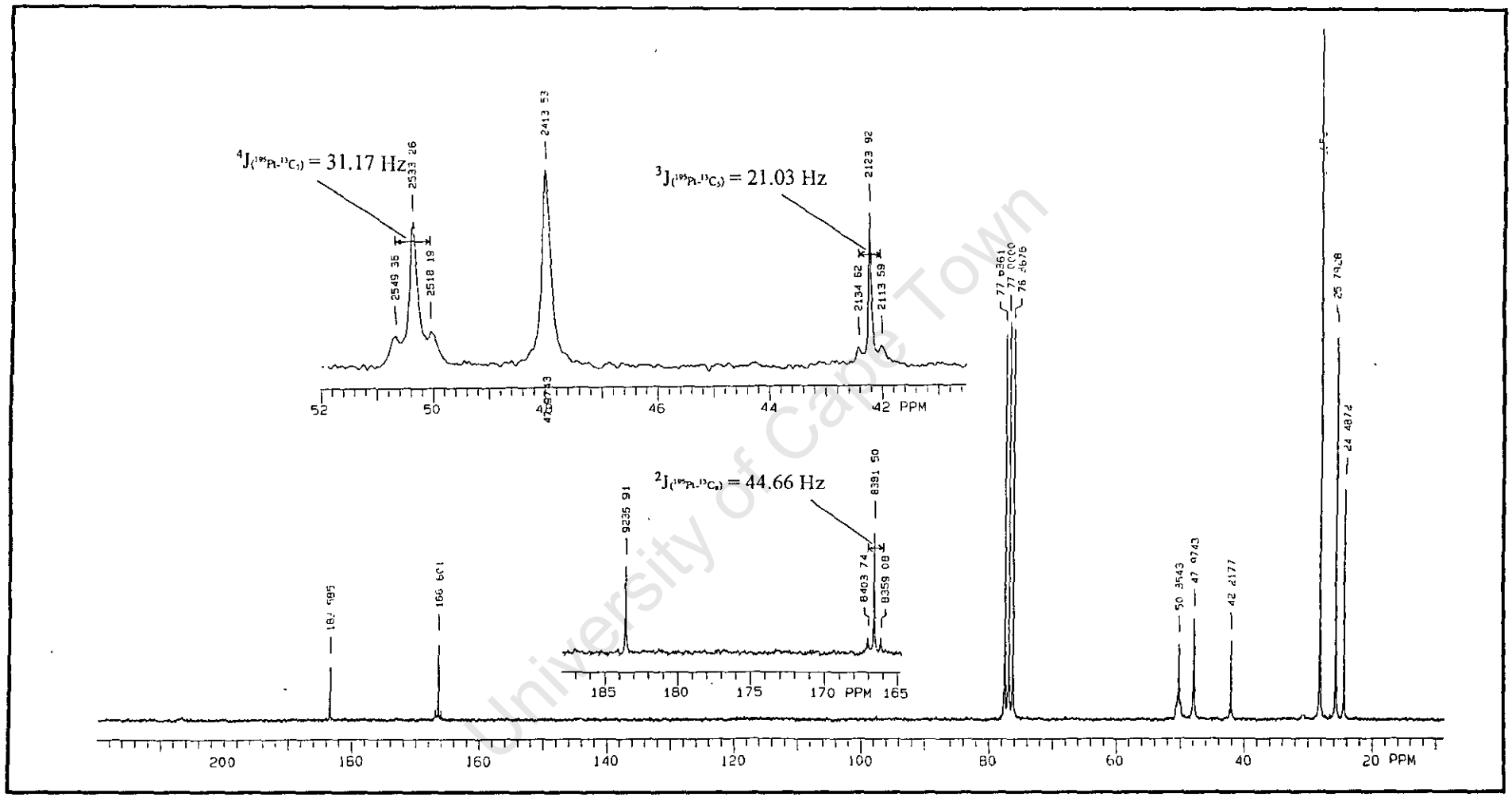

Figure 2.9: A ^{13}C NMR spectrum of *bis*-[*N*-piperidyl-*N'*-(2,2-dimethylpropanoyl)thiourcato]platinum(II) with long range ^{195}Pt-^{13}C couplings.

Table 2.3. Long range couplings between ^{195}Pt and ^{13}C in the W-pathway with respect to platinum. Comparable to those of *cis*-[*N,N*-diethyl- and *N,N*-dibutyl-*N'*-benzoylthioureato]platinum(II)(Pt[L^a-*(S,O)*]$_2$ and Pt[L^b-*(S,O)*]$_2$), reported in reference 61 (written in bold letters).

	Coupling constants / Hz		
	^4J (^{195}Pt-$^{13}C_{3'}$)	^3J (^{195}Pt-$^{13}C_{2''}$)	^2J (^{195}Pt-$^{13}C_2$)
cis-[Pt(L^1-*S,O*)$_2$]	30	21	46
cis-[Pt(L^2-*S,O*)$_2$]	23	20	47
cis-[Pt(L^3-*S,O*)$_2$]	31	21	45
cis-[Pt(L^a-*(S,O)*]$_2$	**27**	**26**	**46**
cis-[Pt(L^b-*(S,O)*]$_2$	**27**	**not observed**	**46**

It has been noted before, on the basis of molecular models, that these four bond couplings occur between ^{195}Pt and specific carbons in the "W" orientation (Figure 2.10) with respect to platinum[6]. Furthermore, it is accepted that long range spin couplings such as these are transmitted through the electronic framework of the molecule. It has been found that the observability of these spin couplings depends on the magnitude of the applied field strength[62]. Palladium(II) complexes, although very similar to platinum(II) complexes in structure, do not show long range couplings since no isotope of palladium is magnetically active.

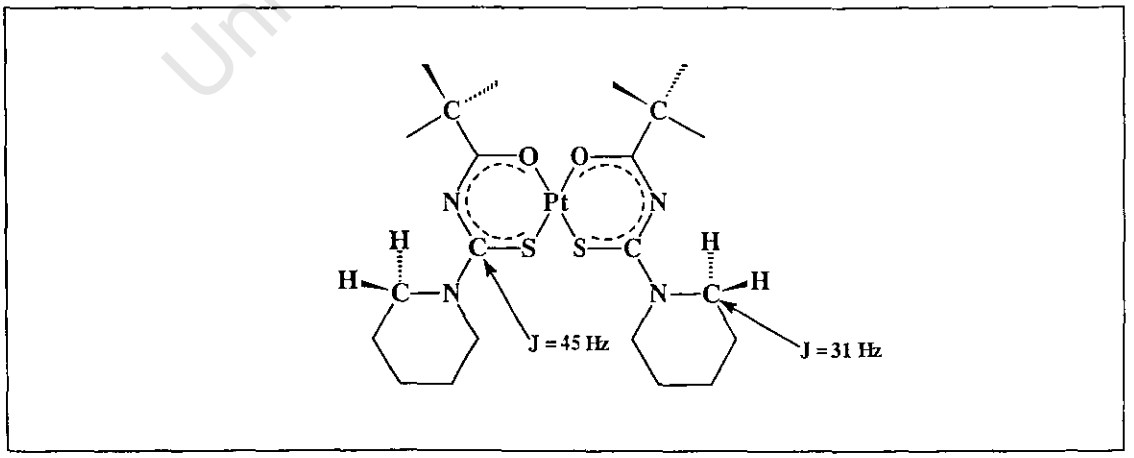

Figure 2.10: The molecular structure of *cis*-Pt[L^3-*(S,O)*]$_2$ illustrating the "W" pathway along which the long range ^2J and ^4J(^{195}Pt-^{13}C) spin couplings occur.

The chemical shifts of the thiocarbonyl carbons, C(S), of free ligands appear to be influenced by the amine substituents, namely dimethylamine (in HL^1), pyrrolidine (in HL^2) and piperidine (in HL^3). The pK_a (electron pair donicity) values of these substituents (as free amines) are 10.78, 11.12 and 11.27, for dimethylamine, pyrrolidine and piperidine, respectively[63]. It appears that the chemical shift of thiocarbonyl carbon of *N*-pyrrolidyl-*N'*-(2,2-dimethylpropanoyl)thiourea (HL^2), 176.66ppm, which is most up-field relative to 178.49 and 180.32ppm of the thiocarbonyl carbon of *N*-piperidyl-*N'*-(2,2-dimethylpropanoyl)thiourea (HL^3) and that of *N,N*-dimethyl-*N'*-(2,2-dimethylpropanoyl)thiourea (HL^1), follows the trend in pK_a values. The thiocarbonyl carbon shifts of all platinum(II), palladium(II) and rhodium(III) complexes in Table 2.2 show this order as well. Based on these observations mentioned above, one could presume that of the three groups of *N,N*-dialkyl-*N'*-acylthiourea complexes, *N,N*-dimethyl-*N'*-acylthiourea complexes will, in theory, have the highest tolerence to acidic conditions since dimethylamine has the lowest pK_a value, and thus the smallest attraction of protons.

In contrast, the chemical shifts of the carbonyl carbons, C(O), of the three free ligands remain virtually the same (within ± 0.4ppm), as do the chemical shifts of the carbonyl carbons in the metal complexes This observation one would expect considering that the acyl function, 2,2-dimethylpropanoyl group, is not changed. The only variation in the structures, is the dialkylamine substituent and since each one has a different electron pair donicity, indicated by the pK_a value, different but predictable changes are induced.

Another interesting observation is that when the chemical shift values of the thiocarbonyl or carbonyl carbons of free ligands are subtracted from their corresponding platinum(II) or palladium(II) complexes, a consistent value is obtained. This is shown in Table 2.4, where the "differences" are represented by $\Delta\delta^{13}C(S)$ and $\Delta\delta^{13}C(O)$.

Table 2.4. $\Delta\delta^{13}C(S)$ and $\Delta\delta^{13}C(O)$ values between ligands and their respective complexes (+ and – denote "up-field" and "down field" shifts, respectively).

	$\{\Delta\delta^{13}C(S)\pm0.5ppm$; $\Delta\delta^{13}C(O)\pm0.5ppm\}$
$Pt[L^1\text{-}(S,O)]_2$	{+12 ; -9}
$Pd[L^1\text{-}(S,O)]_2$	{+8 ; -11}
$Pt[L^2\text{-}(S,O)]_2$	{+12 ; -9}
$Pd[L^2\text{-}(S,O)]_2$	{+8 ; -11}
$Pt[L^3\text{-}(S,O)]_2$	{+12 ; -10}
$Pd[L^3\text{-}(S,O)]_2$	{+8 ; -12}

Apparently, this consistency in $\Delta\delta^{13}C(S)$ and $\Delta\delta^{13}C(O)$ arises from electron densities around platinum and palladium atoms in the complex. The electron density is higher in platinum, being a heavier atom, than in palladium, leading to larger differences in chemical shifts between free and co-ordinated ligands.

The ^{13}C NMR spectra of rhodium complexes were in many respects similar to the palladium(II) and platinum(II) spectra since the molecules are also symmetrical. A $^{2}J(^{103}Rh\text{-}^{13}C)$ coupling was observed (Figure 2.11). However, this coupling is small in magnitude (1.9Hz) and it seems this coupling can only be observed in high resolution NMR. The ^{1}H NMR spectra are also similar to the palladium(II) and platinum(II) spectra and are deceptively simple (Figure 2.12).

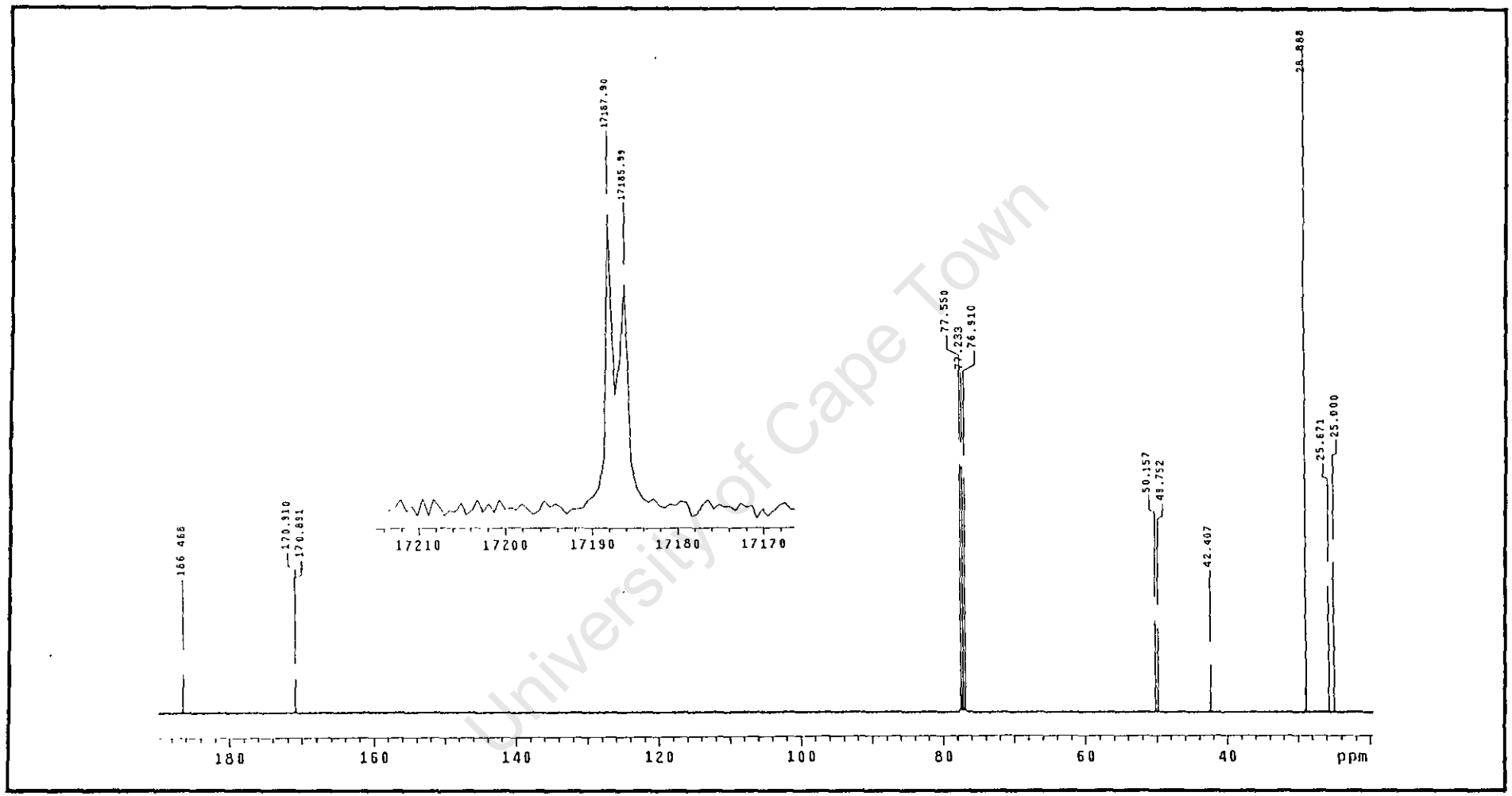

Figure 2.11: A ^{13}C NMR spectrum of *tris*-[*N*-pyrrolidyl-*N'*-(2,2-dimethylpropanoyl)thiourcato]Rh(III) with a long range (^{2}J) ^{103}Rh-^{13}C coupling.

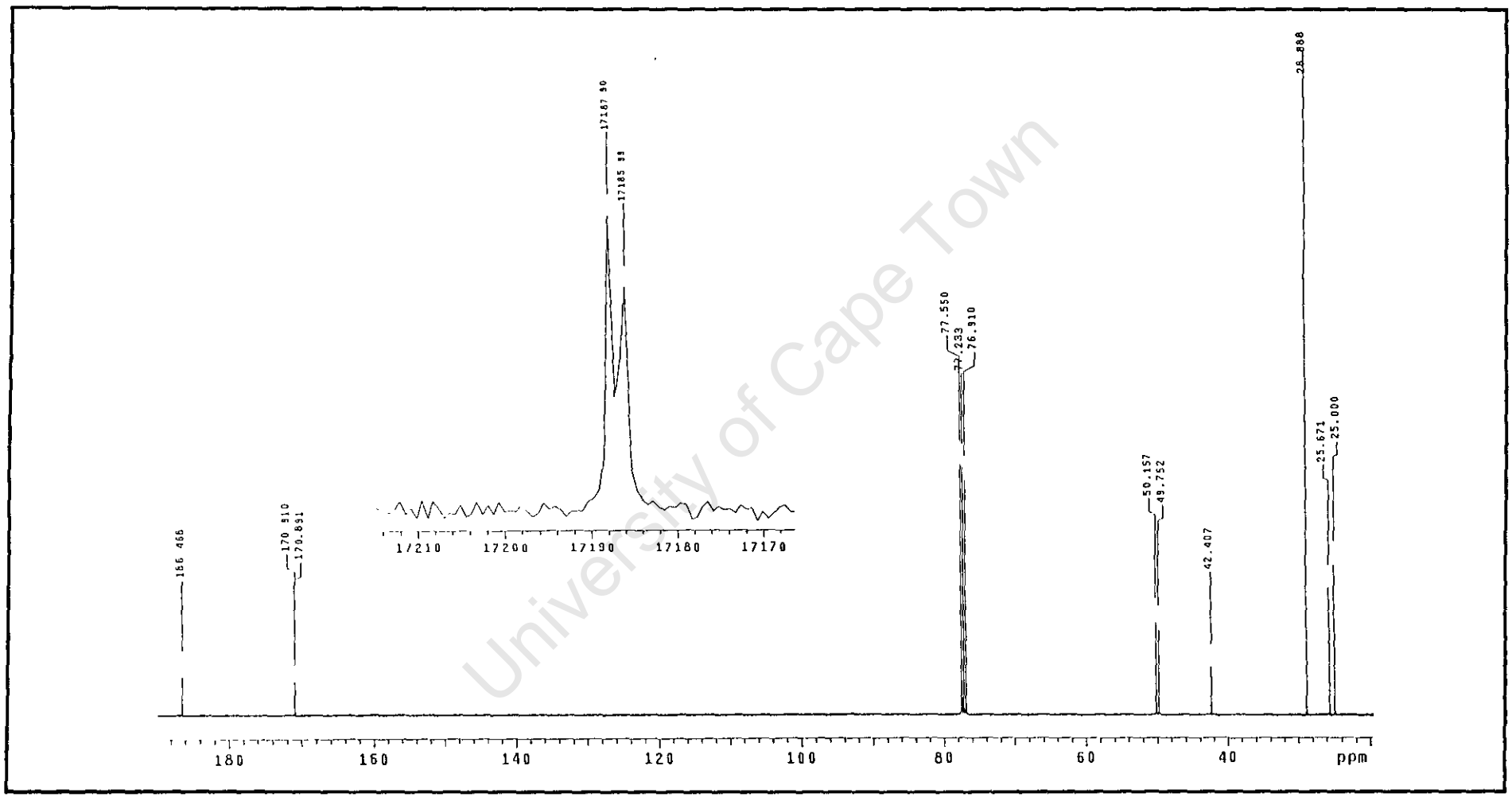

Figure 2.11: A ^{13}C NMR spectrum of *tris*-{*N*-pyrrolidyl-*N'*-(2,2-dimethylpropanoyl)thioureato}Rh(III) with a long range (^{2}J) ^{103}Rh-^{13}C coupling.

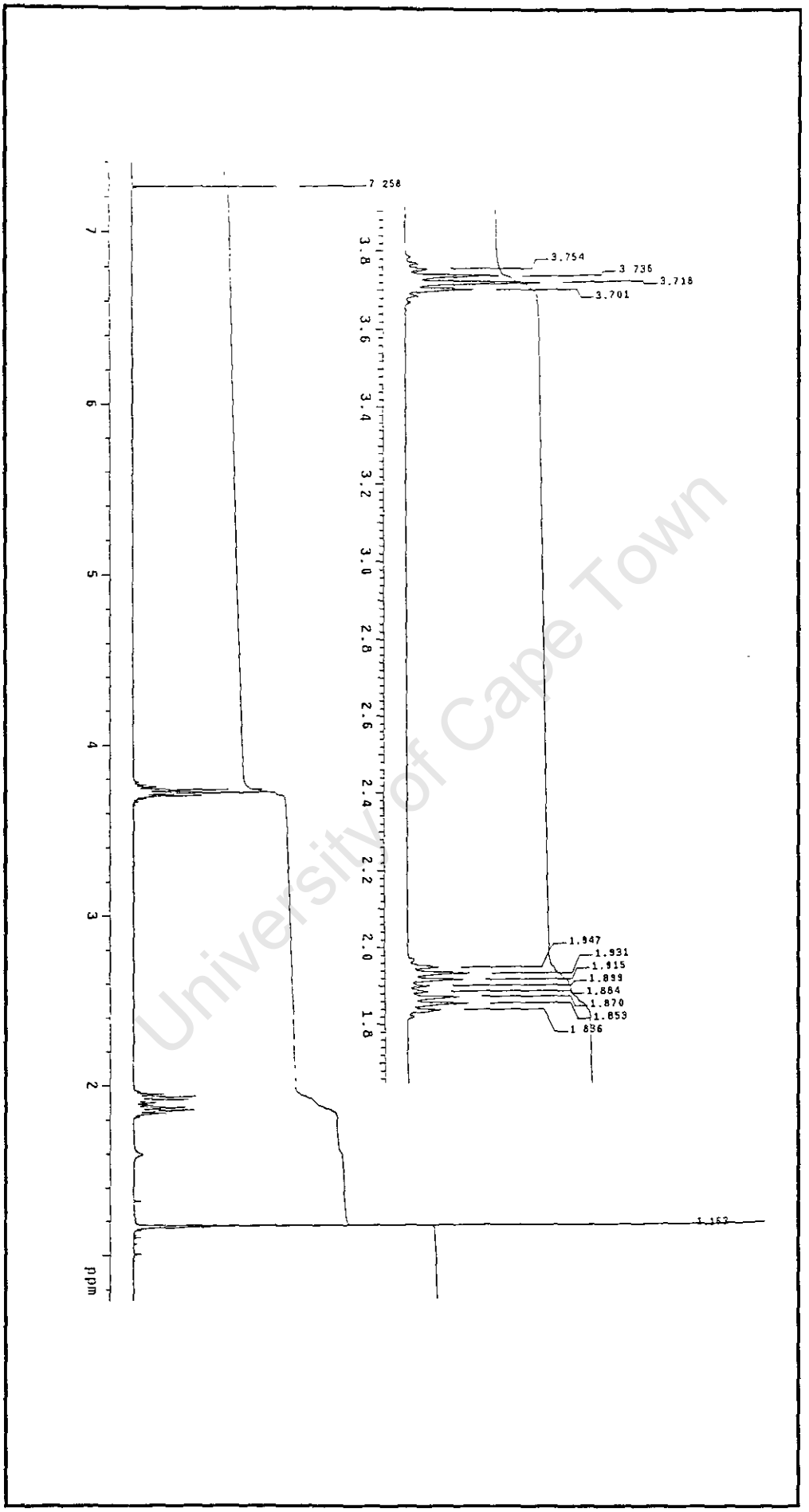

Figure 2.12: A ^{1}H NMR spectrum of *tris*-[*N*-pyrrolidyl-*N'*-(2,2-dimethylpropanoyl)thioureato]rhodium(III).

2.3. X-ray Diffraction

Crystals of *tris*-[*N*-pyrrolidyl-*N'*-(2,2-dimethylpropanoyl)thioureato]rhodium(III) were grown in a $CHCl_3$-CH_3CN (4:1, v/v) mixture. The structure (Figure 2.13) was solved in the space group P1 of the triclinic crystal system using Patterson function in SHELX97 (Sheldrick, 1997) program, which located the rhodium, sulphur and oxygen atoms. The refinement was completed using full matrix least squares refinement on F^2 in SHELX97 program. The final model included anisotropic refinement of all atoms except the carbons in the 2,2-dimethylpropanoyl groups, which exhibited large thermal motion. All hydrogens were placed in geometrically calculated positions and refined with isotropic temperature factors of 120% of their parent atoms. Structure refinement and crystal data are found in Appendix III.

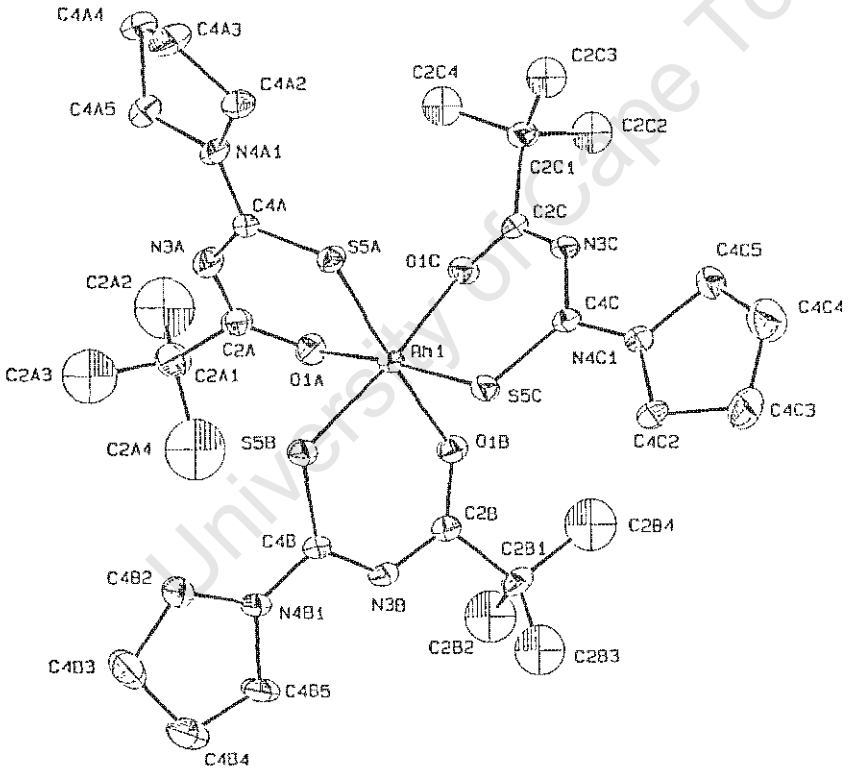

Figure 2.13: The molecular structure of *tris*-[*N*-pyrrolidyl-*N'*-(2,2-dimethylpropanoyl)thioureato]-rhodium(III).

Inspection of the crystal structure reveals that a $CHCl_3$ solvent guest is associated with each complex molecule. The molecular structure of the complex reveals that rhodium atom is in an approximately octahedral environment, with oxygen and sulphur atoms

trans to one another. This results in all three oxygens being on the same face of the molecule and allows for a close contact between each oxygen and the hydrogen of the chloroform guest (C1G-H1G...O1A 3.45(1)Å, 143°; C1G-H1G...O1B 3.60(1)Å, 142°; C1G-H1G...O1C 3.37(1)Å, 140°) (Figure 2.14). No evidence of other interactions involving the chlorine atoms of the chloroform were found.

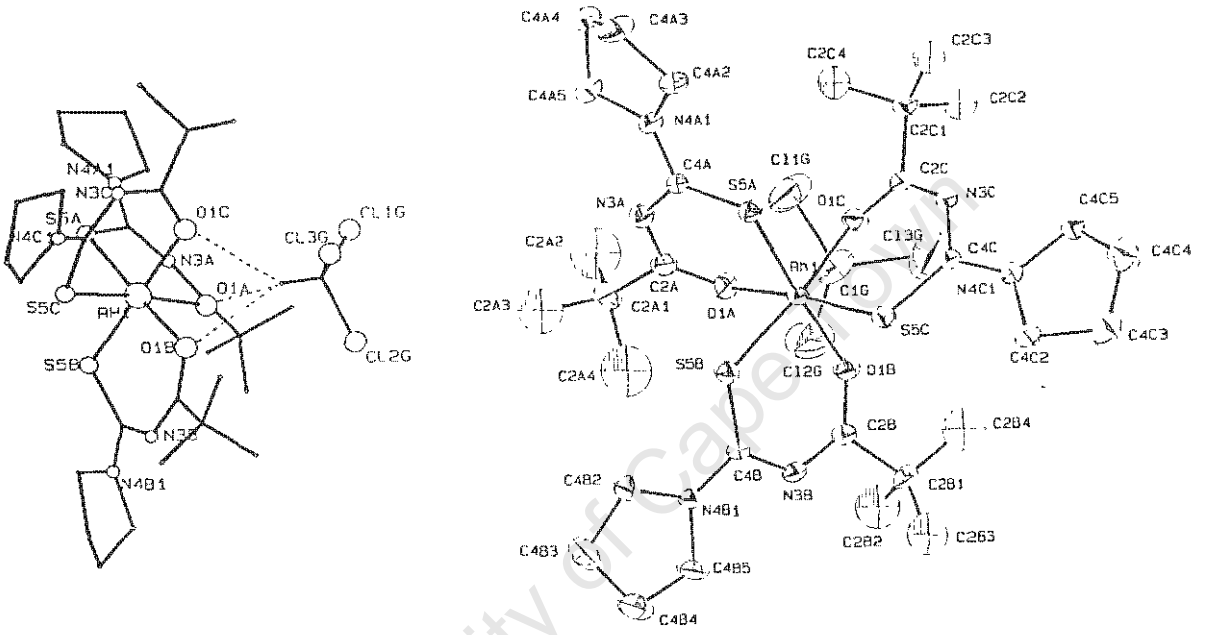

Figure 2.14: Three of oxygens on the same face of the molecule allows for a close contact between each oxygen and the hydrogen of the chloroform guest.

The packing consists of double layers of the coordinated ligands parallel to [100] and [010]. This leaves a channel parallel to [100] and [010] in which the chloroform molecules are packed (Figure 2.15). The presence of a chloroform molecule as part of the complex structure also showed in elemental analysis. The results obtained agree well with the calculated percentages of C, H, N and S, provided the included chloroform molecule is taken into account:

Calculated for $RhC_{30}H_{51}N_6O_3S_3$: C, 48.5; H, 6.9; N, 11.3; and S, 12.9%

Calculated for $RhC_{30}H_{51}N_6O_3S_3.CHCl_3$: C, 43.9; H, 6.2; N, 9.6; and S, 10.9%

Found: C, 45.9; H, 6.6; N, 9.1; and S, 10.6%

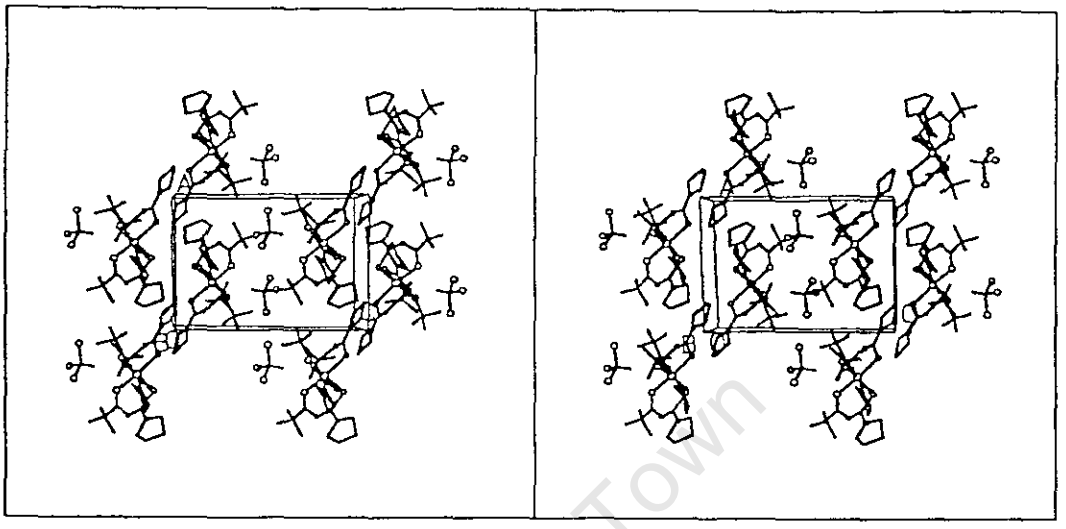

Figure 2.15: The packing consists of double layers of the ligands parrallel to [100] and [010], which leave a channel in which the chloroform molecules are packed.

The average Rh-S and Rh-O bond lengths are 2.2696Å and 2.0597Å, respectively (Appendix V). These Rh-S and Rh-O bond lengths are closely comparable to those found by Bensch and Schuster[64] in the crystal structure analysis of *tris*-[*N,N*-diethyl-*N'*-benzoylthioureato]rhodium(III), where Rh-S bond = 2.284Å and Rh-O bond = 2.033Å in length. The bond angles are also closely comparable as shown in Table 2.5 below.

Table 2.5. Average bond angles of *tris*-[*N*-pyrrolidyl-*N'*-(2,2-dimethylpropanoyl)thioureato]-rhodium(III) ($Rh[L^2\text{-}(S,O)]_3$, in comparison with bond angles of *tris*-[*N,N*-diethyl-*N'*-benzoylthioureato]rhodium(III) ($Rh[L^a\text{-}(S,O)]_3$, in reference 64.

	Bond angles (degrees)	
	$Rh[L^2\text{-}(S,O)]_3$	$Rh[L^a\text{-}(S,O)]_3$
S-Rh-O	95.3(12)	94.2(2)
Rh-S-C_2	104.8(2)	107.7(4)
Rh-O-C_1	124.5(4)	128.6(6)

2.4. UV spectroscopy

2.4.1. Investigation of quantitative complexation by UV spectroscopy

UV spectroscopy was used to investigate the process of complexation using *N*-pyrrolidyl-*N'*-(2,2-dimethylpropanoyl)thiourea and palladium(II). The aim of this study was to confirm quantitative transformation of palladium(II) into *bis*-[*N*-pyrrolidyl-*N'*-(2,2-dimethylpropanoyl)thioureato]palladium(II) complex. In the first part of this investigation, a stoichiometric mixture of *N*-pyrrolidyl-*N'*-(2,2-dimethylpropanoyl)thiourea and palladium(II) (as $PdCl_4^{2-}$) were mixed and scanned by a UV spectrometer. The spectrum of the reaction mixture was compared to the spectrum of a pure, previously synthesised [Pd(L^2-*S,O*)$_2$] complex, at a concentration matched to the expected concentration of the complex formed in the reaction mixture. Shown in Figure 2.16 below, are the overlaid spectra of the pure, previously synthesised [Pd(L^2-*S,O*)$_2$] complex and the reaction mixture.

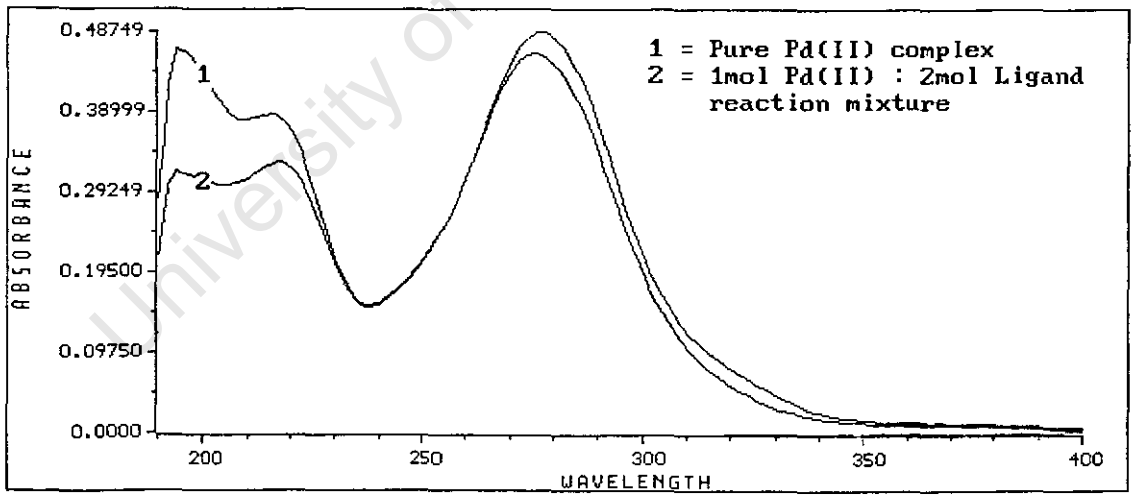

Figure 2.16: The UV spectra of a 1:2, mole Pd(II) to moles *N*-pyrrolidyl-*N'*-(2,2-dimethylpropanoyl)thiourea reaction mixture (2), and a previously synthesised *bis*-[*N*-pyrrolidyl-*N'*-(2,2-dimethylpropanoyl)thioureato]palladium(II) complex (1).

The spectrum of the reaction mixture assumes an identical shape to that of a pure [Pd(L^2-*S,O*)$_2$] complex. The wavelengths of maximum absorbance (276 nm) of the reaction mixture is the same as that of a pure, previously synthesised [Pd(L^2-*S,O*)$_2$] complex. Furthermore, the molar absorption coefficients (ε) obtained are comparable

as shown in Table 2.6 below. This confirms that the [Pd(L^2-*S,O*)$_2$] complex is formed rapidly by mixing $PdCl_4^{2-}$ and HL^2 in solution.

Table 2.6. Molar absorption coefficients of the 1:2 mol Pd(II): mol HL^2 reaction mixture and the pure, previously synthesized [PdL^2-*S,O*)$_2$] complex.

	Complex conc. ($mol.dm^{-3}$)	Absorbance at λ_{max} (or 276 nm)	Molar absorption coefficient (ε) ($dm^{-3}.mol^{-1}.cm^{-1}$)
cis-[Pd(L^2-*S,O*)$_2$]	1.05×10^{-5}	0.48749	46 428
1:2mol, Pd(II):HL^2	1.05×10^{-5}	0.46182	43 983

In the second part of the investigation, concentrations of the complex formed, and that of the ligand were determined according to a spectrophotometric method for the determination of two components with overlapped spectra reported by Blanco *et al*[65]. In this method absorbances of standard solutions of the two mixed components are measured at several wavelengths. A straight line relationship was derived from the Beer-Lambert law for two different compounds [$A_{component1} = (\varepsilon cl)_{component1}$;$A_{component2} = (\varepsilon cl)_{component2}$], from which the concentrations of the components of a mixture can be determined. The straight line relationship is as follows:

$$A_{mix}/A_{comp1(std)} = c_{comp1(mix)}/c_{comp1(std)} + (A_{comp2(std)}/A_{comp1(std)})\ (c_{comp2(mx)}/c_{comp2(std)})$$

where $c_{comp1(mix)}/c_{comp1(std)}$ is the slope and $c_{comp1(mix)}/c_{comp1(std)}$ is the y-intercept.

This graph shown in Figure 2.17, was constructed using data in Table 2.7. The concentration of *bis*[*N*-pyrrolidyl-*N'*-(2,2-dimethylpropanoyl)thioureato]palladium(II) obtained using this method is 1.07×10^{-5} $mol.dm^{-3}$ while that of the ligand is negligibly different from zero (within experimental error, $s_{(n=10)} = 0.24$). The measured concentration of the complex thus agrees very well with the expected concentration (1.05×10^{-5} $mol.dm^{-3}$) that would form if all the palladium in solution is complexed. The conclusion drawn from these results is that *N*-pyrrolidyl-*N'*-(2,2-dimethylpropanoyl)thiourea converts palladium(II) quantitatively and rapidly into the [Pd(L^2-*S,O*)$_2$] complex.

Table 2.7. UV data for simultaneous determination of concentrations of the complex and uncoordinated ligand in the mixture.

Wavelength of Absorption (nm)	A_{HL2}	A_{PdL2}	A_{mix}	A_{mix}/A_{HL2}	A_{PdL2}/A_{HL2}
250	0.09035	0.21158	0.20998	2.32407	2.34178
254	0.11818	0.24368	0.24304	2.05652	2.06194
260	0.18097	0.31082	0 31068	1.71675	1.71752
264	0.23228	0.36964	0.36719	1.58081	1.59136
270	0.29662	0.45073	0.43878	1 47927	1.51955
276	0.31117	0.48749	0 46182	1.48414	1.56664
280	0.28178	0.48039	0.44749	1.58808	1.70484
284	0.22546	0.45107	0.41586	1.84450	2 00067
290	0.12224	0.37070	0 33849	2 76906	3.03256
294	0.06801	0 30460	0 27644	4.06470	4 47875

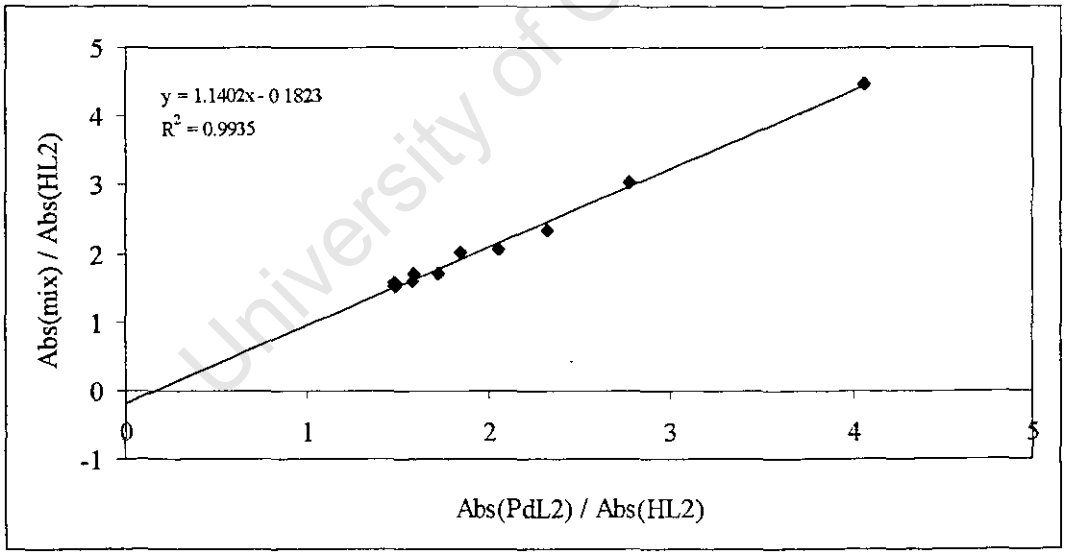

Figure 2.17: The plot of $A_{mix}/A_{HL2(std)}$ *versus* $(A_{PdL2(std)}/A_{HL2(std)})$ for the determination of concentrations of *bis*[*N*-pyrrolidyl-*N'*-(2,2-dimethylpropanoyl)thioureato]palladium(II) and *N*-pyrrolidyl-*N'*-(2,2-dimethylpropanoyl)thiourea in a mixture.

In a similar study using platinum(II), no significant changes were observed in the UV spectrum of the reaction mixture even after the reaction mixture was left to stand for over two weeks. Rhodium(III) was not studied as its reaction is expected to require

extremely long time, or heating as shown in the synthesis of the [Rh(L^2-*S,O*)$_3$] complex in section 2.1.3.

2.4.2. Determination of molar absorption coefficients

The molar absorption coefficients (ε) of all compounds synthesised are given in Table 2.8. These were determined by a graphical method based on the Beer-Lambert law, $\mathbf{A} = \varepsilon c l$, where ε is the molar absorption coefficient, c is the concentration and l is the path length of the absorbing solution. The plot of **A** against c is a straight line that passes through the origin and εl is the slope. The graph, **A** *versus* c, was plotted for each compound, using data obtained from the standard solutions.

Table 2.8. Molar absorption coefficients (ε) of *N,N*-dialkyl-*N'*-(2,2-dimethyl-propanoyl)thioureas and their corresponding Pt(II), Pd(II) and Rh(III) complexes.

Compound	**Wavelength at the apex, λ_{max} (nm)**	**Molar absorption coefficient, ε ($dm^3.mol^{-1}.cm^{-1}$)**
HL^1	276	14 052
cis-[Pd(L^1-*S,O*)$_2$]	276	58 000
cis-[Pt(L^1-*S,O*)$_2$]	254	29 298
HL^2	276	14 711
cis-[Pd(L^2-*S,O*)$_2$]	276	46 900
cis-[Pt(L^2-*S,O*)$_2$]	258	36 871
fac-[Rh(L^2-*S,O*)$_3$]	264	41 309
HL^3	282	14 400
cis-[Pd(L^3-*S,O*)$_2$]	280	60 482
cis-[Pt(L^3-*S,O*)$_2$]	260	31 172
fac-[Rh(L^3-*S,O*)$_3$]	264	42 110

The UV spectra are found in Appendix IX.

2.5. Experimental

2.5.1. Synthesis

Ligands: A 0.02mol of potassium thiocyanate portion was dissolved in 50ml of dry acetone. 0.02mol acyl chloride dissolved in 50ml acetone, was added drop-wise to the solution of potassium thiocyanate. The mixture was heated under refluxed for 30min and allowed to cool to room temperature. 0.02mol of secondary amine solution, also in dry acetone, was added drop-wise and the mixture refluxed for another 30 minutes after which it was allowed to cool to room temperature. The mixture was then transferred into 50ml of water and left to stand in the fumehood overnight. As the acetone evaporated, the product crystallized out in water. In the case where the products formed as oil-like droplets in water the substance could be solidified by repeated agitating and scratching against beaker walls with a glass rod. The product was isolated by filtration and washed with ice-cold water. The products obtained were recrystallized from a 7/3 (v/v) ethanol/water mixture, to yield pure substances.

Pt(II)/Pd(II) complexes: Reaction mixtures of *N,N*-dialkyl-*N'*-acylthiourea and platinum(II) or palladium(II) in 2:1 molar ratio were made in the presence of 4 mole equivalents of sodium acetate. 0.2g *N,N*-dialkyl-*N'*-acylthiourea in 15ml of acetonitrile was mixed with a 10ml solution of sodium acetate (in water). The appropriate mass of K_2PdCl_4 or K_2PtCl_4 was dissolved in 15ml of water and 10ml of acetonitrile was added. The K_2PdCl_4 or K_2PtCl_4 solution was added drop-wise, by means of an addition funnel, to a constantly stirred ligand solution. The reaction mixture was stirred for 2 hours at room temperature. Formation of the complex as a suspended precipitate in solution became evident within 10 minutes.

Rh(III) complexes: A mixture of stoichiometric amounts of sodium acetate, *N*-pyrrolidyl-*N'*-(2,2-dimethylpropanoyl)thiourea or *N*-piperidyl-*N'*-(2,2-dimethyl-propanoyl)thiourea and *tris*-aquo-rhodium(III)-trichloride in 50/50 (%v/v) acetonitrile/water, was heated under reflux at 80°C for 24hrs. The concentration of the reactants was ten times more than the concentration of reactants used in the syntheses of Pt(II) and Pd(II).

In all cases (i.e. Pt, Pd and Rh complex syntheses), exactly 50ml of water was added, and the reaction mixture left to stand overnight in a refrigerator (at 4°C). The precipitates were isolated by centrifugation and decanting off the mother liquor. They were each dried under vacuum and purified by recrystallization in 4/1 (v/v) chloroform/acetonitrile.

Ni(II)/Cu(II) complexes: Similar to the synthesis of platinum(II) and palladium(II) complexes, 200mg of *N,N*-dialkyl-*N'*-acylthiourea was dissolved in 15ml of acetonitrile, mixed with two mole equivalents of CH_3COONa (dissolved in 10ml water), and 100mg Nickel(II) acetate or copper(II) acetate in 15/10, v/v water acetonitrile, was added drop-wise. The reaction was stirred for two hours at room temperature. 50ml of water was added and the reaction was left to stand in the fridge (4°C) overnight. The precipitate was isolated by centrifugation

2.5.2. Characterization

General properties: Melting points were determined on a Reichert-Jung *thermovar* attached to a Dp-4 digital thermometer. Elemental compositions were determined by combustion analysis performed on a Fisons Elemental Analyzer (FEA) model 1108. Experimental yields, calculated as percentage dry mass of recrystallized products obtained (against a theoretical mass), were recorded:

***N,N*-dimethyl-*N'*-(2,2-dimethylpropanoyl)thiourea:** Yield = 83%, mp = 78-81°C; Calculated for $C_8H_{16}N_2OS$: C, 51.0; H, 8.6; N, 14.9; S, 17.0%; Found C, 51.5; H, 9.1; N, 15.2, S, 17.4%; Cream white crystals.

***N*-pyrrolidyl-*N'*-(2,2-dimethylpropanoyl)thiourea:** Yield = 78%, mp = 134-138°C; Calculated for $C_{10}H_{18}N_2OS$: C, 56.0; H , 8.5; N, 13.1, S, 15.0%; Found: C, 55.8, H, 9.2; N, 13.2, S, 14.7%; Cream white crystals.

***N*-piperidyl-*N'*-(2,2-dimethylpropanoyl)thiourea:** Yield = 95%, mp = 86-89°C; Calculated for $C_{11}H_{20}N_2OS$: C, 57.8, H, 8.8; N, 12.3; S, 14.0%; Found: C, 57.9; H, 9.6; N, 12.3; S, 14.6%; white crystals.

***Bis*-[*N,N*-dimethyl-*N'*-(2,2-dimethylpropanoyl)thioureato] palladium(II):** Yield = 100%, mp = 196-198°C, Calculated for $C_{16}H_{30}N_4O_2PdS_2$: C, 40.0; H, 6.3; N, 11.6; and S, 13.3%, Found: C, 40 1; H, 6 4, N, 11 7 and S, 13.4%, Dark orange crystals.

***Bis*-[*N,N*-dimethyl-*N'*-(2,2-dimethylpropanoyl)thioureato]platinum(II):** Yield = 100%, mp = 210-213°C, Calculated for $C_{16}H_{30}N_4O_2PtS_2$: C, 33.7; H, 5.3; N, 9.8; and S, 11.2%, Found: C, 34 0; H, 5.4; N, 9 8; and S, 11 5%, Yellow crystals.

***Bis*-[*N*-pyrrolidyl-*N'*-(2,2-dimethylpropanoyl)thioureato]palladium(II):** Yield = 99%, mp = 212-215°C, Calculated for $C_{20}H_{34}N_4O_2PdS_2$: C, 45.1; H, 6.4; N, 10.5; and S, 12.0%, Found: C, 45.0; H, 6.4; N, 10.3; and S, 11 9%, Dark orange crystals.

***Bis*-[*N*-pyrrolidyl-*N'*-(2,2-dimethylpropanoyl)thioureato]platinum(II):** Yield = 73%, mp = 214-218°C, Calculated for $C_{20}H_{34}N_4O_2PtS_2$: C, 38 6; H, 5.5; N, 9.0; and S, 10.3%, Found: C, 38.5; H, 5.5; N, 9.0; and S, 10.2%, Yellow crystals.

***Bis*-[*N*-pyrrolidyl-*N'*-(2,2-dimethylpropanoyl)thioureato]nickel(II):** Yield = 38%, mp = 206-209°C, Calculated for $C_{20}H_{34}N_4O_2NiS_2$: C, 49.5; H, 7.1; N, 11.5; and S, 13.3%, Found: C, 49.6; H, 6.7; N, 11.5; and S, 12.8%, Purple crystals.

***Bis*-[*N*-pyrrolidyl-*N'*-(2,2-dimethylpropanoyl)thioureato]copper(II):** Yield = 81%, mp = 151-154°C, Calculated for $C_{20}H_{34}N_4O_2CuS_2$: C, 49.0; H, 7.0; N, 11.4; and S, 13.1%, Found: C, 49.3; H, 6.6, N, 11.49, and S, 12.9%, Dark green crystals.

***Tris*-[*N*-pyrrolidyl-*N'*-(2,2-dimethylpropanoyl)thioureato]rhodium(III):** Yield = 75%, mp = 251-254°C, Calculated for $RhC_{30}H_{51}N_6O_3S_3 . CHCl_3$: C, 43.9, H, 6.2; N, 9.6; and S, 10.9%, Found: C, 45.9; H, 6.6; N, 9.1; and S, 10.6%, Orange crystals.

***Bis*-[*N*-piperidyl-*N'*-(2,2-dimethylpropanoyl)thioureato]palladium(II):** Yield = 91%, mp = 192-194°C, Calculated for $C_{22}H_{38}N_4O_2PdS_2$: C, 47.1; H, 6.8; N, 10.0; and S, 11.4%, Found: C, 47.2; H, 6.9; N,10.1; and S, 11.3%, Dark orange crystals.

***Bis*-[*N*-piperidyl-*N'*-(2,2-dimethylpropanoyl)thioureato]platinum(II):** Yield = 78%, mp = 206-210°C, Calculated for $C_{22}H_{38}N_4O_2PtS_2$: C, 40.7; H, 5.9; N, 8.6; and S, 9.9%, Found: C, 40.9; H, 5.9; N, 8.7; and S, 10.0%, Yellow crystals.

***Tris*-[*N*-piperidyl-*N'*-(2,2-dimethylpropanoyl)thioureato]rhodium(III):** Yield = 72%, mp = 210-212°C, Calculated for $RhC_{31}H_{53}N_6O_3S_3$. $CHCl_3$: C, 43.5; H, 6.1; N, 9.8; and S, 11.2%, Found: C, 43.7; H, 6.2; N, 10.0; and S, 11.2%, Orange crystals.

NMR spectroscopy: Fully ^1H de-coupled ^{13}C NMR spectra of the ligands and complexes were recorded at 25°C using a Varian VXR-200 spectrometer at 50.309MHz except for [Rh(L^n-*S,O*)$_3$] complexes which were recorded on Varian Unity-400 at 100MHz. The ^1H NMR spectra were recorded on a Varian VXR-200 at 200.057MHz. For [Rh(L^n-*S,O*)$_3$] complexes, the ^1H NMR spectra were recorded on Unity-400 at 399.951MHz. Approximately 40 mg of sample were dissolved in 2ml of $CDCl_3$. A $CDCl_3$ resonance peak, which occurs at 77.00ppm, was used as a reference relative to which all shifts were measured. A pulse delay of 4s was applied to allow enough relaxation time for non-hydrogen bearing carbons. Good ^{13}C NMR spectra in both cases (50 and 100MHz frequencies), were obtained over an average run time of 16hrs for the complexes, and 30min for the ligands.

X-ray diffraction: Crystals of *tris*-[*N*-pyrrolidyl-*N'*-(2,2-dimethylpropanoyl)-thioureato]rhodium(III) were grown in a $CHCl_3$-CH_3CN (4:1, v/v) mixture. A single crystal (0.3 x 0.35 0.40mm) was mounted on a glass fibre for X-ray data collection on a Nonius CAD4 diffractometer using Mo Kα radiation (λ = 0.7107Å) and the ω-2θ method. The unit cell was refined using angles of reflections in the range $16^\circ \leq \theta \leq 17^\circ$. Reference reflections were monitored periodically for intensity and orientation control. The data were corrected for absorption effects using an empirical ψ scan method[66]. The x-ray data are given in Appendix III - VIII.

UV spectrocopy

i). ***General measurements:*** All UV spectra were recorded between 190 and 450 nm using a Hewlett Packard 8452A photo-diode-array spectrophotometer connected to a

Hewlett Parkard Vectra VL2 (4/33se) computer, equipped with an HP89532A UV-vis software. Characteristic profiles were obtained. Spectra are found in Appendix IX.

ii). ***Preparation of 1:2 metal-ligand reaction mixture for comparison of spectrum with the pure, previously synthesised complex:*** Approximately 1 x 10^{-4} mol.dm^{-3} Pd(II) or Pt(II) stock solutions were prepared by dissolving 0.0033 g and 0.0063 g, K_2PdCl_4 and K_2PtCl_4, respectively, in 100 ml of 80/20 (%v/v) acetonitrile/water mixture. About 2 x 10^{-4} mol.dm^{-3} stock solution of *N*-pyrrolidyl-*N'*-(2,2-dimethylpropanoyl)thiourea was also prepared by dissolving 0.0021 g in 50 ml of 80/20 (%v/v) acetonitrile/water mixture. Exactly 1 ml and 2 ml aliquots of the metal and ligand solutions, respectively, were mixed and made up to 10 ml with 80/20 (%v/v) acetonitrile/water mixture. About 1 x 10^{-4} mol.dm^{-3} solutions of the pure, previously synthesised, metal complexes were also prepared in 80/20 (%v/v) acetonitrile/water mixture. UV spectra of these solutions were recorded.

iii). ***Determination of concentration of complex in the reaction mixture:***
Standard solutions of palladium(II), 0.0036 g K_2PdCl_4/100ml (which represents 1.103 x 10^{-4}mol.dm^{-3} Pd^{2+}), and *N,N*-pyrrolidyl-*N'*-(2,2-dimethylpropanoyl)thiourea i.e. the ligand, 0.0045g/100ml or 2.099 x 10^{-4} mol.dm^{-3} were prepared, using 20/80 (%v/v) water/acetonitrile mixture as a solvent. A reaction mixture, 1mol Pd(II) : 2mol ligand was made by mixing exactly 1ml aliquots in a 10ml volumetric flask and making up to the mark. Standard solutions of the ligand (2.099 x 10^{-5} mol.dm^{-3}) and *bis*[*N*-pyrrolidyl-*N'*-(2,2-dimethylpropanoyl)thioureato]palladium(II) (0.938 x 10^{-5}mol.dm^{-3}), to be used in the determination of concentration in the mixture, were prepared.

iv). ***Preparation of solutions for the determination of molar absorption cofficients (ε):*** Approximately 1 x 10^{-4} mol.dm^{-3} solutions were prepared, using a spectroscopic grade acetonitrile as a solvent. A series of standards of each compound were made by dilutions of the concentrated solution. UV spectra of these solutions were recorded (Appendix IX).

3.

Reversed Phase-High Performance Liquid Chromatography (RP-HPLC) of complexes

3.1. Principles of operation

The basic components of a typical high performance liquid chromatograph (HPLC) are shown in Figure 3.1. The mobile phase is pumped through the chromatographic system by a binary reciprocating pump which produces a constant, pulse-free flow. The components are connected to each other by steel tubing to contain high pressures, usually above 1000psi. Samples are introduced into the system by means of a fixed loop at the injection port shown schematically in figure 3.2. Loops of various sizes (5, 10 or 20μl) exist. The inlet and outlet of the sample loop are joined by a three-way valve, which can be switched to loading and injecting positions (Figure 3.2*a* and *b*). When switched to the injecting position (Figure 3.2*b*), the loop is on line and the sample is carried by the flowing stream of the mobile phase to the column.

The analytical column is a tubular encasing of stainless steel, packed densely with spherical or irregularly-shaped but uniform size micro-particles, called the stationary phase. Typical analytical column particle sizes range from 3 to 10μm in diameter. Columns that are packed with finer particles, give narrower, sharper peaks. Various materials namely silica, alumina (classified as ceramic substrates), polystyrene and methacrylate (classified as polymeric substrates), are used as stationary phases. A major advantage of ceramic packings over polymeric ones is that they are highly rigid and do not swell in any solvent while polymeric packings do not have the same rigidity and give rise to high back-pressures when certain solvents, which can penetrate the particle, are used as mobile phases.

The separation properties of stationary phase materials can sometimes be modified chemically by attaching a non-polar molecule. The molecules are covalently bonded to the stationary phase. A variety of surface chemistries such as ion-exchange, adsorption and partition chromatography can thus be achieved. Alumina, unlike silica and polymeric substrates, does not have easily derivatized functional groups and is not a very stable stationary phase when modified.

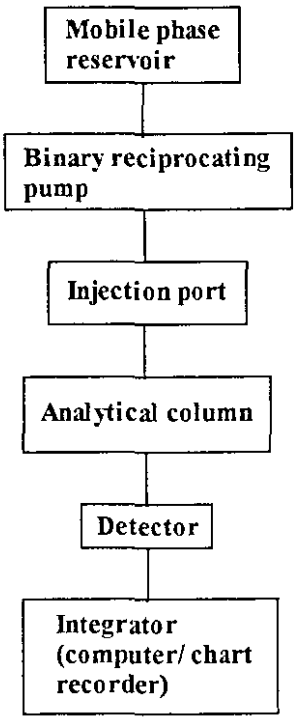

Figure 3.1: A block diagram of HPLC showing the basic components.

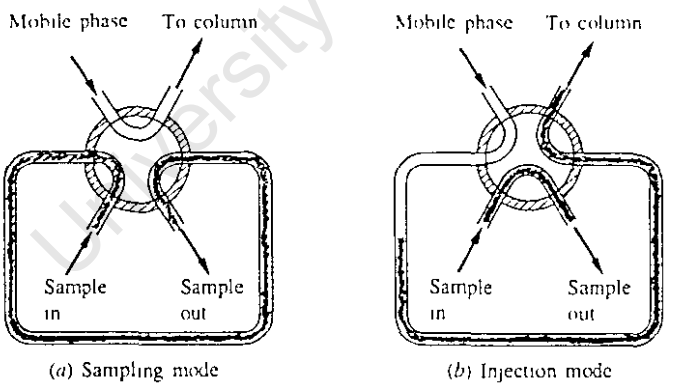

Figure 3.2: A diagram of the injection loop.

Various types of detectors based on the principles of refractive index, fluorescence and electrochemical sensing can be used as detectors in HPLC. Mass spectrometers can also be used as detectors in HPLC, as in various other analytical instruments. The resultant hybrid instrument, LC-MS (for liquid chromatography-mass spectrometry), represents a form of cutting edge technology in modern analytical chromatography. Individual peaks in a chromatogram can be identified and compounds of interest

distinguished from impurities. LC-MS is, therefore, very useful in qualitative analyses but requires specially trained operators. Unfortunately the cost of LC-MS is high.

The most prominent type of detector in many HPLC applications, which is suitable for a wide range of compounds, is a UV/visible detector. The latest model is a photo-diode-array UV detector which allows simultaneous collection of chromatograms at different wavelengths during a single run. Chromatograms of all compounds acquired at their respective wavelengths of maximum UV/visible light absorption can be displayed immediately after separation of the mixture. Moreover, the full UV/visible spectrum of each individual chromatographic peak can be displayed, compared with standards for identification purposes, or used to check the "chromatographic purity" of a peak. These capabilities are particularly desirable in trace analysis with complex mixtures.

Early HPLC separations were based on the principles of partition chromatography in the same way as thin layer and open column chromatography. The name "normal phase HPLC" became more appropriate as other mechanisms of separation such as "reversed phase HPLC" were discovered. The stationary phase material making up the column for normal phase HPLC is polar while the mobile phase is non-polar. The more polar components of a sample are attracted more strongly to the polar stationary phase and eluted at a slower rate than the less polar (or non-polar) components, with the result that the least polar compound is eluted first and the most polar last. The most common stationary phase material used to make up "normal phase" columns is silica gel which, in addition to being polar, is acidic due to the available proton on its hydroxyl groups.

It was later discovered that polar solvents such as water-methanol mixtures could be used for elution in HPLC, provided the stationary phase material was relatively non-polar. Silica was then made non-polar by chemically bonding long chain, saturated hydrocarbons to the silica particle surface[43]. This development led to "reversed phase HPLC" which has shown remarkable versatility.

Various lengths of modifying hydrocarbons exist, for example C_4 and C_8, but the most popular and practical hydrocarbon chain is 18 carbons long, and the columns in which

these were used are referred to as ODS for octadecyl silane or C18 columns. Components of the sample partition into the non-polar, hydrocarbon-modified stationary phase. The extent of the partition varies from one component to another depending on their respective polarities. The more polar components show a small tendency to partition into the non-polar stationary phase and are quickly swept through the column, while relatively non-polar components interact strongly and are more strongly retained by the stationary phase. Retention is therefore shortest for the most polar component and always longer for relatively non-polar (or hydrophobic) components as shown in Figure 3.3.

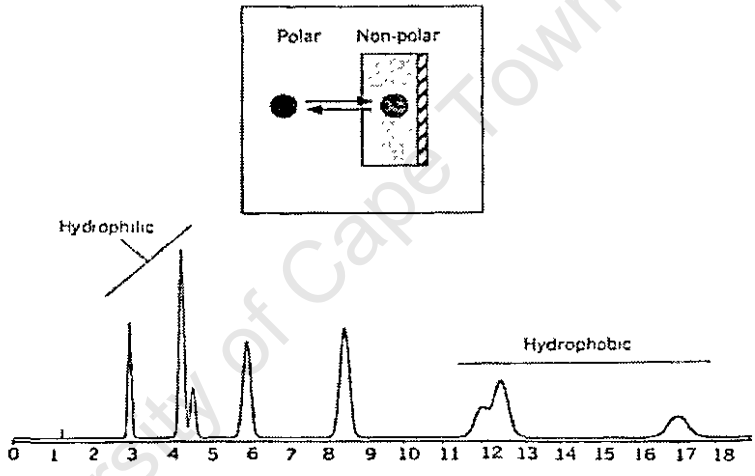

Figure 3.3: A schematic representation of partitioning of a sample molecule between polar mobile phase and non-polar stationary phase and the resultant order of elution in RP-HPLC.

For those compounds which are basic or acidic, the pH of the mobile phase plays a role in determining their retention. When the pH is varied over a wide range, retention exhibits a characteristic S-shaped plot (Figure 3.4). The mid-point of this plot corresponds to the pK_a value of the compound[42]. In other words, the compound is in equilibrium between protonated and unprotonated states. It is reported that the chromatographic peaks obtained with the mobile phase pH equal to pK_a, tend to be broad because two species, the protonated and unprotonated compounds, co-elute[43]. Almost all of the pH-related change in retention is reported to occur for pH values within ±1.5 units of the pKa value and outside this range, the compound is either protonated or unprotonated[42]. As a general rule, therefore, the appropriate mobile

phase pH for basic compounds should be equal to or greater than pK_a + 1.5, and less than or equal to pK_a - 1.5 for acidic compounds.

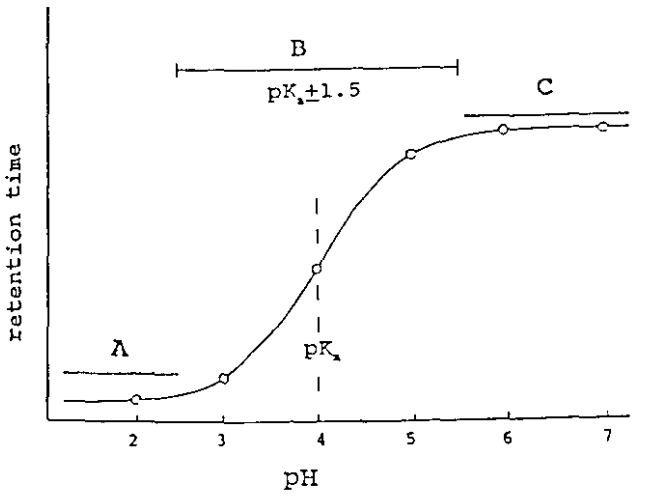

Figure 3.4: Dependence of retention on pH for a basic compound with $pK_a = 4.0$[42].

The chromatographic performance of a reversed-phase silica column can be affected by several factors, the dominant of which is the activity of residual silanol groups. These arise from poor or incomplete functionalisation of the silica by the hydrocarbons. A high level of silanol activity results in tailing peaks for basic or polar compounds, which is due to their tendency to form hydrogen bonds and/or due to dipole-dipole interactions. Silanol activity is usually prevented by "end-capping" where the modified silica packing is reacted with a silanization reagent, usually trimethylchlorosilane, thereby converting residual silanols to trimethylsilyl groups (Figure 3.5).

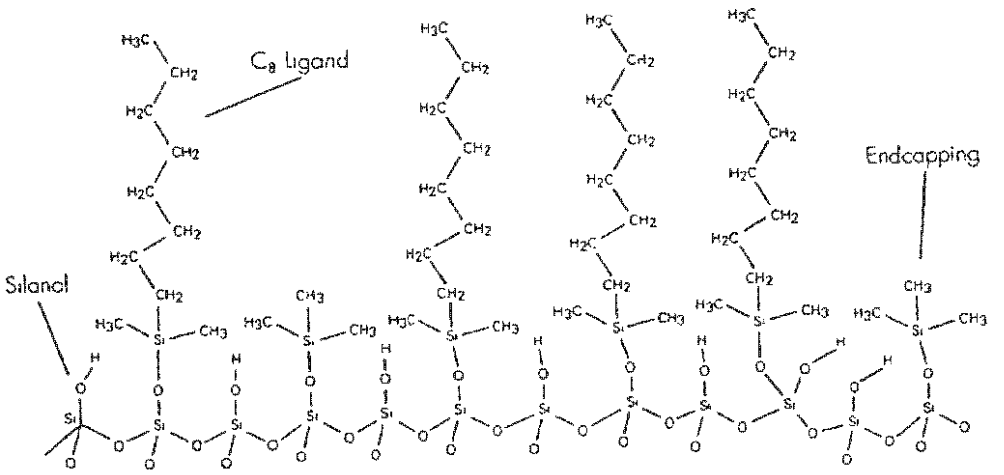

Figure 3.5: The surface of a typical reversed-phase stationary phase; a C8-modified silica.

Fully end-capped bonded stationary phases are indispensable for the chromatography of basic analytes as these are most prone to protonation. Non end-capped stationary phases can, on the other hand, be used with advantage in many other applications to obtain a different selectivity.

3.2. Chromatography of metal complexes

A survey of literature, introduced in chapter 1, shows that among other techniques based on separation, reversed phase HPLC is well suited to analysis of metal complexes. The survey further shows that metal chelates i.e. complexes in which the ligands are bound to the metal center by two or more binding sites, are kinetically stable and well suited to HPLC. It has also emerged that ligands with more than one binding sites (also referred to as *bidentate, tridentate,* and so on) tend to be selective for certain metal ions[34]. One such class of ligands is exemplified by *N,N*-dialkyl-*N'*-acylthioureas. These ligands have been found to be selective to platinum group metals[5,6,55] in acid solutions.

N,N-dialkyl-*N'*-acylthioureas form uncharged, stable complexes with platinum(II), palladium(II) and rhodium(III) as has been shown in chapter 2. Previous reports of

chromatographic separation of the acylthiourea complexes of platinum(II), palladium(II), rhodium(III) include those by Schuster and Unterreitmaier[53,54] and Matoetoe[57]. These separations were based on normal phase chromatography, and although the complexes migrate and separate well on TLC with chloroform-methanol mobile phases, severely broad peaks were obtained in normal phase HPLC using a silica column[57]. Strong interactions with silica, the stationary phase, which lead to slow decomposition reactions were cited as possible causes of broadening.

Considering that metal ions are generally found in aqueous media, and that acylthiourea complexes of platinum group metals are prone to protonation by silanols and thus may undergo strong interactions with silica when it is not chemically modified, we have decided to study the separation of these complexes based on reversed phase chromatography.

3.2.1. Choice of a suitable ligand

The acylthiourea ligands of preference were those whose platinum(II), palladium(II) and rhodium(III) complexes would be soluble in water or water-miscible organic solvents such as methanol and acetonitrile. These ligands would presumably show some water solubility themselves. The *N,N*-dialkyl-*N'*-(2,2-dimethylpropanoyl)-thioureas which we found to be more water soluble than the *N,N*-dialkyl-*N'*-benzoylthioureas including *N,N*-di(2-hydroxyethyl)-*N'*-benzoylthiourea, were thus chosen. We decided to study three derivatives of *N,N*-dialkyl-*N'*-(2,2-dimethylpropanoyl)thiourea, namely *N,N*-dimethyl-*N'*-(2,2-dimethylpropanoyl)-thiourea (HL^1), *N*-pyrrolidyl-*N'*-(2,2-dimethylpropanoyl)thiourea (HL^2) and *N*-piperidyl-*N'*-(2,2-dimethylpropanoyl)thiourea (HL^3). These compounds were also easy to prepare. Chemical structures are shown in Table 2 1.

Standard solutions of the palladium complexes of the three ligands (HL^1, HL^2 and HL^3) mentioned above were injected onto the HPLC column with conditions kept the same, so that retention times could be compared (Table 3.1) Although, *bis*[*N,N*-dimethyl-*N'*-(2,2-dimethylpropanoyl)thioureato]palladium(II) [$Pd(L^1\text{-}S,O)_2$], has the shortest retention time, complexation of *N,N*-dimethyl-*N'*-(2,2-dimethylpropanoyl)thiourea (HL^1) with rhodium(III) is incomplete and leads to a mixture of compounds. This condition is not ideal for the analytical determination of

rhodium(III). The application of *N,N*-dimethyl-*N'*-(2,2-dimethylpropanoyl)thiourea (HL^1) as a complexing agent for the mixture of platinum(II), palladium(II) and rhodium(III) was therefore not pursued further.

Retention time is longest for *bis*-[*N*-piperidyl-*N'*-(2,2-dimethylpropanoyl)thioureato]-palladium(II) [$Pd(L^3\text{-}S,O)_2$], but relatively shorter for *bis*-[*N*-pyrrolidyl-*N'*-(2,2-dimethylpropanoyl)thioureato]palladium(II) [$Pd(L^2\text{-}S,O)_2$]. It was on the basis of relative ease of preparation of complexes of PGMs and the length of retention times and symmetry and sharpness of the peaks that *N*-pyrrolidyl-*N'*-(2,2-dimethylpropanoyl)thiourea (HL^2) was found the most suitable complexing agent.

Table 3.1. Retention of various *bis*-[*N,N*-dialkyl-*N'*-acylthioureato]palladium(II) on RP-HPLC. Column = LUNA C18(2) 5 µm 150 mm x 4.6 mm, Mobile phase 90/10 (%v/v) CH_3CN/0.1 mol.dm^{-3} Acetate buffer (pH = 6.04), Flow rate = 0.6 ml.min^{-1}, Detection = UV at λ_{max}

Complex	Ret. time (min)	Detection λ (nm)
$[Pd(L^1\text{-}S,O)_2]$	12.49	276
$[Pd(L^2\text{-}S,O)_2]$	22.41	276
$[Pd(L^3\text{-}S,O)_2]$	31.36	280

3.2.2. Column efficiency

The efficiency of a column is greatest when conditions of the system are such that the number of theoretical plates (N) is the maximum and the height equivalent of a theoretical plate (H) is the minimum. This theory, originally developed by Martin and Synge[67], is expressed by the following relationship:

$$N = L / H$$

where L is the length of the column (packing).

H is, fundamentally, the number of equilibrations that occur in a given length of the column and is influenced mainly by the flow rate of the mobile phase. Thus, the flow rate at which the performance of the column is an optimum, by measurement of the parameters mentioned above, was determined by plotting **N** against **Flow rate** (Figure 3.6) obtained from the runs of *N,N*-dimethyl-*N'*-(2,2-dimethylpropanoyl)thiourea

complexes of platinum(II) and palladium(II) at varied flow rates (Table 3.2). This exercise, usually described as van Deemter plot, compensates for diffusion and extra-column effects which may cause band spreading (or peak broadening).

Table 3.2. Determination of the optimum flow rate for the *N,N*-dimethyl-*N'*-(2,2-dimethylpropanoyl)thiourea complexes of platinum(II) and palladium(II). Column = LUNA C18(2), 5µm, 150 mm x 4.6 mm. Mobile phase = 90/10 (%v/v), Acetonitrile / 0.1 mol.dm^{-3} Acetate buffer (pH=6). Detection = UV at 254 nm. $N = 2\pi(t_R h/A)^2$ and H = L/N.

	Flow rate (ml/min.)	Retention time, t_R. (min.)	Peak Area. A. (uV.sec.)	(mV.min.)	Peak height (mV)	No of plates, N.	Plate height, H. (mm)
Pt	0.2	50.51	6369.3	382.158	67.1	494	0.3
Pd		59.28	47773.9	2866.43	397.2	424	0.35
Pt	0.4	25.6	8809.9	528.594	194.2	556	0.27
Pd		29.96	33595.9	2015 75	564.5	442	0 34
Pt	0.6	17.33	8357.3	501.438	272	555	0.27
Pd		20.2	23458.4	1407.5	597.3	462	0.32
Pt	0.8	12.7	6470	388 2	285 3	547	0 27
Pd		14.76	17581.4	1054 88	556 3	381	0.39
Pt	1	9.95	5412.3	324.738	294.2	511	0.29
Pd		11.5	14059.9	843 594	502 9	295	0.51
Pt	1.2	8.18	4697.4	281.82	299.6	475	0.32
Pd		9.4	11820.7	709.242	409 8	185	0.81
Pt	1.4	6.9	4096.8	245.808	301.4	450	0.33
Pd		7.87	10121.1	607.266	351.7	131	1.15
Pt	1.6	6	3573.9	214 434	291.4	418	0.36
Pd		6.8	8835.3	530.118	290 1	87	1.72

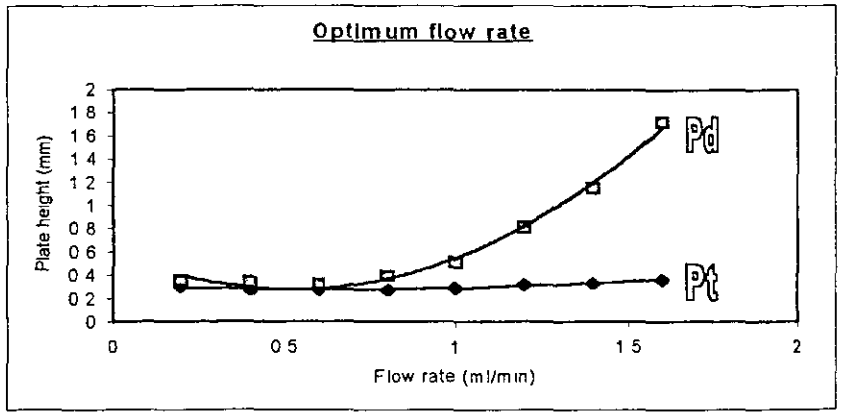

Figure 3.6: van Deemter curves of Pt and Pd complexes on HPLC. Optimum flow rate = 0.6 ml.min^{-1}.

3.2.3. Shelf-life of complexes in solution.

Three separate 100ppm standard solutions of *N,N*-dimethyl-*N'*-(2,2-dimethylpropanoyl)thiourea complexes of platinum(II) and palladium(II) were made in acetonitrile and analysed by HPLC immediately after preparation, after 30 minutes, and after 1, 2, 6, and 24 hours of standing. An additional peak, eluting one minute before the *bis*-[*N,N*-dimethyl-*N'*-(2,2-dimethylpropanoyl)thioureato]platinum(II) peak appeared in a chromatogram. Seemingly, this additional peak grows over time as shown in figure 3.7. The peak area of *bis*-[*N,N*-dimethyl-*N'*-(2,2-dimethylpropanoyl)thioureato]platinum(II) does not seem to decrease significantly. However, in a later time dependence study of the analogue i.e. *bis*-[*N,N*-dimethyl-*N'*-(2,2-pyrrolidylpropanoyl)thioureato]platinum(II) – see section 3.4.1, a gentle decrease in peak area over time was observed which suggests that the additional peak forms at the expense of the major peak.

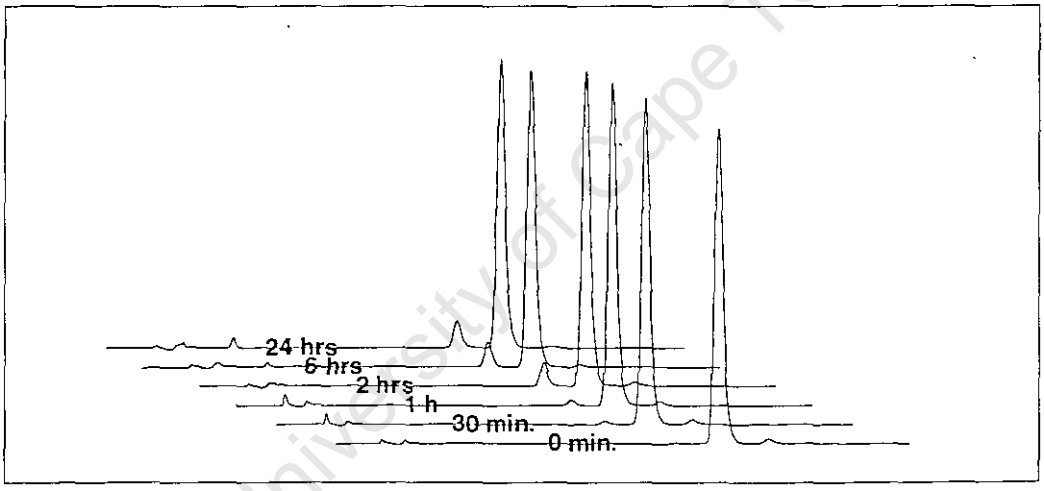

Figure 3.7: The chromatograms of *bis*-[*N,N*-dimethyl-*N'*-(2,2-dimethylpropanoyl)thioureato]-platinum(II) showing the appearance of an additional peak over time. Column = LUNA C18(2) 5 µm 150 mm x 4.6 mm, Mobile phase 90/10 (%v/v) CH_3CN/0.1 $mol.dm^{-3}$ Acetate buffer (pH = 6), Flow rate = 1.0 $ml.min^{-1}$, Detection = UV at 258nm.

No additional peak was detected in a similar study of *bis*-[*N,N*-dimethyl-*N'*-(2,2-dimethylpropanoyl)thioureato]palladium(II) and *tris*-[*N*-pyrrolidyl-*N'*-(2,2-dimethylpropanoyl)thioureato]rhodium(II) complexes.

In order to elucidate the structure of the additional compound observed in a 24 hour-old standard solution of *bis*-[*N,N*-dimethyl-*N'*-(2,2-dimethylpropanoyl)thioureato]-platinum(II) complex, this solution was analysed by high performance liquid chromatography-electrospray mass spectrometry (HPLC-ESMS). In electrospray

mass spectrometry (ESMS), the sample which is converted into a gas by high vacuum together with heating, is bombarded with an electron beam whereby the electrons of the sample molecules are ejected leading to fragmentation into ionic species. Structural determinations of sample molecules are usually facilitated by comparing the mass spectrum of the sample with thousands of spectra of known compounds in electronic databases. When ESMS is interfaced with an HPLC instrument, unknown peaks are individually analyzed as they come out of the analytical column and identified. The mass spectra of the additional, unknown peak and that of the *bis*-[*N,N*-dimethyl-*N'*-(2,2-dimethylpropanoyl)thioureato]platinum(II) peak are shown in Figure 3.8, top and bottom, respectively.

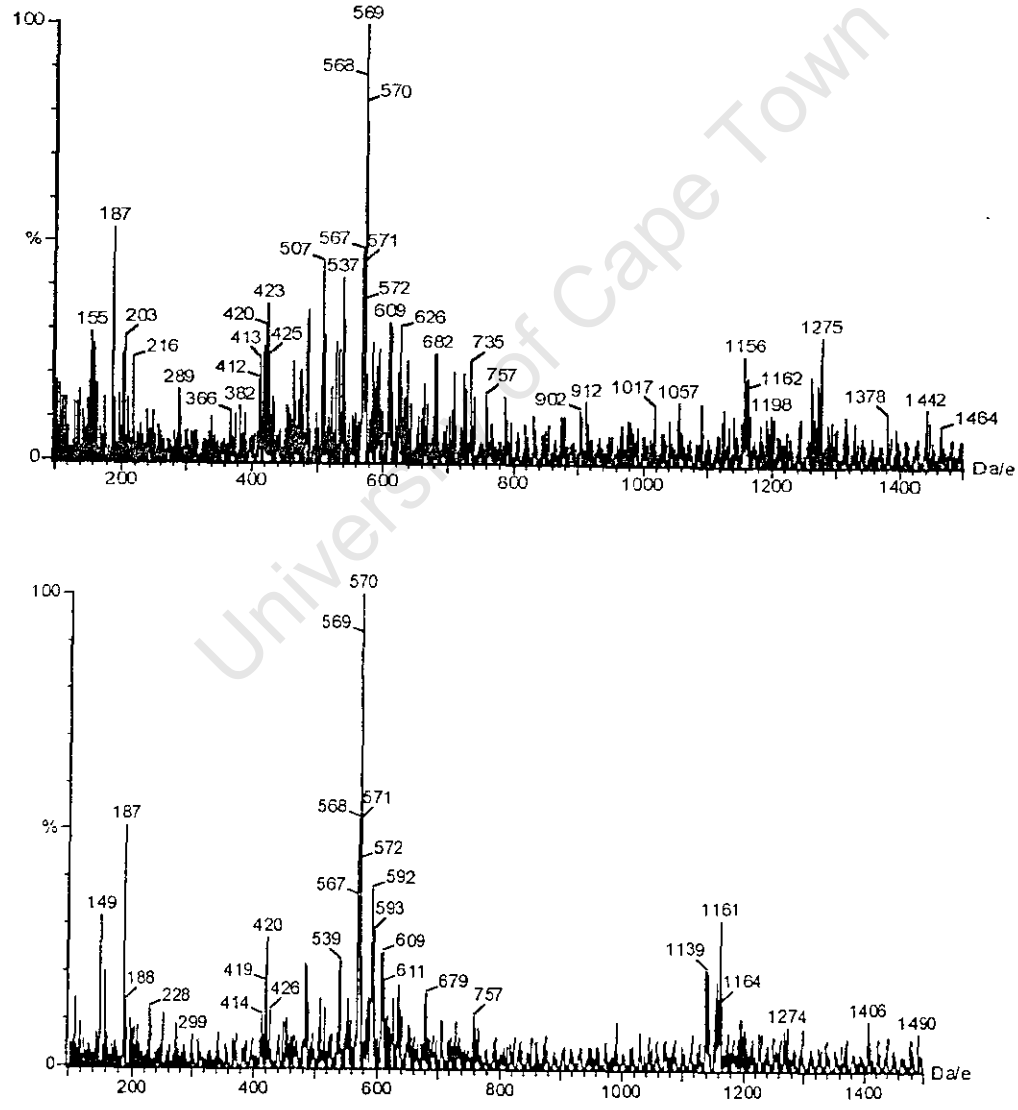

Figure 3.8: ESMS spectra of the unknown peak (top) and the *bis*-[*N*-pyrrolidyl-*N'*-(2,2-dimethylpropanoyl)thioureato]platinum(II) peak (bottom).

The parent ion of the unknown compound has the *m/z* ratio of 569, which agrees well with the calculated molar mass, 569.7g.mol^{-1}, of *bis*-[*N,N*-dimethyl-*N'*-(2,2-dimethylpropanoyl)thioureato]platinum(II). Although it is difficult to assign all the ion fragments, the pattern of ionization of this unknown compound and *bis*-[*N,N*-dimethyl-*N'*-(2,2-dimethylpropanoyl)thioureato]platinum(II), suggests close similarities. Our unconfirmed speculation is that the additional compound is the *trans* isomer, which apparently forms on allowing the complex solutions to stand for prolonged periods.

The additional peak was also observed in the solution of *bis*-[*N*-pyrrolidyl-*N'*-(2,2-dimethylpropanoyl)thioureato]platinum(II) complex.

3.2.4. Stability of complexes towards change in mobile phase pH

Experiments where pH of the mobile phase was varied, showed that platinum(II), palladium(II) and rhodium(III) complexes do not remain stable at acidic conditions. This can be seen from the splitting and severe deformation of chromatographic peaks at pH < 4 (Figure 3.9).

To suggest a possible explanation to this observation, we refer to the S-shaped plot of **retention** *versus* **pH** reported by Snyder *et al*[42] which we discussed in section 3.1. It is possible that the mobile phase pH, 3.4, lies within the ± 1.5 range of the protonation constants of the complexes. At any point in this range, it is reported that broad peaks are obtained since the protonated and unprotonated species co-elute[43].

The mobile phase pH of 6, is presumably outside the **protonation constant ± 1.5** range, since 3.4 + 1.5 = 4.9. At mobile phase pH of 6, sharp, symmetrical peaks were obtained and this was found to be a suitable mobile phase pH to work at.

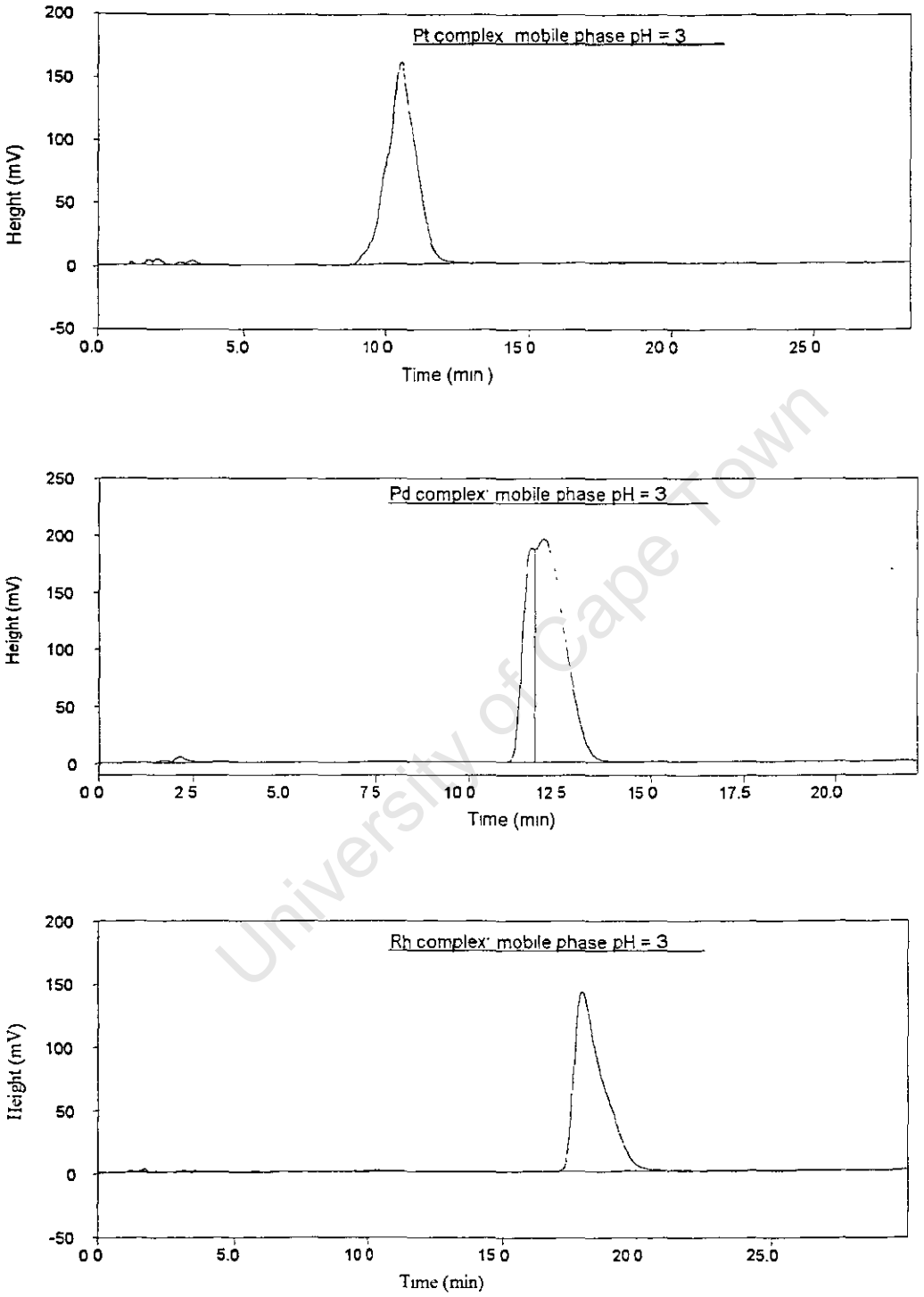

Figure 3.9: Evidence of decomposition of the complexes when acidic buffers are used. Column = LUNA C18(2) 5 µm 150 mm x 4.6 mm, Mobile phase 90/10 (%v/v) CH_3CN/0.1 mol.dm^{-3} Acetate buffer (pH = 3.4), Flow rate = 1.0 ml.min^{-1}, Detection = UV at 254nm.

3.2.5. Chromatography of N-pyrrolidyl-N'-(2,2-dimethylpropanoyl)thiourea complexes of nickel(II) and copper(II).

The *N*-pyrrolidyl-*N'*-(2,2-dimethylpropanoyl)thiourea complexes of nickel(II) and copper(II) showed signs of dissociation in the chromatographic column (Figures 3.10 and 3.11). It is possible that the $[Cu(L^2\text{-}S,O)_2]$ and $[Ni(L^2\text{-}S,O)_2]$ complexes are not stable in the mobile phase at these conditions and disproportionate into other species. From the shape of the peaks shown in Figures 3.10 and 3.11, it seems that these complexes do not pass through the column as well defined bands of single species. From the point of injection, the molecules simply diffuse through the stationary phase as they are not strongly retained.

It is most likely that the metals form strong, irreversible electrostatic bonds with silica, at the residual silanol sites during interaction of the complex molecules with the stationary phase. As a consequence, the separation properties of the column are compromised. Separation of other ordinary compounds could not be achieved any longer using this affected column. Successful analysis of PGM samples then, would require that the formation of base metal complexes be prevented by careful sample preparation. This could be achieved by selective extraction of PGMs from various transition metals with which they are associated, based on the approach of Schuster and Unterreitmaier[53,54]. Fully end-capped analytical columns could also be used with advantage in this regard.

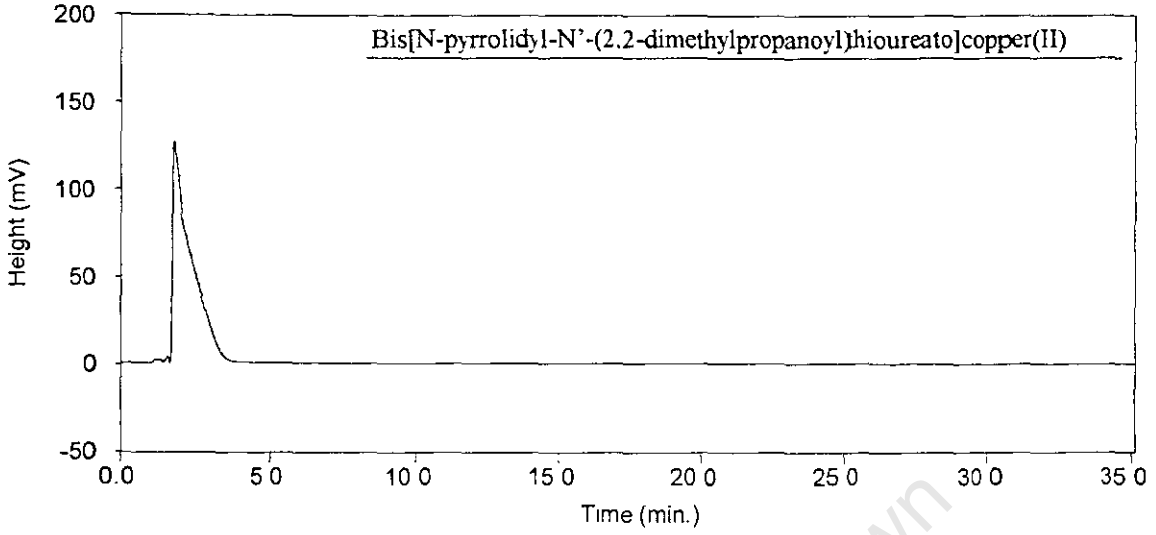

Figure 3.10: A chromatogram of $[Cu(L^2\text{-}S,O)_2]$ complex. . Column = Spherisorb C18, 5 µm, 150 mm x 4.6 mm. Mobile phase = 90/10 (%v/v) CH_3CN / 0.1 mol dm^{-3} Acetate buffer (pH = 6.04). Flow rate = 1.0 ml.min^{-1}. Detection = UV at 254 nm.

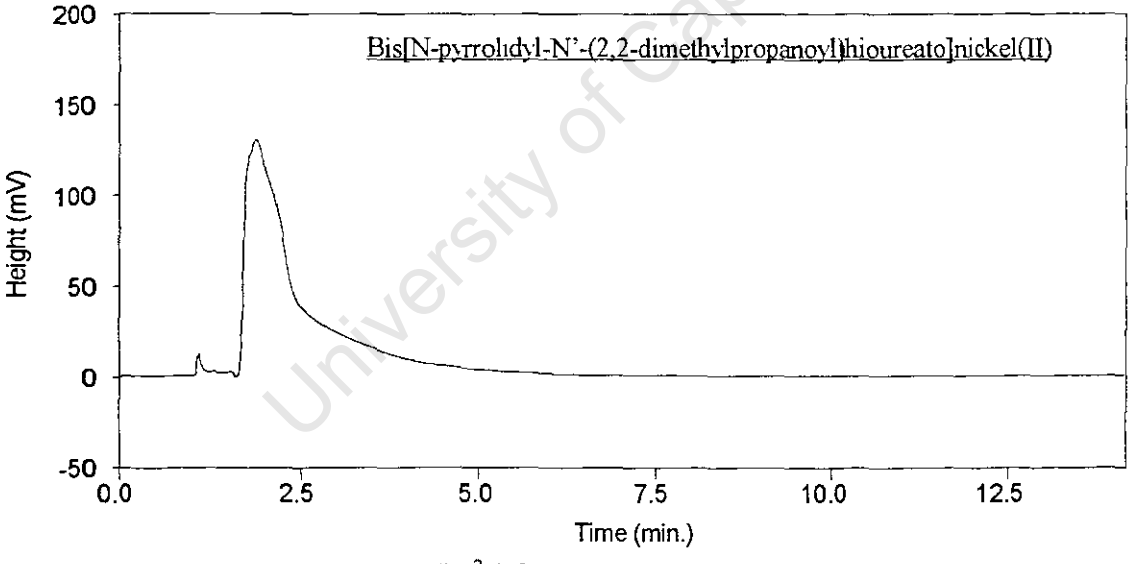

Figure 3.11: A chromatograms of $[Ni(L^2\text{-}S,O)_2]$ complex. . Column = Spherisorb C18, 5 µm, 150 mm x 4.6 mm. Mobile phase = 90/10 (%v/v) CH_3CN / 0.1 mol.dm^{-3} Acetate buffer (pH = 6.04). Flow rate = 1.0 ml.min^{-1}. Detection = UV at 254 nm.

3.2.6. Analytical separation of platinum(II), palladium(II) and rhodium(III) complexes

In the preliminary experiments carried out to obtain analytical separation, a standard non-end-capped, 150 mm long C18 column supplied with the Spectra-Series HPLC

system, was used (Figure 3.12). Tailing was observed in all three, platinum(II), palladium(II) and rhodium(III) complex peaks. Resolution between platinum- and palladium-complex peaks is compromised due to this tailing. Using a buffered mobile phase (pH = 6.04) resulted in some small improvements in peak shape but did not prevent tailing. We thus regarded this observation as evidence of residual silanol activity.

An end-capped column was subsequently purchased. Symmetrical, sharp peaks were obtained as shown later in this chapter.

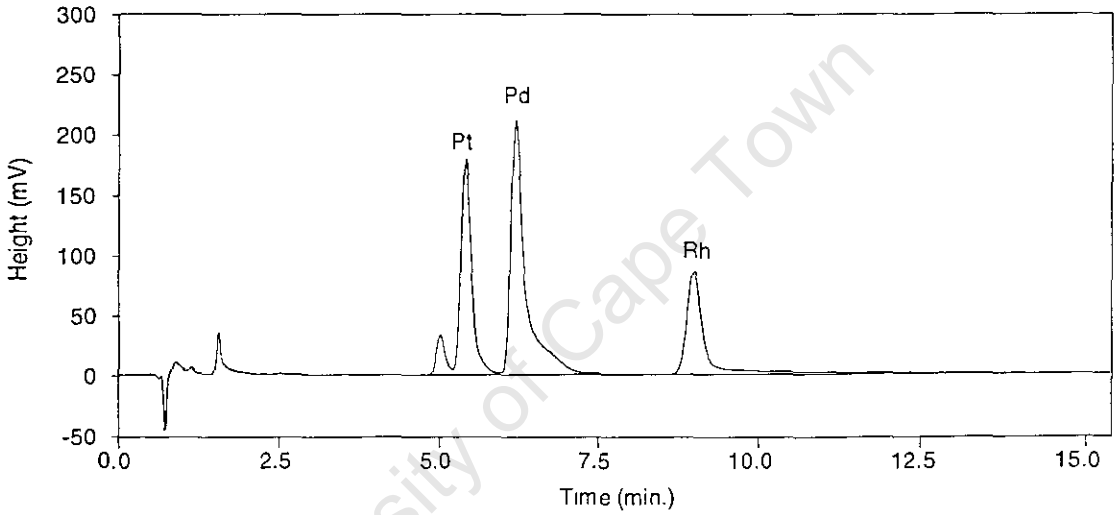

Figure 3.12: Tailing of peaks due to residual silanol activity. Column = Spherisorb C18, 5 µm, 150 mm x 4.6 mm. Mobile phase = 90/10 (%v/v) CH_3CN / 0.1 mol.dm^{-3} Acetate buffer (pH = 6.04). Flow rate = 1.0 ml.min^{-1}. Detection = UV at 254 nm.

A good baseline separation of a mixture of platinum(II), palladium(II) and rhodium(III) complexes was obtained on a high performance liquid chromatograph set up as described below:

Instrument:	A Spectra-Series HPLC system comprised of a P200 pump, a manual injector, a UV150 detector, and a Fujitech pentium computer using Delta 5.0 chromatography data system integration software.
Column:	LUNA ODS (C18(2)) 5 µm, 150 mm x 4.6 mm.
Mobile phase:	90/10 (%v/v) Acetonitrile / 0.1 mol.dm^{-3} Acetate buffer(pH = 6.04)
Flow rate:	1.0 ml.min^{-1}
Injection vol.:	20 µl
Detection:	UV at 254 nm

A chromatogram of a standard mixture of the three complexes is shown in Figure 3.13 and the integration data is given in Table 3.3.

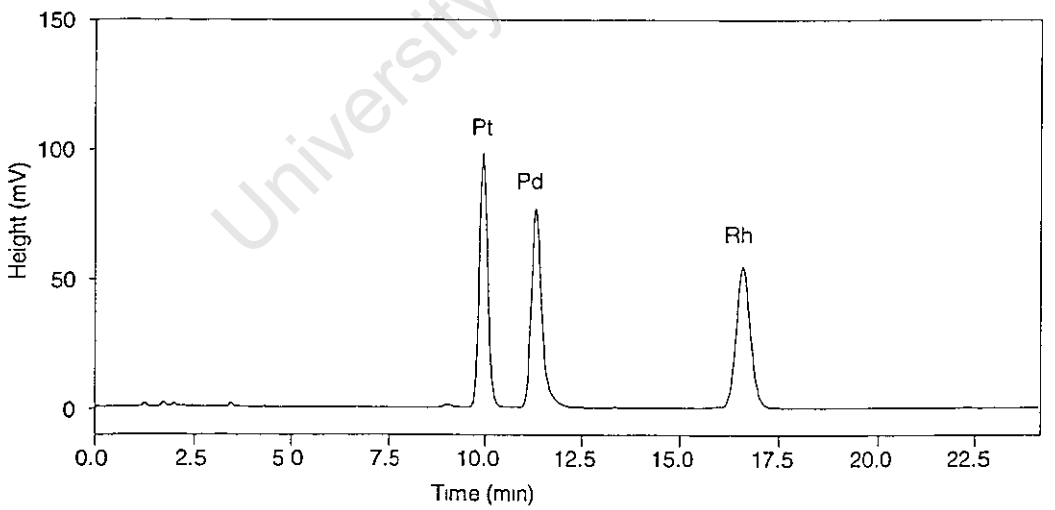

Figure 3.13: A RP-HPLC chromatogram of exactly 29, 20 and 20 ppm, Pt(II), Pd(II) and Rh(III) complexes of *N*-pyrrolidyl-*N'*-(2,2-dimethylpropanoyl)thiourea, respectively. Column = LUNA C18(2), 5 µm, 150 mm x 4.6 mm. Mobile phase = 90/10 (%v/v), Acetonitrile / 0.1 mol.dm^{-3} Acetate buffer (pH 6). Flow rate = 1.0 ml.min^{-1}. Detection = UV at 254 nm.

Table 3.3. Integration report of a standard chromatogram shown in Figure 3.11.

Pk#	Type	Component	t_R(min)	Width(sec)	Area(uVsec)	%
1	VP		1.23	7.00	12.8	0.3
2	PP		1.69	6.10	14.1	0.3
3	PP		1.96	6.50	13.7	0.3
4	BB		9.03	15.90	17.6	0.4
5	BV	Pt	9.94	13.60	1451.5	34.1
6	VB	Pd	11.32	15.80	1406.1	33.0
7	BB	Rh	16.59	22.60	1341.2	31.5
	Totals:				4257.0	100.0

An important condition in the use of HPLC separation for accurate quantitative determinations, is that the baseline resolution between peaks of similar size should be greater than 1.5. This was easily achieved in this study. Resolution was calculated using data shown in Table 3.3 to assess the separation of Pt(II) and Pd(II) complexes which, because of their close retention times, were regarded as critical bands.

A satisfactory resolution value was obtained as can be seen below.

$$R_s = \frac{2(t_{R(Pd)} - t_{R(Pt)})}{W_{(Pt)} + W_{(Pd)}}$$

$$= \frac{2(11.32 \text{ min.} - 9.94 \text{ min.})}{0.226 \text{ min.} + 0.263 \text{ min.}}$$

$$= \underline{5.64}$$

A longer column (250 mm x 3.0 mm in diameter) gives an equally good baseline separation (R_s = 6.65) although the total run time of 40 minutes for all three complexes is undesirably long (Figure 3.14).

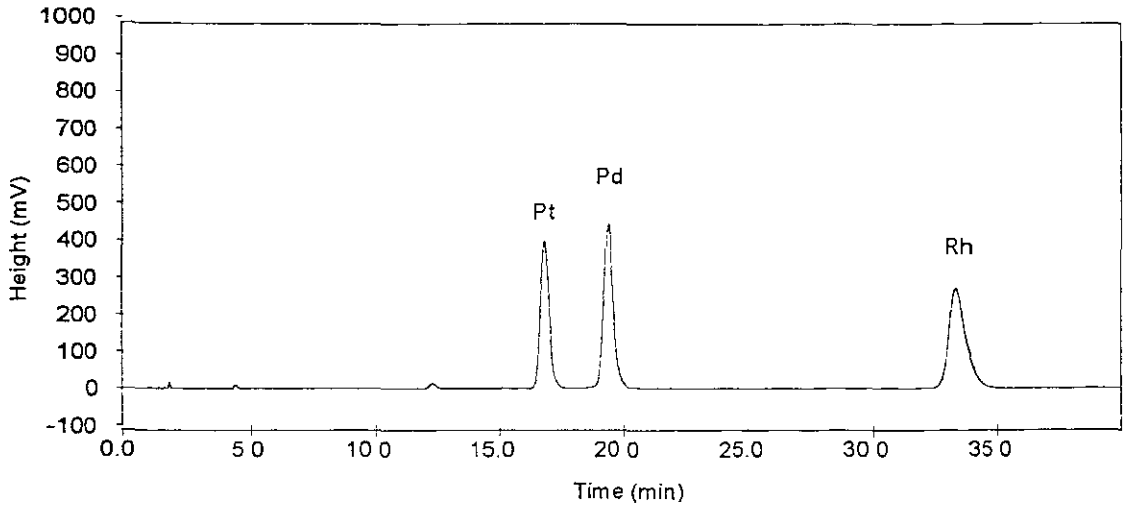

Figure 3.14: RP-HPLC chromatogram of Pt(II), Pd(II) and Rh(III) complexes of *N*-pyrrolidyl-*N'*-(2,2-dimethylpropanoyl)thiourea. Column = LUNA C18(2), 5 µm, 250 mm x 3.0 mm. Mobile phase = 90/10 (%v/v), Acetonitrile / 0.1 mol.dm^{-3} Acetate buffer (pH 6). Flow rate = 0.8 ml.min^{-1}. Detection = UV at 254 nm.

3.2.7. Calibration graphs and limits of detection

A series of standard solutions of platinum(II), palladium(II) and rhodium(III) complexes of *N*-pyrrolidyl-*N'*-(2,2-dimethylpropanoyl)thiourea mixtures between 0.1 and 100ppm each compound, were prepared by dilution of a concentrated stock solution. Acetonitrile was used as a solvent. These standard solutions were injected onto an HPLC system under conditions described in section 3.2.6.

The calibration graphs i.e. **Peak area** *versus* **Concentration**, of platinum(II), palladium(II) and rhodium(III) complexes were all linear with correlation factors (r^2) greater than 0.999. These graphs are shown in figure 3.15. They all have zero intercept which, as generally accepted, indicate that the complexes are kinetically stable.

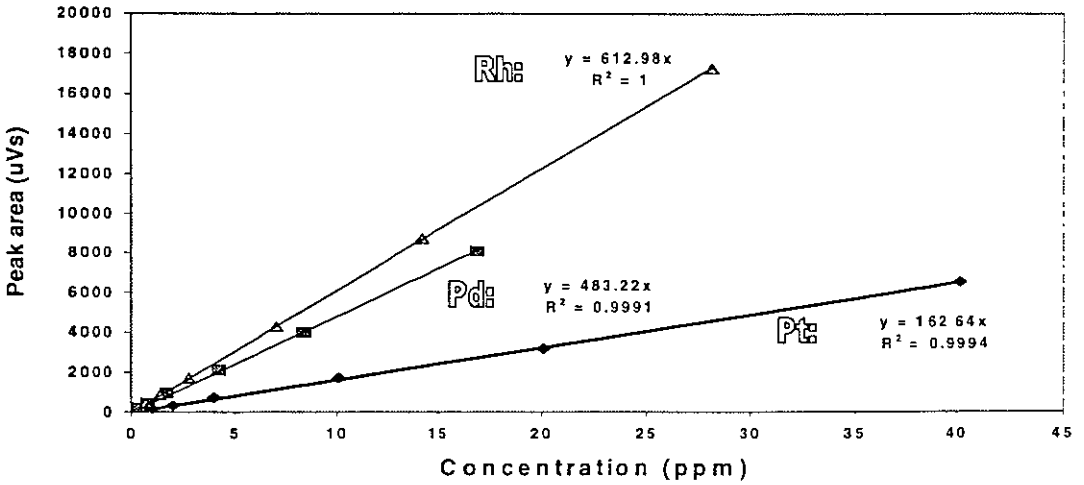

Figure 3.15: RP-HPLC calibration graphs for Pt(II), Pd(II) and Rh(III) as their *N*-pyrrolyl-*N'*-(2,2-dimethylpropanoyl)thiourea complexes. Column = LUNA C18(2), 5 µm, 150 mm x 4 6 mm. Mobile phase = 90/10 (%v/v), Acetonitrile / 0.1 mol.dm^{-3} Acetate buffer (pH 6). Flow rate = 1 0 ml.min^{-1}. Detection = UV at 254 nm.

The limits of detection and quantification (LOD and LOQ) for each of the three complexes were determined at their respective wavelengths of maximum absorption (Table 3.4). The LOD was taken as that concentration of the complex whose signal (or peak) is equivalent to three times the standard deviation of the average baseline noise in terms of peak height. The LOQ was that concentration producing a signal that is equivalent to ten times the standard deviation of the average baseline noise[20,42]. A practical approximation of these two limits is demonstrated with sketches in Figure 3.16.

Table 3.4. RP-HPLC limits of detection and determination (LOD and LOQ).

	Limit of detection (ppm)	Limit of determination (ppm)	UV λ_{max} (nm)
Pt	0.03	0.15	258
Pd	0.02	0.08	276
Rh	0.03	0.12	264

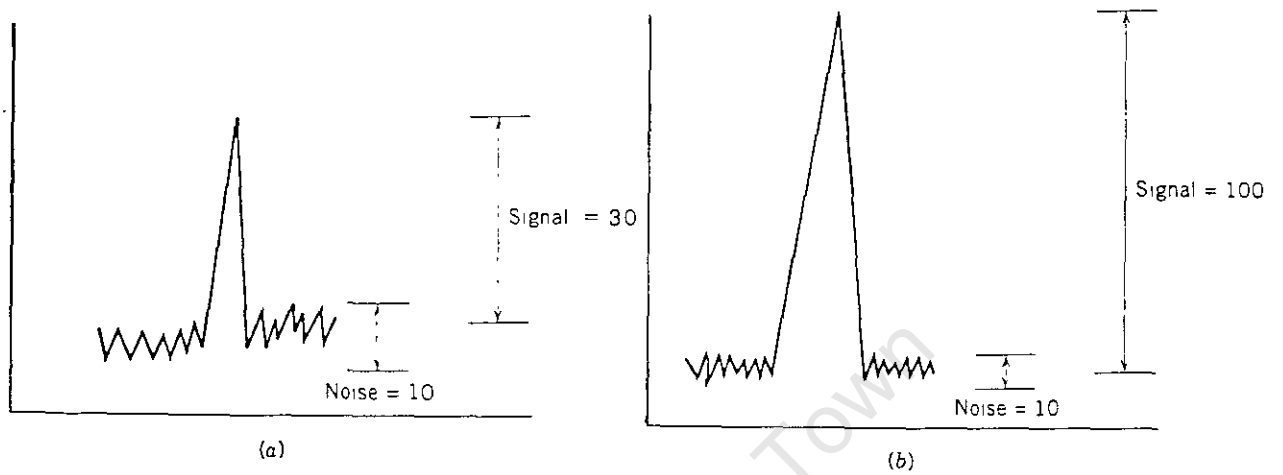

Figure 3.16: Signal-to-Noise ratio at (a) limit of detection (LOD) = 3:1,(b) limit of quantification (LOQ) = 10.1[42].

3.3. Complexation of platinum(II), palladium(II) and rhodium(III) in aqueous samples

The complexation of metals for analysis by HPLC has been carried out in several different ways[44-52]. One way is to introduce the ligand in the mobile phase and inject the aqueous metal ion solution onto HPLC so that the metal complexes are formed on line. Complexation in this way, however, tends to be incomplete for slow reacting metals and usually, there is undesirably high background noise due to excess ligand. Another way is to carry out the complexation reaction separately and isolate the complexes by solvent extraction. This method proves to be tedious. Furthermore, as a precaution in reversed phase HPLC, non-polar solvents such as chloroform should not be introduced into the analytical column as they may cause the chemically bonded hydrocarbon phase to deteriorate over time. The other way is to carry out the complexation reaction in a solvent mixture that is the same as the mobile phase, prior to injection. The disadvantage associated with this last way of complexation is that the metal solution is inevitably diluted. Mueller and Lovett[46] developed a salt-induced phase separation method which was found to have more advantages than the other

ways of complexation. The metal complexes are formed in aqueous-acetonitrile mixture and the acetonitrile phase is separated by the addition of a saturated solution of sodium chloride. The metal complexes are extracted into acetonitrile which can be injected directly into the HPLC system. The major advantage of the salt-induced phase separation method is that the metal complexes are pre-concentrated in the acetonitrile layer.

In the present work, we employed the salt-induced water-acetonitrile phase separation in the treatment of the aqueous mixture of platinum(II), palladium(II) and rhodium(III). Unfortunately, rhodium(III) did not form a complex at room temperature as no peak was observed and we were not able to cover its complexation for determination by HPLC in the present work, using this method of sample preparation.

A flow diagram of the procedure followed in the complexation of platinum(II) and palladium(II) in aqueous media is shown below (Figure 3.17.).

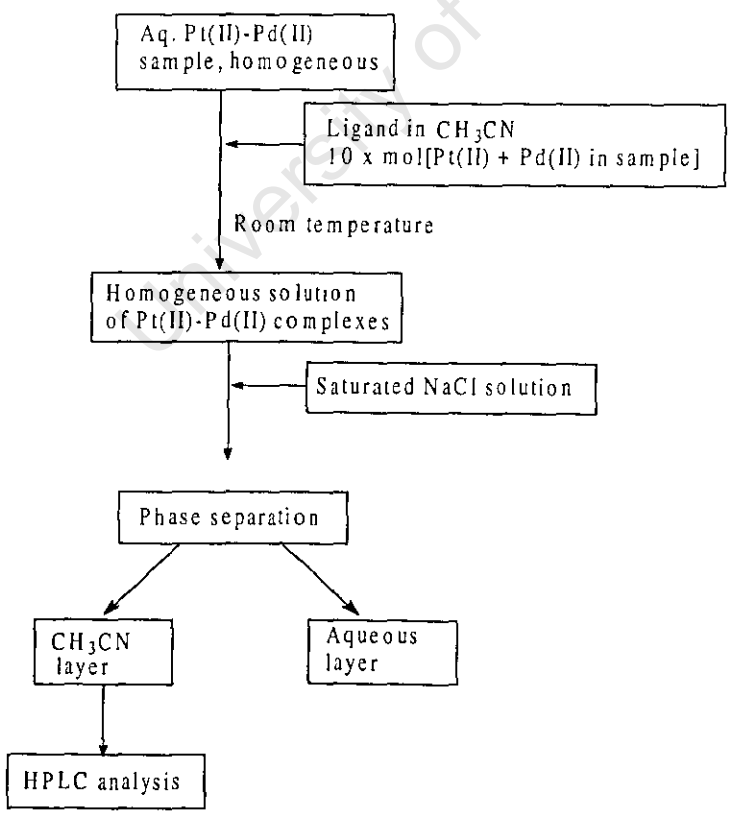

Figure 3.17: Treatment of sample for analysis by RP-HPLC.

While the salt-induced phase separation method is effective, it became evident when comparing the chromatograms of non-acidic (water) samples with acidic samples that the amount of the platinum(II) and palladium(II) complexes formed (in terms of peak area) is affected by the presence of higher acid concentrations as shown in Figure 3.18. The rate of formation of the complex appears to be facilitated in the presence of acid. Salts of platinum(II) and palladium(II) form brownish precipitates at pH values greater than 5 such as in distilled water. The precipitates are thought to be the hydroxy species of these metals[17]. In water therefore, the amount of platinum(II) or palladium(II) available for complexation with acylthiourea is reduced.

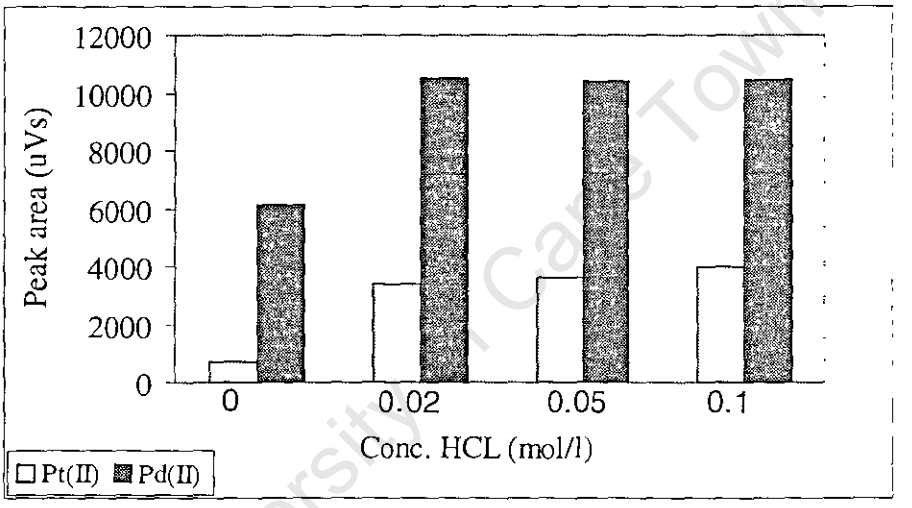

Figure 3.18: Influence of acid concentration on the amount of *N*-pyrrolidyl-*N'*-(2,2-dimethylpropanoyl)thiourea complexes of platinum(II) and palladium(II) formed in aqueous media. Column = LUNA C18(2), 5 µm, 150 mm x 4.6 mm. Mobile phase = 90/10 (%v/v), Acetonitrile / 0.1 mol.dm^{-3} Acetate buffer (pH 6). Flow rate = 1.0 ml.min^{-1}. Detection = UV at 254 nm.

Having seen that the presence of acid results in an increase in peak area, we decided to investigate change in peak area of the complexes as acid concentration increases. Thus 50 ppm platinum(II) and palladium(II) solutions were made in 0.1, 0.5, 1.0, 2.0 and 5.0 mol.dm^{-3} HCl, and complexed with *N*-pyrrolidyl-*N'*-(2,2-dimethylpropanoyl)-thiourea. The complex peak was found to grow increasingly broader as the concentration of hydrochloric acid was increased (Figures 3.19 and 3.21). Solutions in which the acid concentration give rise to narrow and sharp chromatographic peaks range from 0.1 to 0.5 mol.dm^{-3} HCl.

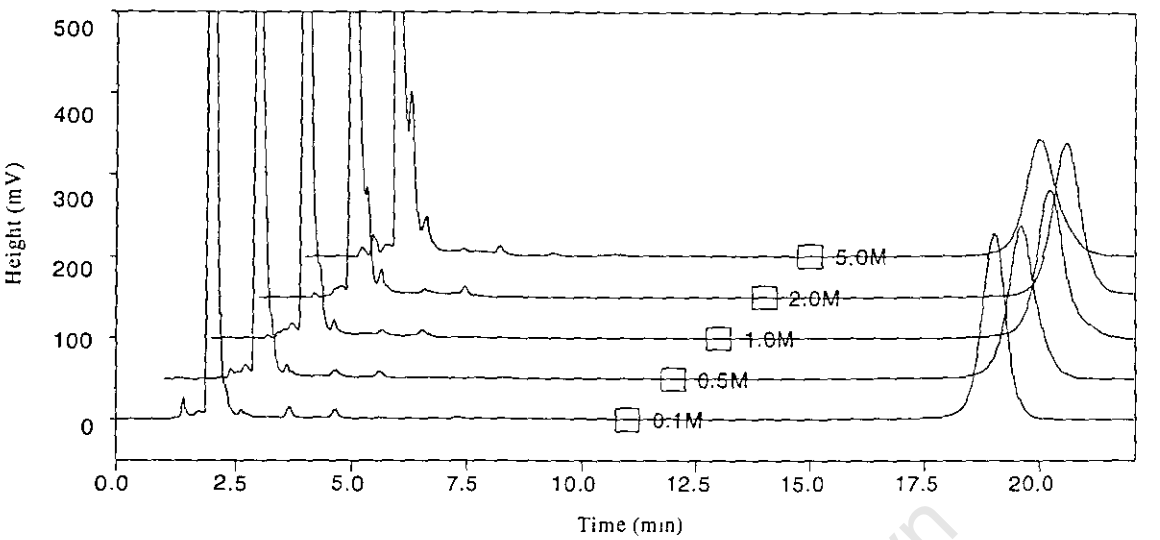

Figure 3.19: Chromatograms obtained from complexation of platinum(II) in aqueous samples of varying HCl concentrations. Column = LUNA C18(2), 5 µm, 150 mm x 4.6 mm. Mobile phase = 90/10 (%v/v), Acetonitrile / 0.1 mol.dm^{-3} Acetate buffer (pH 6). Flow rate = 1.0 ml.min^{-1}. Detection = UV at 254 nm.

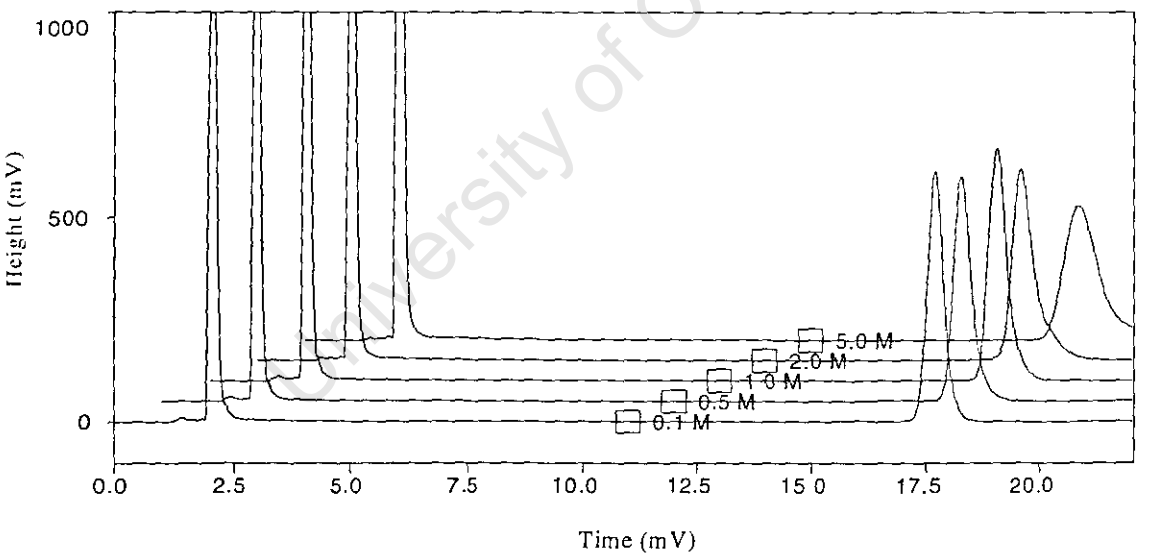

Figure 3.20: Chromatograms obtained from complexation of palladium(II) in aqueous samples of varying HCl concentrations. Column = LUNA C18(2), 5 µm, 150 mm x 4.6 mm. Mobile phase = 90/10 (%v/v), Acetonitrile / 0.1 mol.dm^{-3} Acetate buffer (pH 6). Flow rate = 1.0 ml.min^{-1}. Detection = UV at 254 nm.

Moreover it can be seen that as acid concentration increases, the peak area of the palladium(II) complex increases slightly while in the case of the platinum(II) complex it decreases slightly (Figure 3.21). However, quantitative recoveries (100 ± 3%) were

obtained from samples containing 0.1 mol.dm^{-3} HCl, which is taken as optimum HCl concentration in the aqueous sample (section 3.4.1).

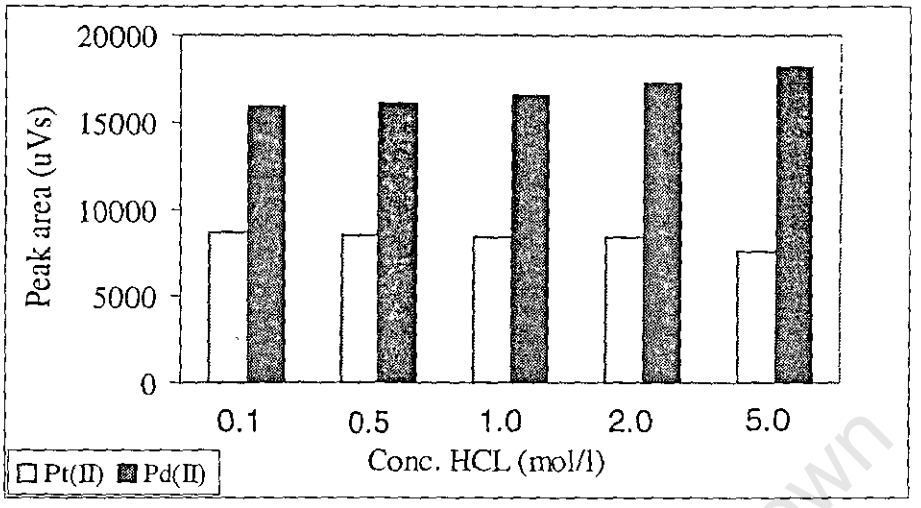

Figure 3.21: The peak area due to the palladium(II) complex seems to increase slightly while in the case of platinum(II) it decreases, as HCl concentration in the aqueous sample is increased. Column = LUNA C18(2), 5 µm, 150 mm x 4.6 mm. Mobile phase = 90/10 (%v/v), Acetonitrile / 0.1 mol.dm^{-3} Acetate buffer (pH 6). Flow rate = 1.0 ml.min^{-1}. Detection = UV at 254 nm.

Broadening of the peaks at between 2 and 5M HCl concentrations could arise from the presence of additional protonated complex species different from the usual *bidentate bis*-Pt[L^2-*(S,O)*]$_2$ and *bis*-Pd[L^2-*(S,O)*]$_2$ complexes, represented by structure **A** in figure 3.22. It is possible that when *N*-pyrrolidyl-*N'*-(2,2-dimethylpropanoyl)thiourea is introduced to platinum(II) or palladium(II) in acidic solutions of between 2 and 5M HCl, *monodentate* coordination *via* sulphur takes place leading to the formation of structure **C** and/or **B** complexes shown in Figure 3.22. It would follow then, that the *bidentate* complexes are formed on-line, soon after injection due to the presence of sodium acetate used as buffer agent in the mobile phase. Supporting evidence that this is indeed so, was that extremely broad peaks of both platinum(II) and palladium(II) complexes were obtained when 0.01M sodium acetate was used to buffer the mobile phase (Figures 3.23 and 3.24) compared to the usual 0.1M. The broadening of peaks as depicted in Figures 3.19 and 3.20 suggests that 0.1M acetate buffer is not enough to reverse all open-ring complexes formed in solutions of higher HCl concentration, typically 2 to 5M HCl.

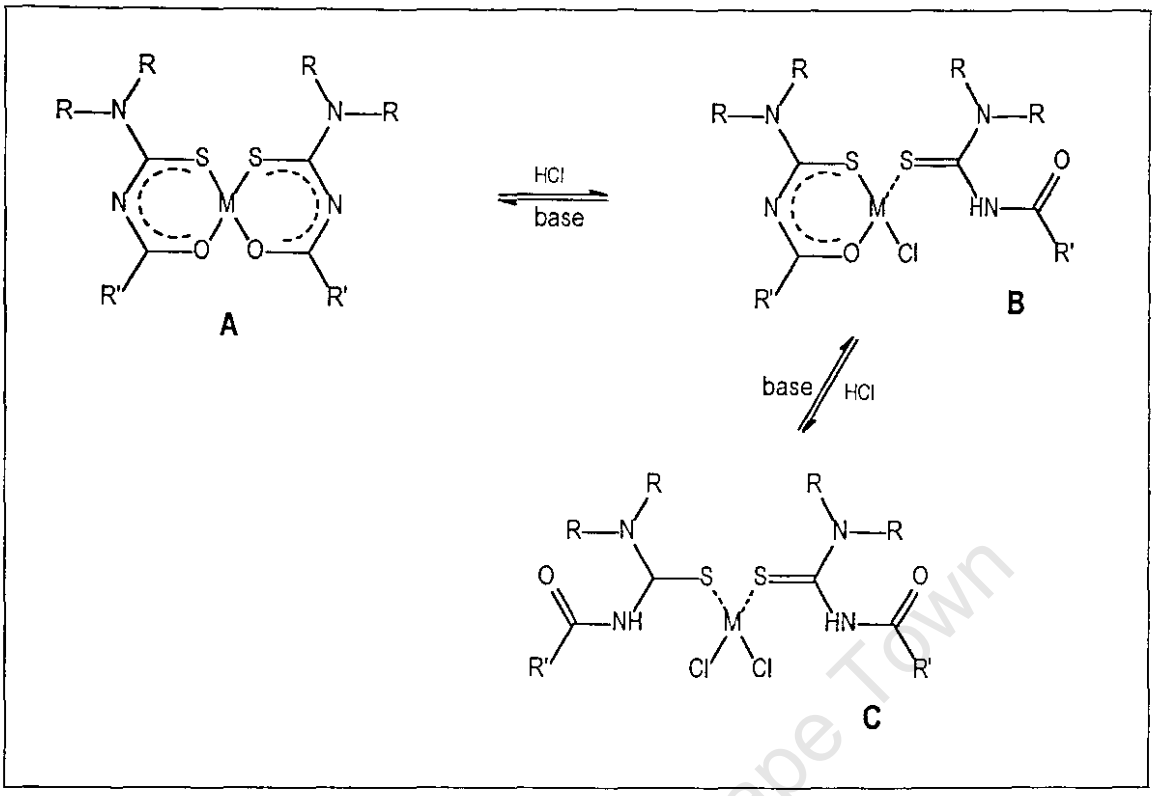

Figure 3.22: Different complex species possibly present at higher HCl concentrations. The structures adapted from the report on protonation studies of *cis*-Pt[L-*(S,O)*]$_2$ complexes[64].

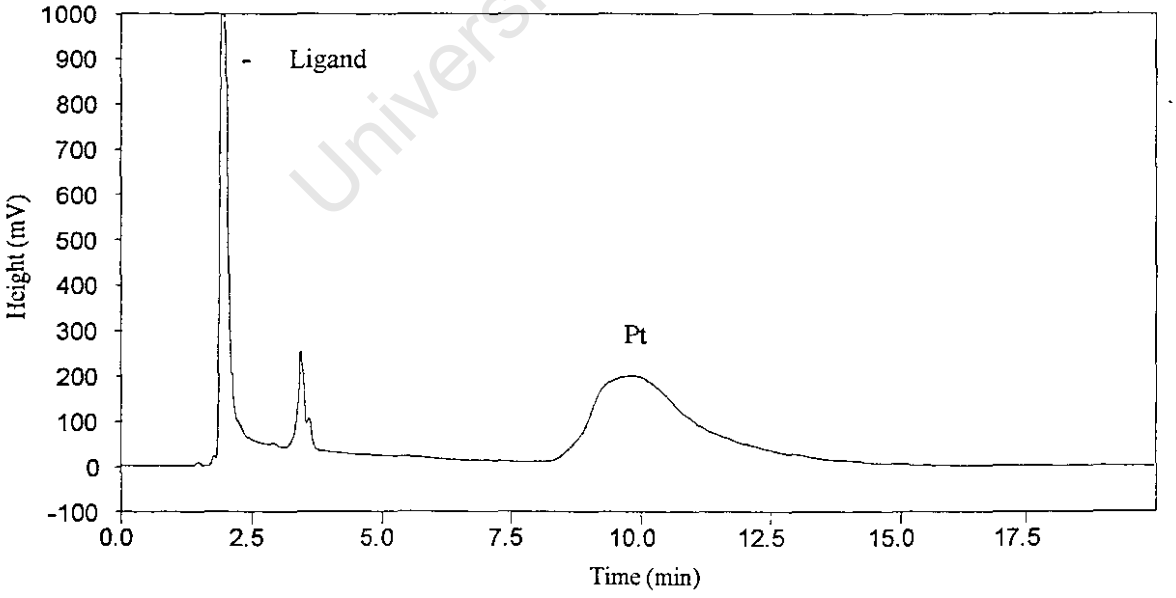

Figure 3.23: Extremely broad platinum(II) complex peak when 0.01M CH_3COONa is used to buffer the mobile phase. Column = LUNA C18(2), 5 µm, 150 mm x 4.6 mm. Mobile phase = 90/10 (%v/v), Acetonitrile / 0.01 mol.dm^{-3} Acetate buffer (pH 6). Flow rate = 1.0 ml.min^{-1}. Detection = UV at 258 nm.

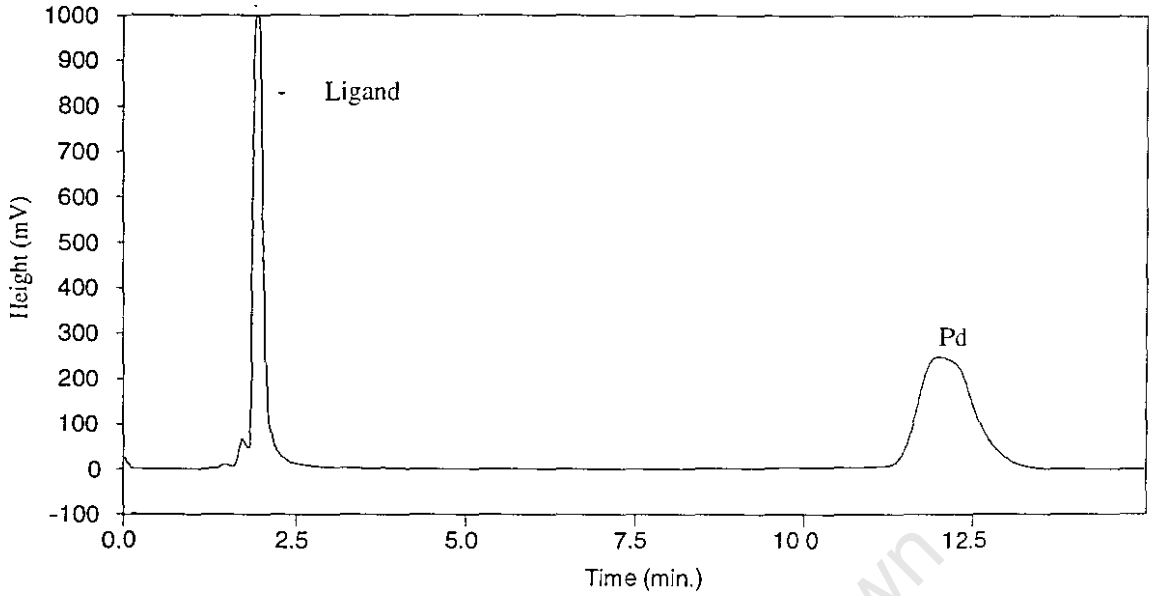

Figure 3.24: A broad palladium(II) complex obtained when 0.01M CH_3COONa is used to buffer the mobile phase. Column = LUNA C18(2), 5 µm, 150 mm x 4.6 mm. Mobile phase = 90/10 (%v/v), Acetonitrile / 0.01 mol.dm^{-3} Acetate buffer (pH 6). Flow rate = 1.0 ml min^{-1}. Detection = UV at 276nm.

3.3.1 Analytical recovery for platinum(II) and palladium(II)

Exactly 1ml of the aqueous platinum(II)-palladium(II) sample was mixed with exactly 2ml of acetonitrile into which *N*-pyrrolidyl-*N'*-(2,2-dimethylpropanoyl)thiourea ligand (ten fold molar excess to combined Pt(II) and Pd(II)) was dissolved. After addition of exactly 1ml of a saturated solution of sodium chloride, following the procedure shown in Figure 3.17, acetonitrile separated out as a layer, extracting the formed complexes. The acetonitrile layer was analysed by HPLC. A typical chromatogram of the sample is shown in figure 3.25.

In the quantitative determination of the concentrations of the complexes it is important to note that the volume of acetonitrile recovered by phase separation is not exactly the same as the volume introduced. The volume of acetonitrile recovered from a 1:2 (v/v) aqueous sample/acetonitrile mixture was determined to be exactly 85%(v/v) of the volume introduced. This is described further in section 3.7.

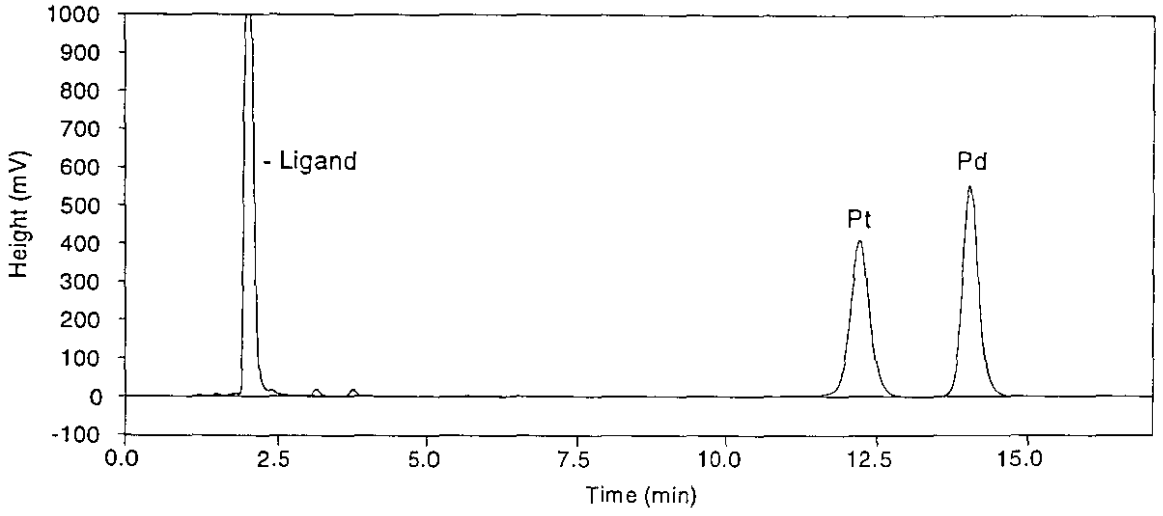

Figure 3.25: A typical chromatogram of the sample treated according to the procedure shown in figure 3.17. Column = LUNA C18(2), 5 µm, 150 mm x 4.6 mm. Mobile phase = 90/10 (%v/v), Acetonitrile / 0.1 mol.dm^{-3} Acetate buffer (pH 6). Flow rate = 1.0 ml.min^{-1}. Detection = UV at 254 nm.

The concentrations of the complexes in the acetonitrile phase obtained after addition of a saturated solution of sodium chloride were calculated using the straight line equations obtained from the calibration graphs. The amounts of platinum and palladium represented were calculated. Data of standards and samples obtained from HPLC are given in Table 3.5 and 3.6, respectively. The calibration graphs constructed are shown in Figures 3.26A and B.

Table 3.5. RP-HPLC data of previously synthesised, pure standard Pt(II) and Pd(II) complexes for calibration.

Pt-complex		Pd-complex	
Conc. (ppm)	Area (µVs)	Conc. (ppm)	Area (µVs)
4	246	3.3	191
40	2055	33	1937
200	10197	165	9478
400	19500	330	18911

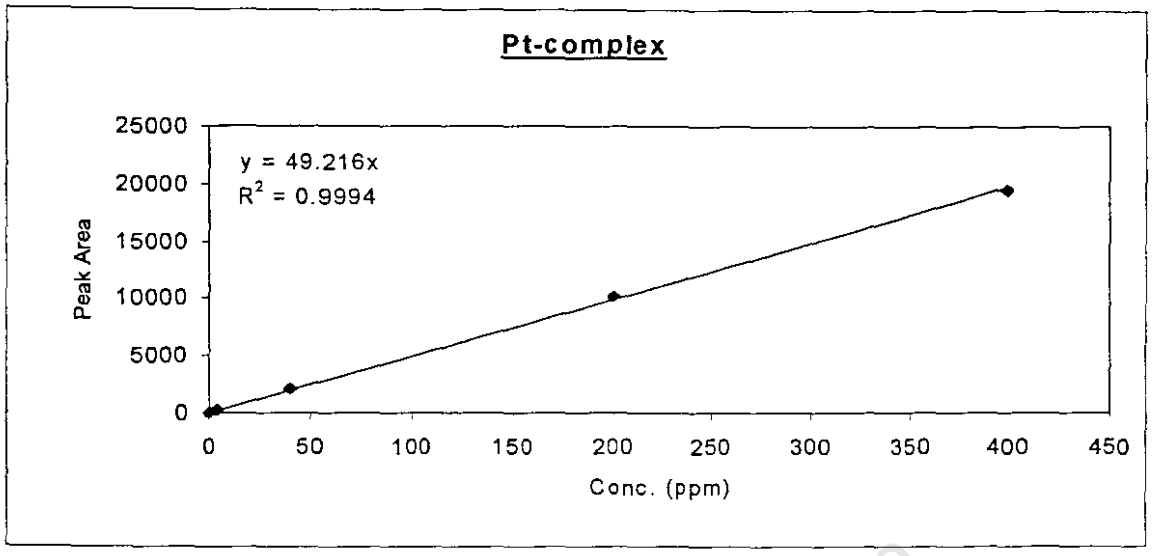

A.

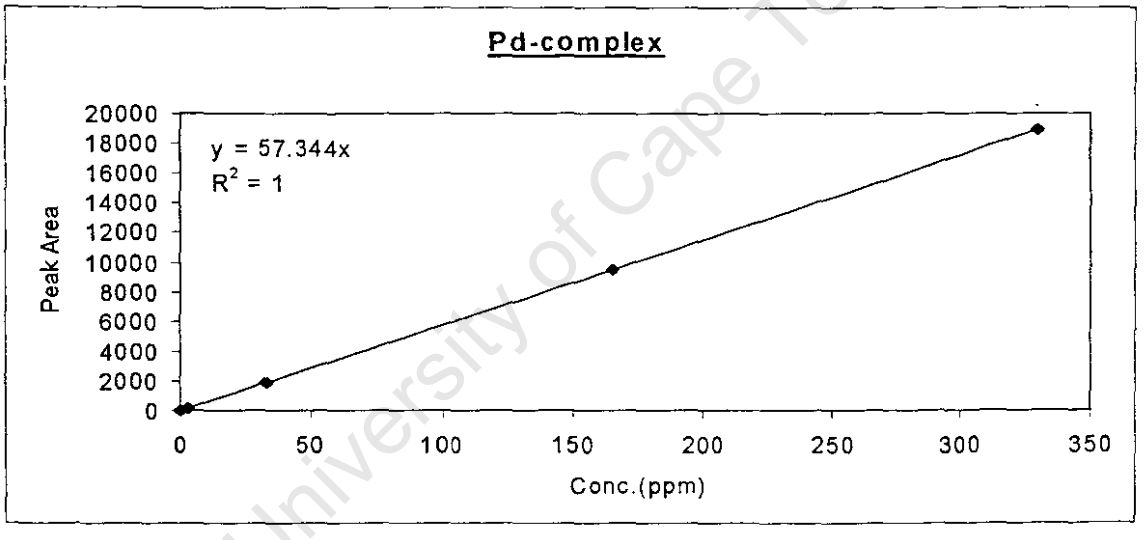

B.

Figure 3.26: RP-HPLC calibration graphs used for quantitative determination of Pt(II) - top, and Pd(II) - bottom, in aqueous samples Column = LUNA C18(2), 5 µm, 150 mm x 4.6 mm. Mobile phase = 90/10 (%v/v), Acetonitrile / 0.1 mol.dm^{-3} Acetate buffer (pH 6). Flow rate = 1.0 ml.min^{-1}. Detection = UV at 254 nm.

Table 3.6. RP-HPLC recovery tests based on an aqueous Pt(II)-Pd(II) sample containing exactly 103.4 and 61.9 ppm, Pt(II) and Pd(II), respectively. The concentrations of platinum(II) and palladium(II) are derived from the concentrations of $[Pt(L^2\text{-}S,O)_2]$ and $[Pd(L^2\text{-}S,O)_2]$ complexes formed.

Concentration obtained (ppm)			
Pt-complex	Pt(II)	Pd-complex	Pd(II)
186.92	100.0	185.28	63.1
192.86	103.2	191.47	65.2
192.41	103.0	186.83	63.6
Average Recovery:	**Pt = 98.7% ± 1.8**		**Pd = 103.3% ± 1.6**

These recoveries confirm the applicability of reversed phase HPLC to metal analysis and more specifically, the efficiency of the salt-induced phase separation method in comparison to several other complexation methods already discussed. Analytical methods that give deviations of ± 3% from the target value are generally regarded as good methods[42]. In many cases analyses are acceptable within ± 5% from the target value.

3.3.2. The limit of detection of platinum(II) and palladium(II) in aqueous samples

The lowest concentrations of platinum(II) and palladium(II) complexed and detected were found to be about 2 ppm and 0.5 ppm, respectively. These were measured at each complex's wavelength of maximum absorbance (258 nm for platinum(II) complex and 276 nm for palladium(II) complex). For the analysis of a mixture of the two metal complexes, a common wavelength of 254 nm was chosen because a single wavelength UV detector was used. At this wavelength 4 ppm Pt(II) was the lowest detectable concentration while 0.5 ppm Pd(II) could still be detected.

Samples containing mixtures of either platinum(II) or palladium(II) at the lowest detectable concentration and about 50 ppm palladium(II) or platinum(II), were prepared and injected into HPLC as a check of whether the lowest metal complex concentration could still be satisfactorily determined in the presence of a large excess of another complex. The chromatograms are shown in Figures 3.27 and 3.28.

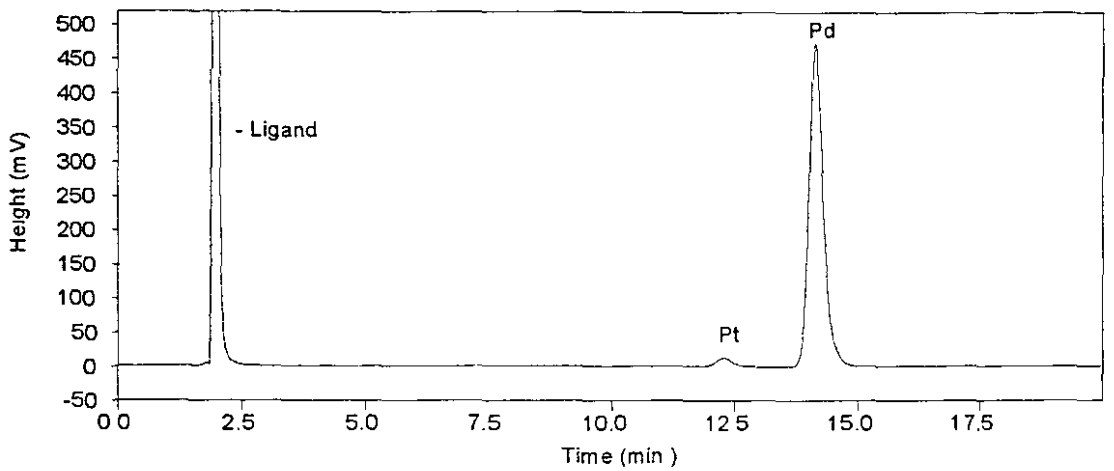

Figure 3.27: A Chromatogram of trace concentration, 4 ppm, of platinum(II) in the presence of 50 ppm palladium(II). Resolution >> 1.5. Column = LUNA C18(2), 5 µm, 150 mm x 4.6 mm. Mobile phase = 90/10 (%v/v), Acetonitrile / 0.1 mol dm^{-3} Acetate buffer (pH 6). Flow rate = 1.0 $ml.min^{-1}$. Detection = UV at 254 nm.

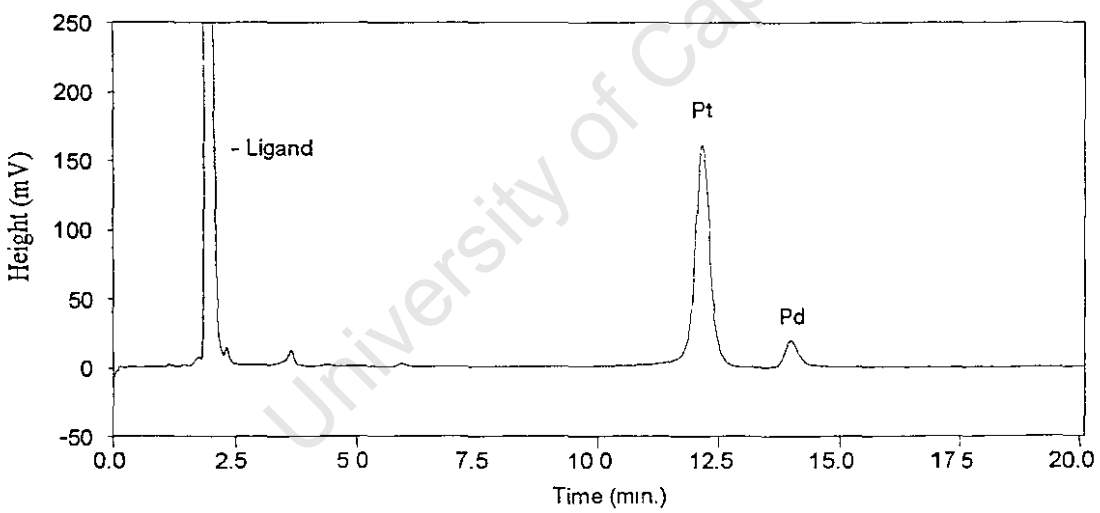

Figure 3.28: A chromatogram of trace concentration, 0.5 ppm, of palladium(II) in the presence of 50 ppm platinum(II). Resolution >> 1 5. Column = LUNA C18(2), 5 µm, 150 mm x 4.6 mm. Mobile phase = 90/10 (%v/v), Acetonitrile / 0.1 $mol.dm^{-3}$ Acetate buffer (pH 6). Flow rate = 1.0 $ml.min^{-1}$. Detection = UV at 254 nm.

Quantitative analysis of additional samples containing 51.7 and 31; 10.3 and 6.2 ppm, platinum(II) and palladium(II) respectively, were carried out.

The percentage error associated with the determination at these levels of concentration was evaluated (Table 3.7) according to the following equation:

$$\%\text{Error} = \frac{100(\text{True} - \text{detected})}{\text{True}}$$

Table 3.7. Average error in the determination of Pt(II) and Pd(II) with decreasing levels of concentration. Samples were prepared in triplicate (n = 3).

Pt(II)		Pd(II)	
Conc.(ppm)	± %Error	Conc.(ppm)	± %Error
103.4	1.3	61.9	3.3
51.7	1.1	31.0	8.7
10.3	26.5	6.2	11.3
		0.62	55.4

3.4. Optimum time for complexation in water/acetonitrile mixtures

3.4.1. Platinum(II) and Palladium(II)

A time dependence study of platinum(II) and palladium(II) complexation with *N*-pyrrolidyl-*N'*-(2,2-dimethylpropanoyl)thiourea was carried out. The reaction was stopped after 5, 10, 20, 30, 60 and after 120 minutes by separating the acetonitrile and water phases using the salt-induced phase separation procedure[46] described in section 3.3.1. Peak areas of the platinum(II) and palladium(II) complexes formed over different time intervals were plotted against reaction time (Figure 3.29).

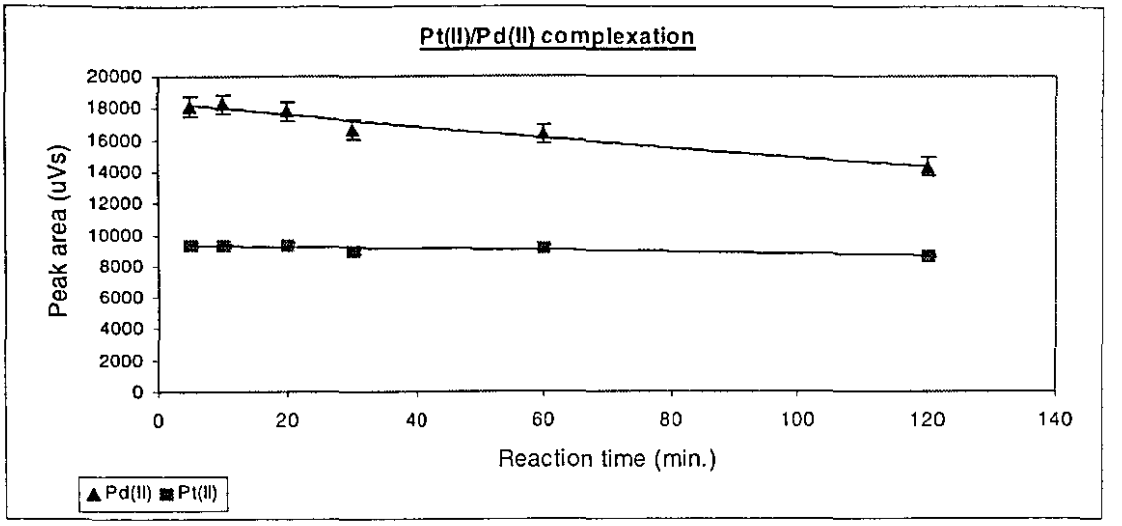

Figure 3.29: Determination of optimum time for quantitative Pt(II)/Pd(II) complexation with *N*-pyrrolidyl-*N'*-(2,2-dimethylpropanoyl)thiourea. Column = LUNA C18(2), 5 µm, 150 mm x 4 6 mm. Mobile phase = 90/10 (%v/v), Acetonitrile / 0.1 mol.dm^{-3} Acetate buffer (pH 6). Flow rate = 1.0 ml.min^{-1}. Detection = UV at 254 nm.

It appears that the peak areas of both complexes decrease over time. The decrease is more rapid for the palladium(II) complex than the platinum(II) complex. The appearance of an additional peak over time shown in section 3.2.3, indicates formation of an additional compound which is seemingly at the expense of the desired *cis*-[PtL^2-*(S,O)*] and *cis*-[PdL^2-*(S,O)*] complexes. Clearly, the amount of *cis*-[PdL^2-*(S,O)*] decreases at a faster rate than *cis*-[PtL^2-*(S,O)*] as would be expected given the reactivities of palladium(II) compounds and platinum(II) compounds. The highest amount of detectable complex is formed in less than five minutes. See experimental details in section 3.7. This observation further suggests that when determining the concentration of these complexes, using the same procedure, it would not be necessary to wait for longer than five minutes.

3.4.2. Rhodium(III)

A very small amount of rhodium(III) complex was detected on HPLC after a reaction time of four hours. However, the amount did not seem to increase in 8, 16, 20 and 24 hours. This observation demonstrates that reactions of rhodium at room temperature are very slow. A catalyst accompanied by heating could increase the rate of the reaction, but the latter leads to solvent losses by evaporation and can cause explosions if solvents are contained. A commonly used catalyst in PGM reactions, tin(II) chloride, leads to formation of polynuclear complex species which contain both tin and the PGM of interest[68]. These reactions need to be studied before tin(II) chloride is

used as a catalyst in the synthesis of *tris*-[*N,N*-dialkyl-*N'*-acylthioureato]rhodium(III) complexes for the analysis of rhodium in solutions.

3.5. Evaluation of errors

Types of errors associated with experimental data can be grouped into determinate and indeterminate errors. An additional grouping might be gross errors which arise from lack of due attention and carefulness during experimental measurements. In many cases, gross errors affect only a single result but in other cases such as using a wrong scale, the entire set of results is affected. Gross errors are, however, very infrequent and once identified can be corrected.

Determinate errors (also called systematic errors) originate from a definite source, usually the instrument, the analyst or the method used. Indeterminate errors on the other hand are due to inevitable, uncontrollable random variables that exist in every physical or chemical measurement. The sources of indeterminate errors cannot be identified. It is generally assumed, however, that indeterminate errors arise from combination of various types of errors. Perhaps more challenging, are the personal and method errors. In effect, these errors can only be minimized and cannot be completely eliminated. It is helpful and necessary in this regard and in dealing with indeterminate errors, to apply statistical methods to the experimental data as they reflect analytical results in a meaningful way.

Applying the statistical methods described in Appendix X, we found the 95% confidence limits for the results given in Table 3.6 to be 102.07 ppm ± 3.29 and 63.97ppm ± 2.15, for platinum and palladium, respectively. These ranges do indeed cover the true values namely 103.4ppm platinum and 61.9ppm palladium, so that the HPLC method, together with the sample preparation procedure can be judged reasonably accurate and precise.

Table 3.8 gives data of replicate measurements of peak area obtained in the present RP-HPLC method, which we used to asses reproducibility of the instrument

Table 3.8. Reproducibility of peak areas on the Spectra Series HPLC. (Instrument reproducibility)

Injection no.	Peak area
1	12561.5
2	12755.3
3	12475.4
4	13217.1
5	13061.7
6	12954.4
7	12737.7
8	12562 1
9	12906.3
10	12931.1
Average:	12816.26
Std. Dev.:	239 6444
Rel. Std. Dev.(%):	1 87

Additional determinate errors such as operational ones incurred in the course of study were also determined Experimental details are given in section 3.7. The analytical data obtained from this exercise is given in Table 3.9 below.

Table 3.9. Reproducibility of the analyses including the sample treatment procedure shown in figure 3.17. Data obtained from Pd(II) complexation.

Reaction no.	Peak area
1	3978.7
2	3891.0
3	3736.8
4	4233 0
5	3915 9
6	3784.4
7	3623.8
8	3961.0
9	3645.8
8	4109.3
9	3701.1
Average:	3871.0
Std. Dev.:	193.9
Rel. Std. Dev.(%):	5.01

The statistical error incurred in the performing of experiment alone, or operational error, is given by the difference between total determinate error (5%RSD) and error due to the instrument (2%RSD). Error incurred in the performing of experiments, or sample preparation is, therefore ± 3% RSD.

In all HPLC determinations carried out in the present study the results obtained are estimated to be precise with a 3% relative standard deviation because error introduced by the instrument is eliminated by a calibration graph of standards.

3.6. Validation

Two "unknown" mixtures containing platinum and palladium, prepared by mixing the commercially available standard solutions, were analysed by the RP-HPLC method developed in the present work, which includes the sample preparation procedure shown in Figure 3.17, as well as by Inductively Coupled Plasma (ICP). The RP-HPLC analysis was done by the author while ICP analysis was performed by a different analyst. Results obtained are given in Table 3.10.

Table 3.10. RP-HPLC and ICP Results of unknown mixtures of platinum and palladium.

	Concentration (ppm)			
	RP-HPLC		ICP	
Sample mixture	Pt	Pd	Pt	Pd
1	4.8*	25.4 ± 1.4	43.5 ± 0.8	24.4± 0.6
2	39.6 ± 1.0	25.0 ± 1.4	44.4± 0.3	24.4± 0.2

* Mixture contained platinum(IV).

Mixture 1 contained platinum in its oxidation state IV. The resultant complex, if formed, is charged and therefore not retained. Seemingly, there is a minor fraction of platinum(II) ions. A 20 fold molar excess of tin(II) chloride was added to mixture 1 in order to reduce Pt(IV) to Pt(II) prior to complexation. This led to a slight increase in peak area of the platinum(II) complex. In order to achieve quantitative reduction, however, more studies are necessary.

Statistical tests have been developed to compare two sets of results obtained either from two independent analytical laboratories using the same method or from two different methods. The *F*-test (also called variance ratio test) is the most common. In this method, the value of *F* is calculated from the equation:

$$F = s^2_{(A)} / s^2_{(B)}$$

where $s_{(A)}$ and $s_{(B)}$ are the relative standard deviations of the results of methods A and B, respectively.

The value of *F* is then checked for its significance against values in the *F*-table (Table 3.11) calculated from an *F*-distribution corresponding to the number of degrees of freedom for the two sets of results.

Table 3.11. Values of the parameter, *F*, at various confidence levels[69].

	Confidence limits		
v	80%	90%	96%
1	39.9	161.4	4052
2	8.53	18.5	98.5
3	5.54	10.1	34.1
4	4.54	7.71	21.2
5	4.06	6 61	16.3
6	3.78	5.99	13.7

The *F*-test was applied to the results (of sample 2) obtained from the present RP-HPLC method and those from the ICP method given in Table 3.10.

$$F = s^2_{(RP\text{-}HPLC)} / s^2_{(ICP)}$$

For platinum(II):

$$F = (1.0)^2 / (0.34)^2$$

$$= \underline{8.65}$$

For palladium(II):

$$F = (1.4)^2 / (0.2)^2$$

$$= \underline{49}$$

In the case of platinum the value of *F* is less than 18.5 for two degrees of freedom ($n = 3$) at 90% confidence level, but greater than 8.53 at 80% confidence level. See

Table 3.11. In the case of palladium the value of F is less than 98.5 for two degrees of freedom at 96% confidence level, but greater than 18.5 at 90% confidence level.

It is therefore possible to say that at 90% confidence level there is no significant difference between the precisions of the present RP-HPLC method and ICP method in the determination of platinum(II). For the determination of palladium(II), there is no difference between precisions of the two methods at 96% confidence level.

3.7. Experimental

General HPLC operation: Only de-ionized water and HPLC grade acetonitrile supplied by BDH Laboratories were used to make up the mobile phase. De-ionized water was filtered through a 0.45μm nitrocellulose filters supplied by Microsep (Pty)Ltd, before use The solvents were degassed by bubbling helium gas in the reservoirs for 1 to 2 hours. The tubing leading to the pump were purged by pumping each solvent at 10ml.min^{-1} to remove air bubbles. The pump was programmed to deliver a 90:10 (%v/v), acetonitrile-water mixture usually at 1.0ml.min^{-1}. A 30 minute equilibration delay was allowed before commencing with sample injections.

Preparation of acetate buffer (pH = 6.04): Acetate buffer of pH ≈ 6, was prepared by mixing exactly 25 ml of 0.1 ml.dm^{-3} acetic acid and 475 ml of 0.1 mol.dm^{-3} sodium acetate making up a total volume of 500 ml. The appropriate volumes of acid and its conjugate base solutions were derived from the equilibrium equation stated below:

$$\mathbf{pH = pK_a + \log [base]/[acid]}$$

The dissociation constant, K_a, for acetic acid is 1.75 x 10^{-5} mol.dm^{-3} and its pK_a = 4.76 (see reference 69).

All solutions were made up with de-ionized water. The resultant buffer solution was filtered through a 0.45 μm (pore sized) filter.

Maintenance of the pump and analytical column: At the end of analyses, the system was flushed by pumping 50:50, methanol-water mixture for 1 hour at 0.5ml/min^{-1} to wash out residual, buffered mobile phase which may form precipitate over time and subsequently scratch the plunger and seals of the pump, leading to leakage. The number of theoretical plates in the column was determined regularly by analysing the column manufacturer's test mixture which was a 100ml acetonitrile solution of 7.3, 20.0, 23.2 and 22.0 mg of acetophenone, benzene, toluene and naphthalene, respectively, under the following system conditions:

Mobile phase:	65/35 (%v/v), acetonitrile/water
Flow rate:	0.5 ml.min^{-1}
Injection vol :	20 µl
Detection:	UV, 254 nm

The number of theoretical plates were determined for each compound using the following formula:

$$N = 2\pi (t_R h/A)^2,$$

where t_R is the retention time, **h** is the peak height and **A** is the peak area[42].

The number of theoretical plates were compared with the number of theoretical plates obtained when the column was new, for each compound, so that the performance of a column after long use could be assessed relative to its original performance.

Analytical separation: A standard mixture of pure platinum(II), palladium(II) and rhodium(III) complexes of *N*-pyrrolidyl-*N'*-(2,2-dimethylpropanoyl)thiourea was prepared by dissolving 0.0140, 0.0100 and 0.0140 g, respectively, in 100 ml of acetonitrile. Speedy dissolution was achieved by ultrasonic agitation (for ±10 minutes). Dissolution in a small amount of tetrahydofuran, 2% (v/v), prior to making up to volume with acetonitrile is another way to prepare a concentrated solution of a mixture of standards. Both solvents are transparent to UV and absorbance of the compounds remains the same as in pure acetonitrile.

Complexation of Pt(II)/Pd(II) in aqueous media: Four, 10 ml of 50 ppm platinum(II) solutions were made by dissolving appropriate amounts of K_2PtCl_4 or K_2PdCl_4, using 0.1 , 0.05, 0.02 mol.dm^{-3} HCl and H_2O, respectively, as solvents. A 10ml solution of *N*-pyrrolidyl-*N'*-(2,2-dimethylpropanoyl)thiourea whose concentration was such that the number of moles (of ligand) in a 2ml aliquot would be ten times the number of moles of Pt(II) in 1ml, was prepared in acetonitrile. Exactly 1ml aliquot of each Pt(II) solution was mixed with 2ml of the ligand solution. After 2 hours stirring (of each solution) at room temperature, the reaction mixture was mixed with exactly 1ml of a saturated solution of NaCl, which made the aqueous and organic phases separate into two layers. A sample of the acetonitrile phase was injected onto the HPLC system, each time.

Optimum complexation time for Pt(II) and Pd(II): A solution of a mixture of Pt(II) and Pd(II), about 100 ppm each, was made by dissolving appropriate amounts of K_2PtCl_4 or K_2PdCl_4 in 20 ml of 0.1 mol.dm^{-3} HCl. A 20 ml solution of *N*-pyrrolidyl-*N'*-(2,2-dimethylpropanoyl)thiourea (the ligand) whose concentration was such that the number of moles in 2 ml aliquot would be ten times the combined number of moles of Pt(II) and Pd(II) in 1 ml, was prepared in acetonitrile. Several identical mixtures, 2 ml ligand solution added to 1 ml of Pt(II)-Pd(II) solution, were made and stirred at room temperature for 5, 10, 20, 30, 60 and 120 minutes, respectively. At the end of each time interval, exactly 1 ml of a saturated solution of sodium chloride was added to enforce acetonitrile/aqueous phase separation, and 20 µl of the acetonitrile phase was injected onto HPLC.

Construction of calibration graphs: A standard solution containing exactly 400 ppm *bis*-[*N*-pyrrolidyl-*N'*-(2,2-dimethylpropanoyl)thioureato]platinum(II) and 330 ppm *bis*-[*N*-pyrrolidyl-*N'*-(2,2-dimethylpropanoyl)thioureato]palladium(II) was made by dissolving 0.0040 g and 0.0033 g respectively, in 0.2 ml tetrahydrofuran (THF) and making up to 10 ml with acetonitrile. Exactly 5 ml and 1 ml were diluted to 10 ml and 1 ml to 100 ml with 2/98 (%v/v) THF/CH_3CN. The HPLC data obtained from these standard solutions was used to plot the Pt(II) and Pd(II) complex calibration graphs against which the samples were measured.

Quantitative analysis: A sample, which was a solution of a mixture of Pt(II) and Pd(II), exactly 103.4 and 61.9 ppm respectively, was made by dissolving 0.0044 g K_2PtCl4 and 0.0038 g K_2PdCl_4 in 10 ml of 0.1 mol.dm^{-3} HCl. A 20 ml solution of *N*-pyrrolidyl-*N'*-(2,2-dimethylpropanoyl)thiourea whose concentration was such that the number of moles (of ligand) in 2 ml aliquot would be ten times the combined number of moles Pt(II) and Pd(II) in 1 ml, was prepared in acetonitrile. Exactly 1 ml of Pt(II)-Pd(II) solution was mixed with 2ml ligand solution. The mixture was shaken briefly. Exactly 1ml of a saturated solution of sodium chloride was added and the mixture shaken briefly again, and then allowed to settle. The acetonitrile phase was analysed. This was repeated three times.

The volume of acetonitrile that gets separated by addition of a saturated solution of sodium chloride was determined by mixing exactly 10 ml of 0.1 mol.dm^{-3} HCl with 20 ml of CH_3CN and adding 10 ml of a saturated solution of sodium chloride in a 50 ml ground-neck measuring cylinder. The layer of acetonitrile that formed was exactly 17 ml. Proportionally, 1.7 ml of 2 ml acetonitrile is recovered in the treatment of samples.

Determination of error: A sample of Pd(II) in 0.1 mol.dm^{-3} HCl was prepared. A ligand solution, *N*-pyrrolidyl-*N'*-(2,2-dimethylpropanoyl)thiourea in CH_3CN was also prepared. The concentrations of these two solutions and were such that the number of moles of *N*-pyrrolidyl-*N'*-(2,2-dimethylpropanoyl)thiourea in a 2 ml aliquot were ten times those of Pd(II) in 1 ml. A total of ten HPLC samples in which Pd(II) was transformed into a complex, were prepared following the same procedure as given in Figure 3.17. Each sample was analysed immediately after the two layers have separated out completely.

4.

Determination of Pt, Pd and Rh by Laser Ablation-Inductively Coupled Plasma Mass Spectrometry (LA-ICP MS), after pre-concentration as complexes of *N*,*N*-di(2-hydroxyethyl)-*N'*-benzoylthiourea

4.1. Introduction

In chapter 3, it was shown that it is possible to determine platinum(II) and palladium(II) in aqueous solutions by RP-HPLC, after these metals have been complexed with *N,N*-dialkyl-*N'*-acylthioureas. At the metal concentrations below one part per million, however, RP-HPLC results appear to have wide error margins. As a way of establishing "proof of the principle" of quantitative complexation of the platinum group metals in aqueous solutions with *N,N*-dialkyl-*N'*-acylthioureas at even lower concentrations, we decided to investigate complexation (with *N,N*-di(2-hydroxyethyl)-*N'*-benzoylthiourea) in the analysis of platinum, palladium and rhodium by Laser Ablation - Inductively Coupled Plasma Mass Spectrometry (LA-ICP MS).

LA-ICP MS is a micro-analytical technique for the determination of trace elements in solid materials. A pulsed laser beam is used to ablate a small quantity of sample material, which is transported into the plasma by a stream of carrier/nebulizer gas. Molecular dissociation and subsequent ionization of atoms takes place in the plasma. The positively charged analyte ions generated are extracted from the high temperature, atmospheric pressure environment of the plasma into a high vacuum enclosure *via* an interface region, which has small apertures. The analyte isotopes are then separated according to their mass to charge ratio by a mass spectrometer and detected and measured by the detector (commonly an electron multiplier). Intensities of the signals due to analytes are directly proportional to the analytes' respective concentrations. A representation of the laser ablation section of the instrument is shown in Figure 4.1.

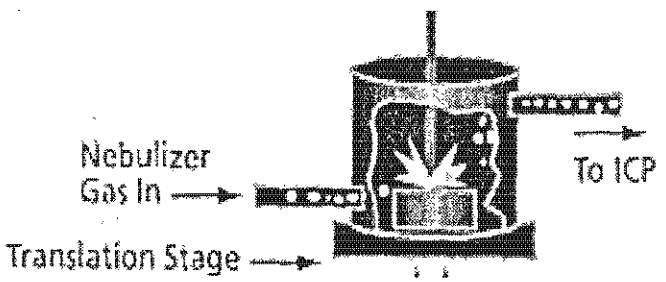

Figure 4.1: A representation of the laser ablation section of LA-ICP MS.

A mass spectrometer provides a more sensitive detection as compared to the measurement of the intensity of emitted or absorbed spectral line[20]. The measurement is, however, not without potential for error and interference. The signals from the ion of interest and other atomic groups, which differ from the analyte by less than 0.5 atomic mass units, can overlap. This tendency is predominant in quadrupole mass spectrometers due to their limited resolution. Three types of interference occur in ICP MS:

(i) **Isobaric interference** occur due to the presence of isotopes of the same mass as the analyte.

(ii) **Molecular interference** is due to recombination of sample ions with argon or other matrix components such as O, H, N, etc, in the cooler regions of the plasma.

(iii) **Doubly-charged ion interference** is due to doubly-charged matrix ions with twice the mass of the analyte because the mass/charge ratio is the same. $^{179}Hf^{16}O^{+}$, for example, produces a signal which overlaps with that of $^{195}Pt^{+}$, $^{66}Zn^{40}Ar^{+}$, $^{90}Zr^{16}O^{+}$, $^{106}Cd^{+}$ and $^{89}Y^{16}O^{1}H^{+}$ signals overlap with that of $^{106}Pd^{+}$, while $^{63}Cu^{40}Ar^{+}$, $^{206}Pb^{2+}$, $^{86}Sr^{16}O^{1}H^{+}$, $^{87}Sr^{16}O^{+}$ and $^{87}Rb^{16}O^{+}$ produce signals which overlap with that of $^{103}Rh^{+}$.

A useful table of ICP interferences has been compiled by May and Wiedmeyer[70]. It is important to understand that the analyte ions are mainly singly charged because argon (plasma) has an ionization potential of 15.76eV, which is only just or slightly greater than the first ionization potential of most elements.

The selective complexation of *N,N*-dialkyl-*N'*-acylthioureas of the platinum group metals[53,54] has two potential advantages in trace and ultra-trace analysis of these metals. Firstly, interfering matrix elements can be eliminated, and secondly, it is possible to pre-concentrate the complexes. Interference by matrix elements and working at extremely low concentrations of the metals of interest are the major causes of error in many ICP MS determinations.

This method can only be used for the preparation of phenazines bearing the same substituents in the 2 and 7 positions. It has recently[5] been used for the synthesis of 2,7-dicarboxyphenazine.

Phenazine (III) was obtained by the self-condensation of o-bromoaniline in boiling nitrobenzene[6]:

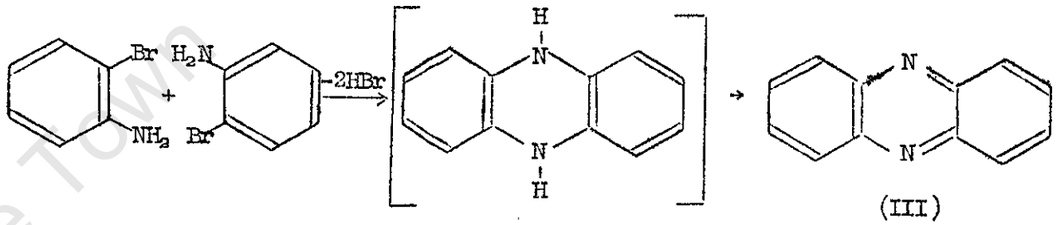

(III)

This is the only example to be found of this type of condensation. Gray[7] was unsuccessful in his attempt to obtain 2,7-dinitrophenazine from 2-bromo-5-nitroaniline.

A method has been described[8] by which phenazine can be obtained in 60 - 70% yield by heating 2-aminodiphenylamine (IV), 2-nitrodiphenylamine (V) and sodium acetate at 250 - 300°:

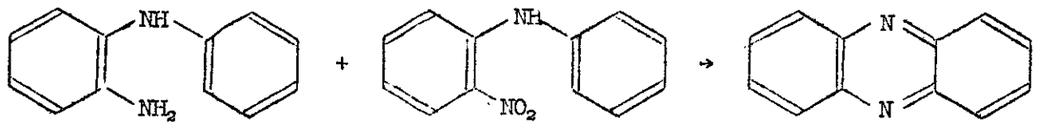

(IV) (V)

However, a number of authors[9,10,11] reported very low yields on repeating this reaction.

A reaction which has been investigated very thoroughly[12-20] is the oxidation of o-phenylenediamine to give 2,3-diaminophenazine (VI):

4.2. Procedure of PGM pre-concentration and analysis

Exactly 200µl of methanol solution of *N,N*-di(2-hydroxyethyl)-*N'*-benzoylthiourea, calculated to be a sixteen fold molar excess of the combined Pt, Pd and Rh, was added to the 0.1M HCl solution of known concentrations of Pt, Pd and Rh. We chose this ligand design to exploit the lipophilicity of the aromatic ring (useful for adsorption onto non-polar surfaces) on the one hand, and hydrophilicity of di-(2-hydroxyethyl)amine substituent (useful for solubility in aqueous medium) on the other. An equivalent of 10 fold molar excess (relative to Pt, Pd and Rh), of catalyst (exactly 600µl of a 0.02M $SnCl_2$ solution) was added, and the mixture was heated to about 80°C while stirring. The reaction was allowed to proceed for 1h in a sealed flask. Tin(II) chloride was used successfully as a catalyst by Schuster *et al*[71] in solvent extraction of PGMs with benzoylthiourea.

Six standard solutions between 0.009 and 0.5ppm of Pd, Pt and Rh, were made by dilution of the reaction mixture. Each solution was passed by buchner funnel filtration through a commercially available "ENVI-18DSK", which is a C18 modified, silica disk supplied by Supelco, Incorporated (Figure 4.2). For consistency in this solid phase extraction process of the PGM complexes, a consistent, low vacuum was used.

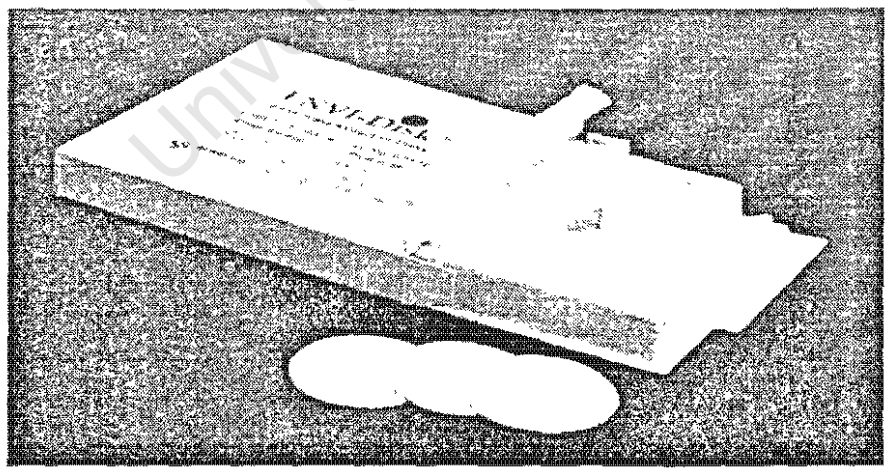

Figure 4.2: The C18 modified silica disks used for the solid phase extraction of complexes.

The disks were allowed to dry in air, followed by LA-ICP MS analysis using a peak-hopping mode of acquisition. A flow diagram of the steps of standard and sample preparation is shown in Figure 4.3.

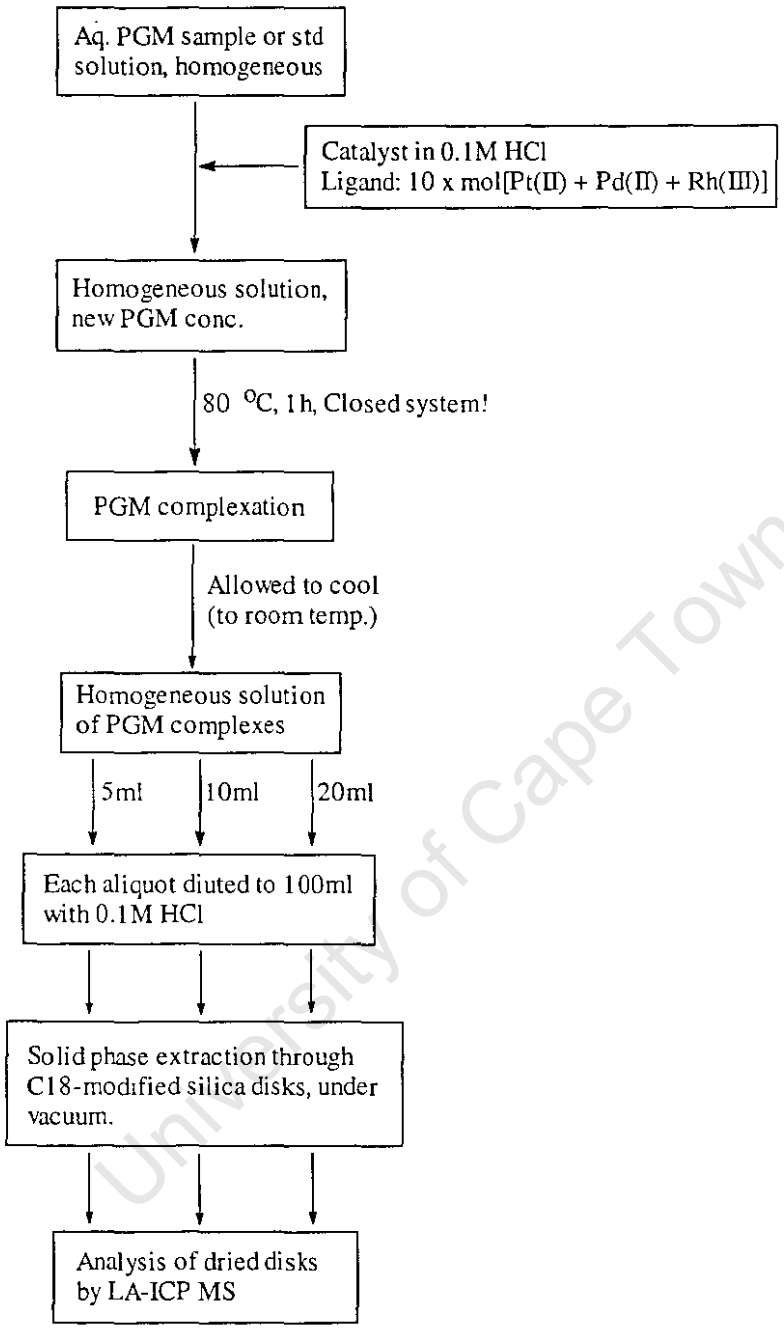

Figure 4.3: Preparation of standards and samples for analysis with LA-ICP MS.

The efficiency of the extraction was determined by measuring the amount of PGMs remaining in solution after extraction (using three standard solutions prepared according to the procedure shown in Figure 4.3) by a conventional ICP MS. From this, the amount of complex adsorbed could be determined to calculate recoveries. Quantitative recoveries (Table 4.1) were obtained.

Table 4.1. Recoveries obtained in the solid phase extraction procedure.

	Std sltn	Pt	Pd	Rh
Conc.(g/l) before adsorption	1	2×10^{-3}	2×10^{-3}	2×10^{-3}
	2	4×10^{-3}	4×10^{-3}	4×10^{-3}
	3	6×10^{-3}	6×10^{-3}	6×10^{-3}
Conc.(g/l) after adsorption	1	0.58×10^{-6}	$0.26 \times 10^{6-}$	14.9×10^{-6}
	2	1.34×10^{-6}	0.26×10^{-6}	28.1×10^{-6}
	3	2.34×10^{-6}	0.16×10^{-6}	42.5×10^{-6}
Average % Recovery		**99.97**	**99.99**	**99.28**

Further assessment of the present methodolgy was undertaken by the inspection of the surface of the C18 silica disks with an electron-microscope equipped with an x-ray probe. Since the solubility of Pt(II), Pd(II) and Rh(III) complexes of *N,N*-di(2-hydroxyethyl)-*N'*-benzoylthiourea is very low in the aqueous solvent medium, the process of retention of the complexes on the disk could well be filtration of a fine precipitate rather than chemical sorption by the C18 phase. To examine this possibility, various sections of a used disk were examined and photographed under an electron microscope for investigation of the presence of Pt(II), Pd(II) and Rh(III) complex precipitates that may have been filtered or entrapped within the disk matrix, after it was used. These disks were also examined by means of Energy Dispersive X-ray Spectroscopy. Some electron microscope photographs are shown in Figure 4.5 and a typical x-ray spectrum of a section of a used C18 silica disk is shown in Figure 4.6.

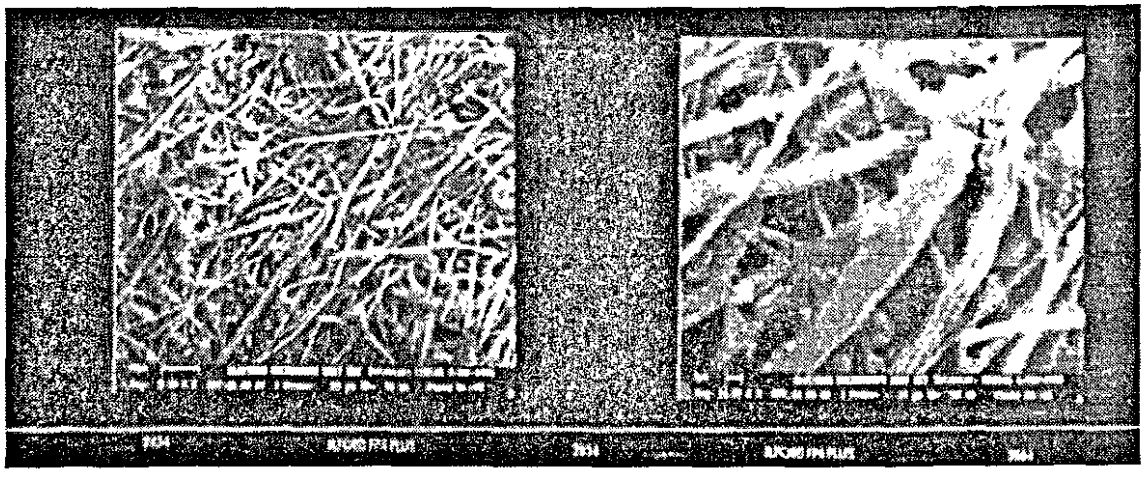

Figure 4.5: Electron microscope photographs of sections of a used C18 silica disk, magnified 3.5×10^3 and 14.9×10^3 times, left and right, respectively.

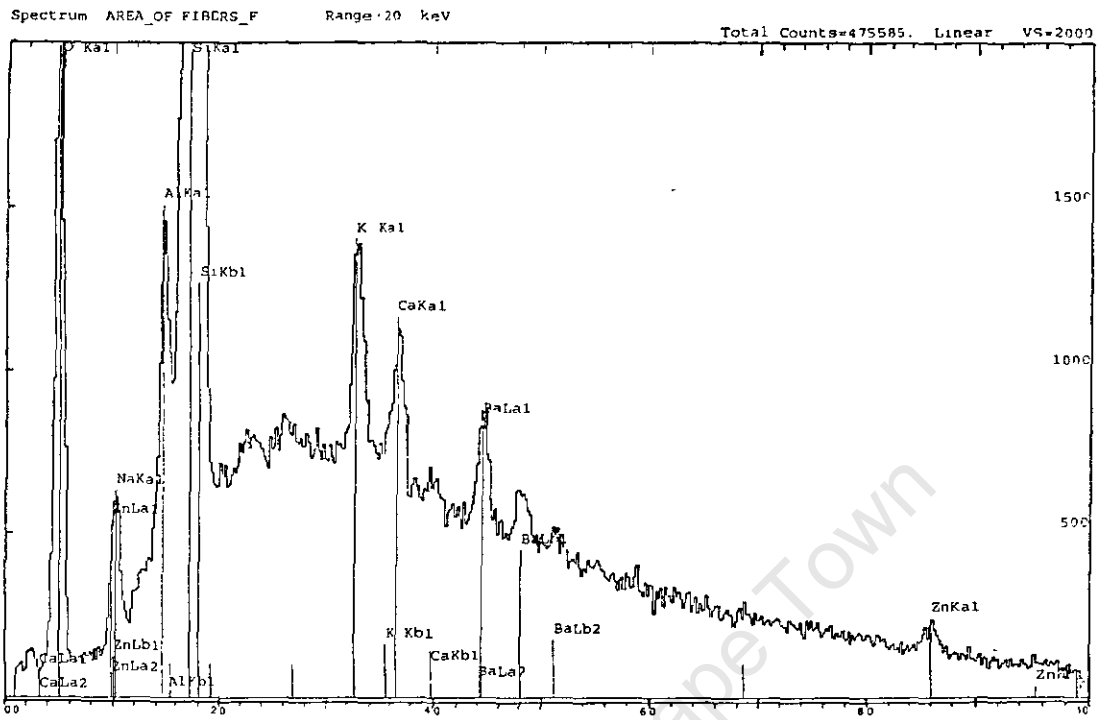

Figure 4.6: A typical x-ray spectrum of a section of a used C18 silica disk.

It was found that the silica particles are not shaped or arranged in any regular form, which would make it easier for the identification of foreign particulates (figure 4.5). The x-ray analysis of the particles, including the 1μm (in diameter) ones, show the same elemental composition in all sections (Figure 4.6). No evidence for the precipitation of metal complexes of *N,N*-di(2-hydroxyethyl)-*N'*-benzoylthiourea could be found, which suggests that true adsorption of the Pt(II), Pd(II) and Rh(III) complexes onto the C18 phase (of the silica disk) had taken place.

Among other elements detected by energy dispersive x-ray spectroscopy in the disks, are Zn, Si, Al and Ca from which a suitable internal standard was selected, in view of the advantages of internal standard calibration method over external standard calibration in ICP MS. Six different disks were quantitatively analysed for the amounts of these elements by LA-ICP MS, to check the concentration levels and consistency from one disk to the next. The intensity of $^{44}Ca^{+}$ appeared to fall in the calibration range of the platinum, palladium and rhodium standards (0.009 to 0.5ppm)

while intensities of Si, Zn and Al ions did not. It was thus decided to study $^{44}Ca^{+}$ as an internal standard for the determination of platinum, palladium and rhodium by LA-ICP MS. The calibration graphs are shown in Figures 4.7, 4.8 and 4.9. In all the cases (i.e. Pt, Pd and Rh), the external standard method of calibration gives a better linear correlation of co-ordinates than the (^{44}Ca) internal standard method. The concentration of $^{44}Ca^{+}$ appear to vary significantly and leads to poor linearity of the calibration graphs.

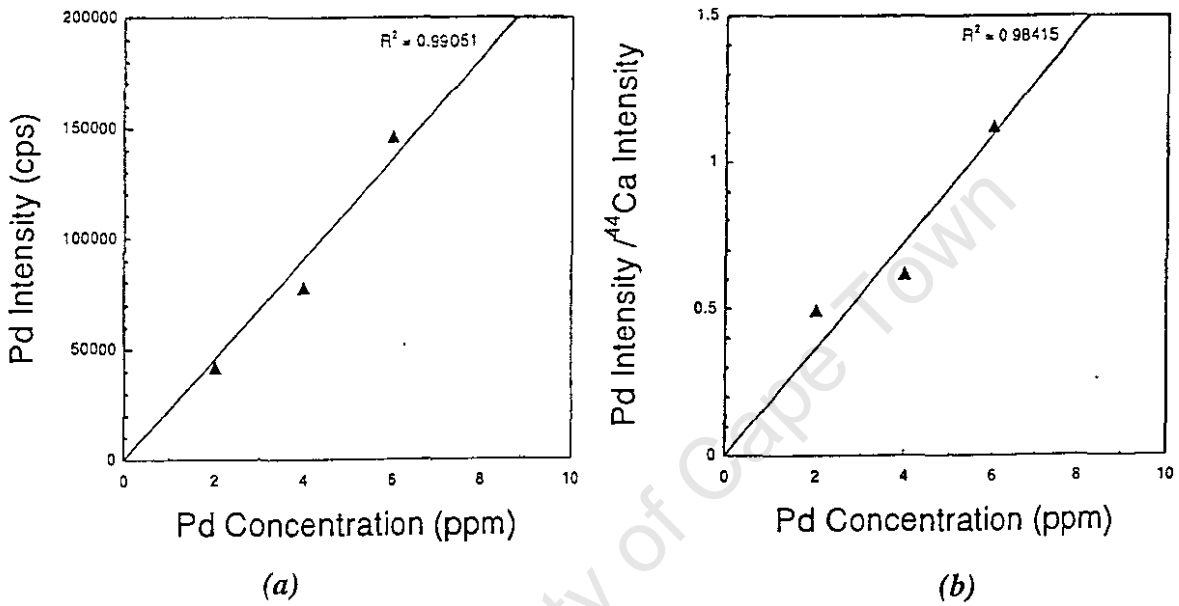

Figure 4.7: External standard calibration (a) gives better linear correlation for palladium. The internal standard calibration (b) gives poor linear correlation due to inconsistent concentration of Ca in the disk (the internal standard).

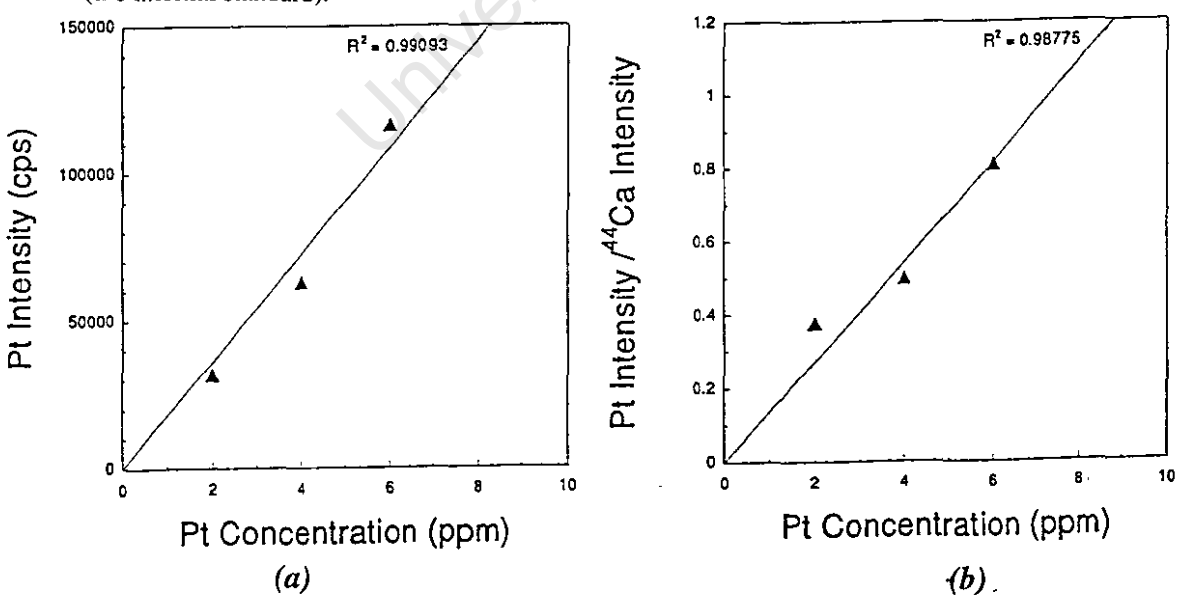

Figure 4.8: External standard calibration (a) gives better linear correlation for platinum. The internal standard calibration (b) gives poor linear correlation due to inconsistent concentration of Ca in the disk (the internal standard).

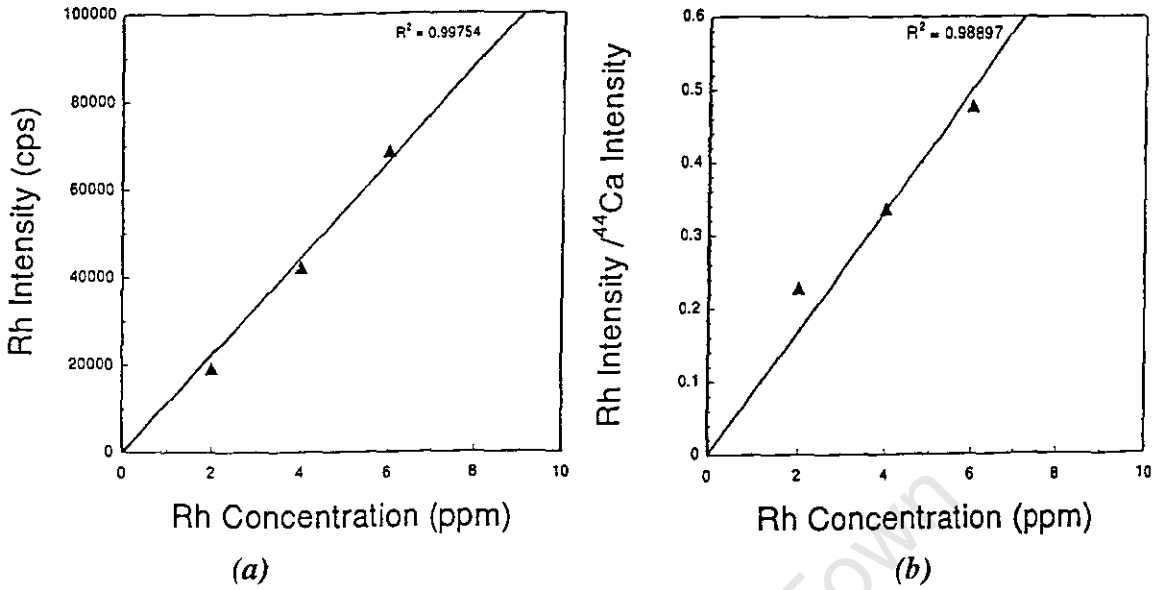

Figure 4.9: External standard calibration (a) gives better linear correlation for rhodium. The internal standard calibration (b) gives poor linear correlation due to inconsistent concentration of Ca in the disk (the internal standard).

Quantitative analyses of platinum, palladium and rhodium were therefore carried out using the external calibration method. The data obtained from the disks (Table 4.2) was used to construct the calibration graphs (Figure 4.4).

Table 4.2. The LA-ICP MS calibration data (n = 6).

	Std solution	Conc.(ppm)	Av. Intensity (cps)
Pt	1	0.00921	25170.5
	2	0.01842	50296.2
	3	0.04605	138811.7
	4	0.09211	273190.3
	5	0.18422	566999.9
	6	0.46055	1411512.0
Pd	1	0.00911	25877.5
	2	0.01822	53394.7
	3	0.04555	154553.3
	4	0.09111	304028.1
	5	0.18222	645515.2
	6	0.45555	1434548.0
Rh	1	0.00929	7487.2
	2	0.01858	16091.9
	3	0.04646	41069.0
	4	0.09292	81133.4
	5	0.18584	170937.7
	6	0.46460	444882.6

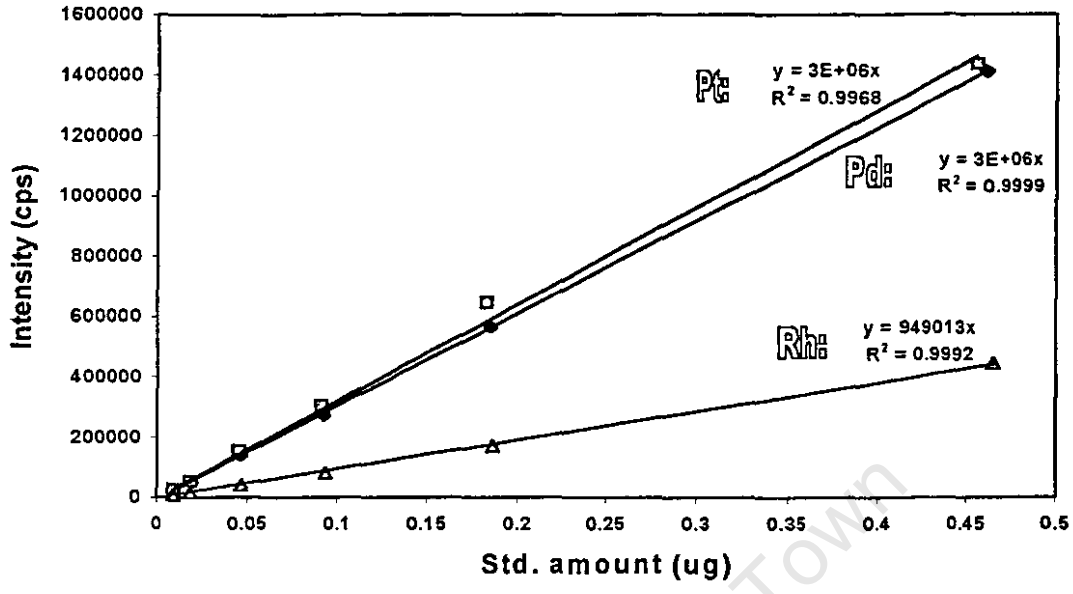

Figure 4.4: LA-ICP MS calibration graphs of platinum, palladium and rhodium.

For each standard solution, six measurements were taken. Standard deviations associated with these measurements were calculated (Table 4.3).

Table 4.3: Relative standard deviations, $\sigma_{n=6}$ [= (std dev.)/(mean) x 100], associated with LA-ICP MS measurements at different levels of concentration (n = 6).

Concentration (ppm)	Platinum [%RSD]	Palladium [%RSD]	Rhodium [%RSD]
0.01	7.64	6.30	8.97
0.02	7.14	5.75	8.96
0.05	21.35	22.05	23.62
0.10	14.12	14.67	15.12
0.20	15.28	15.72	16.92
0.50	16.11	29.85	16.22

Some replicate measurements tend to have wide relative standard deviations, presumably because the disks are not perfectly homogeneous. Nonetheless, average values give linear calibration graphs with correlation factors > 0.999 for Pd and Rh,

and > 0.996 for Pt as can be seen in figure 4.4. Results of a sample of post-process effluent supplied by Anglo American Platinum Limited (AMPLATS), obtained by the present method were closely comparable to those obtained by a conventional ICP method (Table 4.4).

Table 4.4. Analytical results of a sample (344-TK-03) of real post-process effluent.

	Platinum (ppm)	Palladium (ppm)	Rhodium (ppm)
Present method:	164.0 ± 18.0%	53.1 ± 19.9%	54.9 ± 20.8%
Conventional ICP:	167.0	44.9	Not analysed

4.3. Discussion

The scope of the application of LA-ICP MS in the analysis of PGMs after their complexation with *N,N*-dialkyl-*N'*-acylthioureas is potentially much wider than has been covered by the present study. It has been demonstrated in this study by recoveries obtained in the solid phase extraction procedure (Table 4.1), however, that transformation of PGMs into C18 adsorbed *N,N*-dialkyl-*N'*-acylthiourea complexes is quantitative.

Refinements of this method could include the measurement of maximum PGM loading capacity of the disk. The optimum surface area for adsorption could be determined leading to extractions of ultra-low concentrations. In the final stage, the method of determination of traces of PGMs in post-process effluents by LA-ICP MS could be fully automated and adapted on-line.

Advantages of the application of LA-ICP MS for the trace analysis of PGMs exceed those of reversed phase high performance liquid chromatography (RP-HPLC). These include the impressively low detection limits of platinum group elements which are estimated at 10 ppt[20]. While retention is thought to be lipophilic, van der Waal type attraction between neutral complex molecules and the C18 hydrocarbon chains, any adsorbed PGM species regardless of their molecular form and mechanism of retention, get ablated and are counted in the determination. On the same note, however, the cost of LA-ICP MS is much higher than that of HPLC.

5.

Conclusions

5.1. Synthesis and Characterisation of ligands and complexes

The synthesis of relatively hydrophilic derivatives of *N,N*-dialkyl-*N'*-acylthioureas, namely *N,N*-dimethyl-, *N*-pyrrolidyl- and *N*-piperidyl-*N'*-(2,2-dimethylpropanoyl)-thioureas, has been a simple two step process. High yields were obtained. Preparation of the complexes of platinum(II) and palladium(II) using these ligands has been simple and was carried out at room temperature. However, the rate of rhodium(III) complexation was slow and required heating under reflux. These complexes and the ligands showed sharp melting points and were well characterised by ^{13}C NMR and elemental analysis.

The structure of *tris*-[*N*-pyrrolidyl-*N'*-(2,2-dimethylpropanoyl)thioureato]rhodium(III) was determined by x-ray diffraction analysis, which revealed that it is an octahedral, *facial* isomer. The bond lengths and angles compare closely with those of a similar complex, *tris*-[*N,N*-diethyl-*N'*-benzoylthioureato]rhodium(III), reported by Bensch and Schuster[64].

5.2. Reversed Phase - High Performance Liquid Chromatography (RP-HPLC) of complexes

Using mainly *N*-pyrrolidyl-*N'*-(2,2-dimethylpropanoyl)thiourea ligand, we have been able to demonstrate that *N,N*-dialkyl-*N'*-acylthiourea complexes of platinum(II), palladium(II) and rhodium(III) are suitable for reversed phase-liquid chromatography (RP-HPLC). A simple and convenient method of sample preparation has been developed, with which it is possible to determine platinum(II) and palladium(II) directly in dilute HCl concentrations (between 0.1 to 0.5M) by *in situ* complex formation followed by salt-induced phase separation of an acetonitrile phase. While RP-HPLC results of a sample of a real post-process effluent for platinum(II) and palladium(II) are closely comparable with results from a more established Inductively Coupled Plasma (ICP) method, platinum(IV) requires further study. Rhodium(III) complexation proved to be extremely slow at room temperature, however. It has consequently, not been possible to determine rhodium(III) by RP-HPLC using the same complexation procedure as for platinum(II) and palladium(II).

The RP-HPLC limits of detection for palladium(II) and platinum(II) in 0.1M HCl solutions are 0.5 and 2ppm, respectively, while the limits of determination are about 5ppm for palladium(II) and 10ppm for platinum(II). In general, the relative error of the RP-HPLC results at concentrations higher than 10ppm for platinum(II) and 5ppm for palladium(II), falls within ± 5%. At lower concentrations the relative error increases as expected and reaches ± 20%.

5.3. Determination of Pt, Pd and Rh by Laser Ablation - Inductively Coupled Plasma Mass Spectrometry (LA-ICP MS), after pre-concentration as complexes of *N,N*-di(2-hydroxyethyl)-*N'*-benzoylthiourea

In this section of the work, the results (which are preliminary) have shown that platinum, palladium and rhodium can be quantitatively pre-concentrated on commercially available "ENVI-18", C18-modified silica disks, as complexes of *N,N*-di(2-hydroxyethyl)-*N'*-benzoylthiourea and determined by means of Laser Ablation-Inductively Coupled Plasma (LA-ICP MS) in principle. Concentrations down to 1μg.dm^{-3} of platinum, palladium and rhodium could be detected.

Calibration graphs extending down to 9 μg.dm^{-3} for all three metals, were linear with correlation factors (r^2) greater than 0.997, which confirm that after complexation with a suitable *N,N*-dialkyl-*N'*-acylthiourea to enable pre-concentration, determination of very low concentrations of platinum, palladium and rhodium can be achieved. This work should be extended to the development of a method for the determination of PGMs in real process effluents.

5.4. Future work

For the determination of rhodium(III) by reversed phase-high performance liquid chromatography (RP-HPLC), it appears that a catalyst is necessary in order to achieve quantitative complexation of rhodium(III) with *N,N*-dialkyl-*N'*-acylthioureas in a shorter, practical time and at room temperature. It is also necessary to find a means of reducing platinum(IV) to platinum(II) prior to complexation of this metal with a

suitable *N,N*-dialkyl-*N'*-acylthiourea ligand. On this point, several reducing agents have been reported by House *et al*[72], which include tin(II), ascorbic acid, iron(II), hydroxylamine hydrochloride and sodium thiosulfate. It is known that tin(II) chloride can help catalyse ligand co-ordination onto metal ions such as rhodium(III), which should be explored.

References

1. Neucki K., *Berichte der Deutschen Gesellschaft, 6(1873)598.*
2. Douglas I.B. and Dains F.B., *J. Amer. Chem. Soc., 56(1934)719.*
3. Miller J., *PhD thesis - University of Cape Town, 2000.*
4. Shome S.C., Mazumder M., Haldar P.K. and Das D.K., *J. Indian Chem. Soc., LIV(1977)947.*
5. Schuster M., *Fres. J. Anal. Chem., 342(1992)791.*
6. Koch K.R., Sacht C., Grimmbacher T. and Bourne S., *S. Afr. J. Chem., 48(1995)71.*
7. Annual report 1999, Anglo American Platinum Corporation Limited, Johannesburg, South Africa, 1999.
8. Patterson J.W. and Passino R, *Metal speciation, separation and recovery*, Lewis publishers, Michigan, USA, 1990.
9. Savitskii E.M., *Handbook of precious metals*, Hemisphere publishing corporation, New York, 1989.
10. Hartley F.R., *Chemistry of the platinum group metals*, Elsevier, Amsterdam, 1991.
11. Robinson D., Personal communication: Amplats PGM refinery - Rustenburg.
12. Reece P.A., McCall J.T., Powis G. and Richardson R.L., *J. Chrom., 306(1984)417-423.*
13. Bannister S.J., Sternson L.A. and Repta A.J., *J. Chrom., 173(1979) 33-342.*
14. Reedijk J., *Pure and applied chemistry, 59(1987)181.*
15. Balcerzak M., *Analyst, 122(1997)67R.*
16. Cotton F.A. and Wilkinson G., *Advanced Inorganic Chemistry 5th Edition*, John Wiley and Sons, New York, 1988.
17. Cotton S.A., *Chemistry of precious metals 1st Edition*, Chapman and Hall, London, 1997.
18. Pyrzynska K., *Talanta, 47(1998)841.*
19. De Soete D., Gijbels R. and Hoste J., *Neutron activation analysis, volume 34*, Wiley-interscience, London, 1972.
20. Skoog D.A. and West D.M., *Principles of instrumental analysis*, Saunders College, Philadelphia, 1980.
21. Reddi G.S. and Rao C.R.M., *Analyst, 124(1999)1531.*

22. Wildhagen D. and Krivan V., *Anal. Chim. Acta, 274(1993)257.*

23. Lajunen L.H.J., *Spectrochemical analysis by atomic absorption and mission,* Royal society of chemistry, Cambridge, 1992.

24. Pinta M., *Modern methods for trace element analysis,* Ann Arbor science, Michigan, 1978.

25. Farago M.E., Kavanagh P., Blanks R., Kelly J., Kazantzis G, Thornton I., Simpson P.P., Cook J.M., Delves H.T., and Hall G.E.M., *Analyst, 123(1998)451.*

26. Jarvis I., Totland M.M. and Jarvis K.E., *Analyst, 122(1997)19.*

27. Brajter K. and Slonawska K., *Talanta, 30(1983)471.*

28. Brajter K. and Slonawska K., *Fres. J. Anal. Chem., 323(1986)145.*

29. Coedo A.G., Dorado M.T., Padilla I., and Alguacil F., *Anal. Chim. Acta 340(1997)31.*

30. Borisov O.V., Coleman D.M. and Carter III R.O., *J. Anal. Atomic Spectroscopy, 12(1997)231.*

31. Kanicky V., Otruba V. and Mermet J.M., *Talanta, 48(1999)859.*

32. Schuster M. and Schwarzer M., *Anal. Chim. Acta, 328(1996)1.*

33. Jones P. and Schwedt G., *Anal. Chimica Acta, 220(1989)195.*

34. Robards K. and Starr P., *Analyst, 116(1991)1247.*

35. Tong A., Akama Y. and Tanaka S., *Anal. Chim. Acta, 230(1990)170.*

36. Konig K.H., Ehmcke H.U., Schneeweis G. and Steinbrech B., *Fres. J. Anal. Chem. 297(1979)411.*

37. Steinbrech B., Schneeweis G. and Konig K.H., *Fres. J. Anal. Chem., 311(1982)499.*

38. Kohler J. and Schomburg G., *J. Chrom., 255(1983)311.*

39. Nickless G., *J. Chrom., 313(1985)129.*

40. Munder A., and Ballschmiter K., *Fres. J. Chem., 323(1986)869.*

41. Ichinoki S., and Yamazaki M., *J. Chrom. Sc., 29(1991)184.*

42. Snyder L.R., Kirkland J.J and Glajch J.L., *Practical HPLC method development,* John Wiley & Sons Inc., New York, 1997.

43. McMaster M.C., *HPLC - a practical user's guide,* VCH publishers Inc., New York, 1994.

44. Alimarin I.P., Ivanov V.M., Bol'shova T.A. and basova E.M., *Fres. Z. Anal. Chem., 335(1989)63.*

45. Mueller B.J. and Lovett R.J., *Anal. Chem., 57(1985)2693.*

46. Mueller B.J. and Lovett R.J., *Anal. Chem., 59(1987)1405.*
47. Gurira R.C. and Carr P.W., *J. Chrom. Sc., 20(1982)461.*
48. Wuping L. and Qiping L., *Fres. J. Anal. Chem., 350(1994)671.*
49. Qiping L.,Yuanchao W.,Jinchun L. and Jieke C., *Talanta, 42(1995)901.*
50. Zhang H.S., Mou W.Y. and Cheng J.K., *Talanta, 41(1994) 1459.*
51. Ramesh A., *Talanta, 41(1994)355.*
52. Wang H., Zhang H.S. and Cheng J.K., *Talanta, 48(1999)1.*
53. Schuster M. and Unterreitmaier E., *Anal. Chim. Acta 309(1995)339.*
54. Schuster M. and Unterreitmaier E., *Fres. J. Anal. Chem., 346(1993)630.*
55. Koch K.R., Sacht C. and Bourne S., *Inorg. Chim. Acta 232(1995)109.*
56. Koch K.R., Irving A. and Matoetoe M.C., *Inorganica Chim. Acta, 206(1993)193.*
57. Matoetoe M.C., *M.Sc. thesis - University of Cape Town, 1990.*
58. Pearson R.G., *Chemical hardness*, Wiley - VCH, Weinheim, 1997.
59. Bourne S. and Koch K.R., *J. Chem. Soc. Dalton Trans., (1993)2071.*
60. Wang Y., *M.Sc. Thesis - University of Cape Town, 1997.*
61. Koch K.R. and Matoetoe M.C., *Magnetic resonance in chemistry, 29(1991)1158.*
62. Lallemand J.Y., Soulie J. and Chottard J.C., *Chem. Comm. (1980)436.*
63. Perrin D.D., Dempsey B. and Sergeant E.P., *pKa prediction for organic acids and bases*, Chapman and Hall, London, 1981.
64. Bensch W. and Schuster M., *Z. Anorg. Allg. Chem., 615(1992)93.*
65. Blanco M., Iturriaga H., Maspoch S. and Tarin P., *J. Chem. Education, 66(1989)178.*
66. North A.C.T., Phillips D.C. and Matthews F.S., *Acta Crystallogr., A24(1968)351.*
67. Martin A.J.P. and Synge R.L.M., *Journal of Biochemistry*, **35**(1941)1358.
68. Harrison P.G., *Chemistry of Tin*, Blackie & Son Limited, Glasgow 1989.
69. Jeffrey G.H., Bassett J., Mendham J. and Denney R.C., *Vogel's textbook of quantitative chemical analysis* 5^{th} ***edition***, Longman Scientific & Technical, London, 1989.
70. May T.W. and Wiedmeyer R.H., *Atomic spectroscopy 19(1998)150.*
71. Schuster M., Vest P. and Konig K.H., *Fres. J. Anal. Chem. 339(1991)142.*
72. Hindmarsh K., House D.A. and van Eldik R., *Inorg. Chim. Acta 278(1998)32.*
73. Skoog D.A., West D.M. and Holler F.J., *Fundamentals of analytical chemistry,* 5^{th} ***Edition***, Saunders College, New York, 1988.

Appendix I

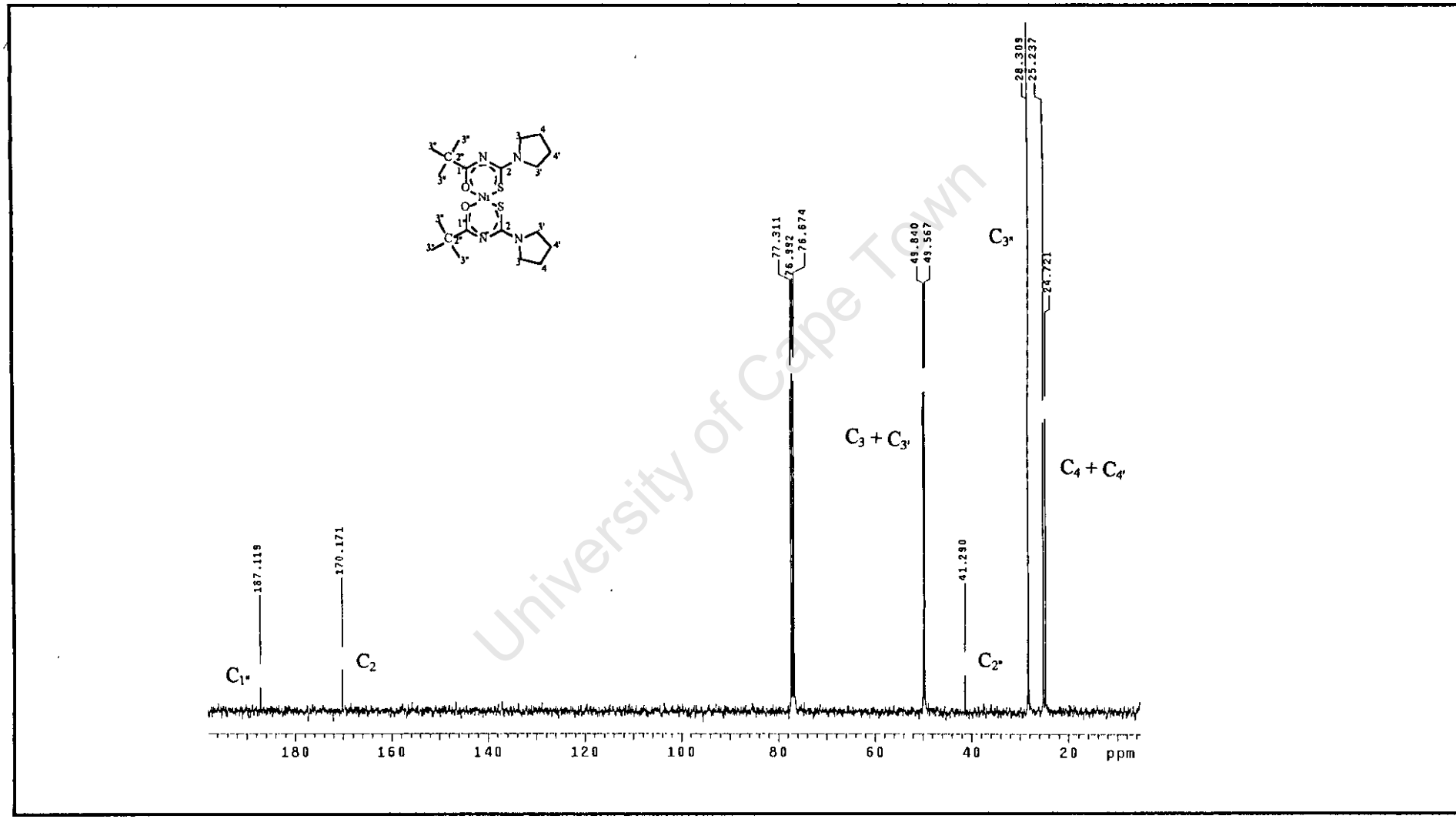

Figure I(Appendix): A ^{13}C NMR spectrum of *bis*-[*N*-pyrrolidyl-*N'*-(2,2-dimethylpropanoyl)thiourcato]nickel(II).

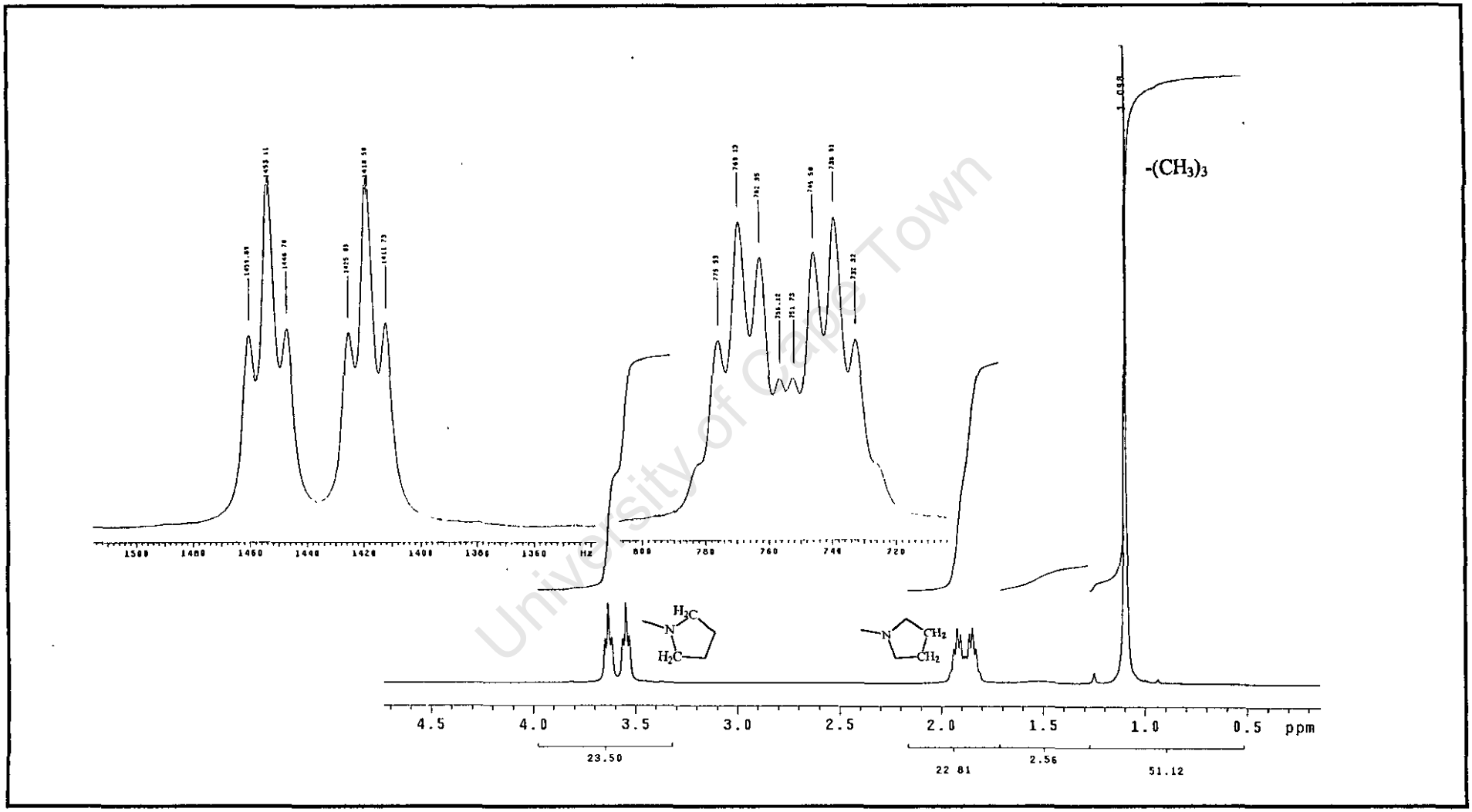

Figure II (Appendix): A ^{1}H NMR spectrum of *bis*-[*N*-pyrrolidyl-*N'*-(2,2-dimethylpropanoyl)thioureato]nickel(II).

Table I (Appendix). Crystal data and structure refinement for *bis*-[*N*-pyrrolidyl-*N'*-(2,2-dimethylpropanoyl)thioureato]rhodium(III).

Empirical formula	$C_{30}H_{51}N_6O_3RhS_3$. $CHCl_3$	
Formula weight	862.23	
Temperature	293(2) K	
Wavelength	0.71070 Å	
Crystal system, space group	Triclinic. P1	
Unit cell dimensions	a = 10.697(4) Å b = 13.454(6) Å c = 14.432(6) Å	alpha = 84.77(3)° beta = 89.81(3)° gamma= 78.88(3)°
Volume	2029.3(15) $Å^3$	
z, Calculated density	2, 1.411 $mg.m^{-3}$	
Absorption coefficient	0.811 mm^{-1}	
F(000)	896	
Crystal size	0.30 x 0.35 x 0.40 mm	
Theta range for data collection	1.42 to 24.98°	
Limiting indices	$-12 \le h \le 12$, $0 \le k \le 15$, $-16 \le l \le 17$	
Reflections collected / unique	7123 / 7123 [R(int) = 0.0000]	
Completeness (to theta = 24.98°)	99.8%	
Maximum and minimum transmission	0.7930 and 0.7375	
Refinement method	Full-matrix least-squares on F^2	
Data / restraints / parameters	7123 / 0 / 379	
Goodness-of-fit on F^2	1.040	
Final R indices [I > 2sigma(I)]	R1 = 0.0773, wR2 = 0.2124	
R indices (all data)	R1 = 0.0954, wR2 = 0.2259	
Largest diff. peak and hole	2.293 and -2.611 $e.Å^{-3}$	

Table II (Appendix). Atomic coordinates (x 10^4) and equivalent isotropic displacement parameters ($Å^2$ x 10^3) for *bis*-[*N*-pyrrolidyl-*N'*-(2,2-dimethylpropanoyl)thioureato]rhodium(III).

	x	y	z	U(eq)
Rh(1)	6510(1)	7166(1)	7914(1)	33(1)
O(1A)	5245(4)	7422(3)	6813(3)	43(1)
C(2A)	4064(6)	7755(5)	6874(4)	44(1)
N(3A)	3470(5)	8420(4)	7430(4)	49(1)
C(4A)	3957(5)	8803(4)	8116(4)	36(1)
S(5A)	5332(1)	8324(1)	8783(1)	40(1)
C(2A1)	3198(7)	7366(6)	6220(5)	59(2)
C(2A2)	2872(18)	8074(14)	5421(11)	168(6)
C(2A3)	1988(13)	7185(12)	6681(9)	131(4)
C(2A4)	3786(17)	6301(13)	6045(12)	167(7)
N(4A1)	3269(5)	9666(4)	8382(4)	45(1)
C(4A2)	3506(6)	10160(5)	9200(5)	53(2)
C(4A3)	2279(8)	10920(6)	9299(6)	71(2)
C(4A4)	1759(8)	11180(6)	8293(7)	76(2)
C(4A5)	2089(6)	10200(5)	7866(5)	58(2)
O(1B)	7657(4)	6183(3)	7114(3)	43(1)
C(2B)	7806(5)	5228(4)	7201(4)	39(1)
N(3B)	7013(5)	4647(4)	7554(4)	44(1)
C(4B)	5935(5)	4922(4)	8021(4)	38(1)
S(5B)	5442(1)	5999(1)	8590(1)	42(1)
C(2B1)	9023(6)	4635(5)	6807(5)	48(1)
C(2B2)	8690(12)	4305(10)	5890(8)	118(4)
C(2B3)	9574(12)	3750(10)	7388(8)	111(4)
C(2B4)	9944(13)	5331(10)	6562(9)	118(4)
N(4B1)	5196(5)	4236(4)	8099(4)	45(1)
C(4B2)	4001(6)	4343(5)	8614(5)	52(2)
C(4B3)	3461(9)	3431(7)	8404(8)	87(3)
C(4B4)	4558(9)	2667(7)	8183(9)	92(3)
C(4B5)	5504(8)	3250(5)	7713(6)	66(2)
O(1C)	7321(4)	8321(3)	7269(3)	40(1)
C(2C)	7967(5)	8822(4)	7702(4)	37(1)
N(3C)	8811(4)	8487(3)	8390(4)	42(1)
C(4C)	9044(5)	7566(4)	8845(4)	36(1)
S(5C)	8016(1)	6726(1)	9058(1)	41(1)
C(2C1)	7824(6)	9957(4)	7367(4)	45(1)
C(2C2)	8833(8)	10052(7)	6653(6)	73(2)
C(2C3)	8037(8)	10563(7)	8164(6)	72(2)
C(2C4)	6523(8)	10348(7)	6939(6)	68(2)
N(4C1)	10185(4)	7291(4)	9256(4)	42(1)
C(4C2)	10637(6)	6328(5)	9806(5)	53(2)
C(4C3)	12007(7)	6377(7)	10055(7)	81(3)
C(4C4)	12075(9)	7440(8)	9985(8)	98(3)
C(4C5)	11112(6)	7963(5)	9253(5)	57(2)
C(1G)	7250(9)	7871(7)	5011(6)	82(3)
Cl(1G)	6240(3)	8993(2)	4611(2)	116(1)
Cl(2G)	7072(4)	6885)	4390(3)	139(1)
Cl(3G)	8839(3)	8031(4)	4918(3)	149(2)

Table III (Appendix). Bond lengths (Å) and angles (degrees) for *bis*-[*N*-pyrrolidyl-*N'*-(2,2-dimethylpropanoyl)thioureato]rhodium(III).

Rh(1)-O(1A)	2.051(4)	O(1A)-Rh(1)-O(1B)	85.93(17)
Rh(1)-O(1B)	2.058(4)	O(1A)-Rh(1)-O(1C)	86.79(16)
Rh(1)-O(1C)	2.070(4)	O(1B)-Rh(1)-O(1C)	87.72(16)
Rh(1)-S(5B)	2.2654(17)	O(1A)-Rh(1)-S(5B)	89.43(13)
Rh(1)-S(5C)	2.2686(17)	O(1B)-Rh(1)-S(5B)	95.85(12)
Rh(1)-S(5A)	2.2749(17)	O(1C)-Rh(1)-S(5B)	174.61(11)
O(1A)-C(2A)	1.262(7)	O(1A)-Rh(1)-S(5C)	173.63(12)
C(2A)-N(3A)	1.325(8)	O(1B)-Rh(1)-S(5C)	87.96(13)
C(2A) C(2A1)	1.518(9)	O(1C)-Rh(1)-S(5C)	94.79(11)
N(3A)-C(4A)	1.311(8)	S(5B)-Rh(1)-S(5C)	89.39(6)
C(4A)-N(4A1)	1.337(8)	O(1A)-Rh(1)-S(5A)	95.25(13)
C(4A)-S(5A)	1.742(6)	O(1B)-Rh(1)-S(5A)	176.29(11)
C(2A1)-C(2A2)	1.425(17)	O(1C)-Rh(1)-S(5A)	88.84(13)
C(2A1)-C(2A4)	1.493(18)	S(5B)-Rh(1)-S(5A)	87.69(6)
C(2A1)-C(2A3)	1.504(14)	S(5C)-Rh(1)-S(5A)	90.96(6)
N(4A1)-C(4A2)	1.454(8)	C(2A)-O(1A)-Rh(1)	124.5(4)
N(4A1)-C(4A5)	1.491(8)	O(1A)-C(2A)-N(3A)	128.3(5)
C(4A2)-C(4A3)	1.516(10)	O(1A)-C(2A)-C(2A1)	116.8(6)
C(4A3)-C(4A4)	1.541(12)	N(3A)-C(2A)-C(2A1)	114.9(6)
C(4A4)-C(4A5)	1.487(10)	C(4A)-N(3A)-C(2A)	128.0(5)
O(1B)-C(2B)	1.258(7)	N(3A)-C(4A)-N(4A1)	115.7(5)
C(2B)-N(3B)	1.331(7)	N(3A)-C(4A)-S(5A)	129.8(4)
C(2B)-C(2B1)	1.527(8)	N(4A1)-C(4A)-S(5A)	114.4(4)
N(3B)-C(4B)	1.340(7)	C(4A)-S(5A)-Rh(1)	104.4(2)
C(4B)-N(4B1)	1.324(7)	C(2A2)-C(2A1)-C(2A4)	116.6(11)
C(4B)-S(5B)	1.723(6)	C(2A2)-C(2A1)-C(2A3)	108.6(11)
C(2B1)-C(2B3)	1.421(13)	C(2A4)-C(2A1)-C(2A3)	99.9(10)
C(2B1)-C(2B2)	1.499(14)	C(2A2)-C(2A1)-C(2A)	110.4(9)
C(2B1)-C(2B4)	1.505(14)	C(2A4)-C(2A1)-C(2A)	108.8(8)
N(4B1)-C(4B5)	1.464(8)	C(2A3)-C(2A1)-C(2A)	112.2(8)
N(4B1)-C(4B2)	1.466(8)	C(4A)-N(4A1)-C(4A2)	126.2(5)
C(4B2)-C(4B3)	1.508(10)	C(4A)-N(4A1)-C(4A5)	121.5(5)
C(4B3)-C(4B4)	1.459(13)	C(4A2)-N(4A1)-C(4A5)	112.3(5)
C(4B4)-C(4B5)	1.517(11)	N(4A1)-C(4A2)-C(4A3)	103.3(6)
O(1C)-C(2C)	1.257(7)	C(4A2)-C(4A3)-C(4A4)	103.8(6)
C(2C)-N(3C)	1.332(8)	C(4A5)-C(4A4)-C(4A3)	104.1(6)
C(2C)-C(2C1)	1.538(8)	C(4A4)-C(4A5)-N(4A1)	103.4(6)
N(3C)-C(4C)	1.327(7)	C(2B)-O(1B)-Rh(1)	126.1(4)
C(4C)-N(4C1)	1.329(7)	O(1B)-C(2B)-N(3B)	128.9(5)
C(4C)-S(5C)	1.731(6)	O(1B)-C(2B)-C(2B1)	116.9(5)
C(2C1)-C(2C4)	1.503(10)	N(3B)-C(2B)-C(2B1)	114.1(5)
C(2C1)-C(2C2)	1.506(10)	C(2B)-N(3B)-C(4B)	128.5(5)
C(2C1)-C(2C3)	1.512(10)	N(4B1)-C(4B)-N(3B)	114.6(5)
N(4C1)-C(4C2)	1.455(7)	N(4B1)-C(4B)-S(5B)	116.3(4)
N(4C1)-C(4C5)	1.465(8)	N(3B)-C(4B)-S(5B)	128.9(4)
C(4C2)-C(4C3)	1.524(10)	C(4B)-S(5B)-Rh(1)	105.2(2)
C(4C3)-C(4C4)	1.440(13)	C(2B3)-C(2B1)-C(2B2)	107.9(9)
C(4C4)-C(4C5)	1.505(11)	C(2B3)-C(2B1)-C(2B4)	113.1(8)
C(1G)-Cl(2G)	1.708(11)	C(2B2)-C(2B1)-C(2B4)	104.1(8)
C(1G)-Cl(1G)	1.730(9)	C(2B3)-C(2B1)-C(2B)	113.2(7)
C(1G)-Cl(3G)	1.756(10)	C(2B2)-C(2B1)-C(2B)	107.8(7)...

Table III (Appendix). Bond lengths (Å) and angles (degrees) for *bis*-[*N*-pyrrolidyl-*N'*-(2,2-dimethylpropanoyl)thioureato]rhodium(III).

C(2B4)-C(2B1)-C(2B)	110.2(7)
C(4B)-N(4B1)-C(4B5)	123.9(5)
C(4B)-N(4B1)-c(4B2)	124.6(5)
C(4B5)-N(4B1)-C(4B2)	111.4(5)
N(4B1)-C(4B2)-C(4B3)	104.0(6)
C(4B4)-C(4B3)-(C(4B2)	105.3(7)
C(4B3)-C(4B4)-C(4B5)	106.0(7)
N(4B1)-C(4B5)-C(4B4)	103.0(6)
C(2C)-O(1C)-Rh(1)	122.9(3)
O(1C)-C(2C)-N(3C)	128.3(5)
O(1C)-C(2C)-C(2C1)	116.4(5)
N(3C)-C(2C)-C(2C1)	115.2(5)
C(4C)-N(3C)-C(2C)	126.9(5)
N(3C)-C(4C)-N(4C1)	115.4(5)
N(3C)-C(4C)-S(5C)	128.5(4)
C(4C)-S(5C)-Rh(1)	104.9(2)
C(2C4)-C(2C1)-C(2C2)	110.1(6)
C(2C4)-C(2C1)-C(2C3)	110.4(6)
C(2C2)-C(2C1)-C(2C3)	108.4(6)
C(2C4)-C(2C1)-C(2C)	109.8(5)
C(2C2)-C(2C1)-C(2C)	107.4(6)
C(2C3)-C(2C1)-C(2C)	110.7(5)
C(4C)-N(4C1)-C(4C2)	125.0(5)
C(4C)-N(4C1)-C(4C5)	123.2(5)
C(4C2)-N(4C1)-C(4C5)	111.7(5)
N(4C1)-C(4C2)-C(4C3)	103.4(5)
C(4C4)-C(4C3)-C(4C2)	106.3(7)
C(4C3)-C(4C4)-C(4C5)	106.6(7)
N(4C1)-C(4C5)-C(4C4)	103.6(6)
Cl(2G)-C(1G)-Cl(1G)	112.0(6)
Cl(2G)-C(1G)-Cl(3G)	108.2(5)
Cl(1G)-C(1G)-Cl(3G)	109.6(6)

Table IV (Appendix). Anisotropic displacement parameters ($Å^2 \times 10^3$) for *bis*-[*N*-pyrrolidyl-*N'*-(2,2-dimethylpropanoyl)thioureato]rhodium(III).
The anisotropic displacement factor exponent takes the form: $-2\pi^2[h^2 a^{*2} U11 + ... + 2hk\, a^* b^* U12]$.

	U11	U22	U33	U23	U13	U12
Rh(1)	31(1)	25(1)	43(1)	-8(1)	-2(1)	-2(1)
O(1A)	40(2)	47(2)	42(2)	-14(2)	-8(2)	-5(2)
C(2A)	46(3)	35(3)	51(3)	-6(3)	-8(3)	-3(3)
N(3A)	40(3)	44(3)	62(3)	-19(2)	-8(2)	0(2)
C(4A)	30(2)	26(3)	52(3)	-7(2)	0(2)	-4(2)
S(5A)	37(1)	35(1)	48(1)	-17(1)	-6(1)	1(1)
C(2A1)	57(4)	55(4)	68(4)	-19(3)	-20(3)	-13(3)
N(4A1)	38(2)	32(3)	64(3)	-13(2)	-8(2)	2(2)
C(4A2)	55(4)	37(3)	67(4)	-22(3)	5(3)	-2(3)
C(4A3)	75(5)	48(4)	84(5)	-24(4)	11(4)	12(4)
C(4A4)	62(4)	36(4)	126(7)	-14(4)	-15(5)	5(3)
C(4A5)	46(3)	43(4)	79(4)	-4(3)	-7(3)	5(3)
O(1B)	42(2)	33(2)	52(2)	-8(2)	10(2)	-5(2)
C(2B)	38(3)	30(3)	48(3)	-9(2)	1(2)	-3(2)
N(3B)	37(2)	27(2)	66(3)	-10(2)	11(2)	-2(2)
C(4B)	37(3)	24(3)	50(3)	-3(2)	0(2)	-1(2)
S(5B)	42(1)	33(1)	52(1)	-13(1)	9(1)	-9(1)
C(2B1)	40(3)	38(3)	62(4)	-11(3)	11(3)	5(3)
N(4B1)	43(3)	26(2)	69(3)	-14(2)	11(2)	-7(2)
C(4B2)	49(3)	46(4)	65(4)	-15(3)	8(3)	-14(3)
C(4B3)	76(6)	74(6)	126(8)	-34(5)	33(5)	-42(5)
C(4B4)	88(6)	49(5)	149(9)	-26(5)	29(6)	-27(5)
C(4B5)	68(4)	30(3)	105(6)	-23(4)	27(4)	-16(3)
O(1C)	45(2)	33(2)	42(2)	1(2)	-8(2)	-9(2)
C(2C)	30(3)	28(3)	52(3)	-7(2)	3(2)	0(2)
N(3C)	37(2)	24(2)	62(3)	-2(2)	-10(2)	-1(2)
C(4C)	33(3)	27(3)	47(3)	-7(2)	-2(2)	1(2)
S(5C)	40(1)	31(1)	51(1)	1(1)	-9(1)	-6(1)
C(2C1)	46(3)	28(3)	59(3)	3(3)	-12(3)	-3(2)
N(4C1)	34(2)	32(3)	57(3)	4(2)	-7(2)	-4(2)
C(4C2)	45(3)	33(3)	74(4)	10(3)	-15(3)	2(3)
C(4C3)	50(4)	74(6)	108(6)	19(5)	-26(4)	3(4)
C(4C4)	72(5)	79(6)	143(9)	18(6)	-50(6)	-22(5)
C(4C5)	44(3)	46(4)	82(5)	2(3)	-14(3)	-14(3)
C(1G)	79(6)	77(6)	76(5)	-8(4)	4(4)	20(5)
Cl(1G)	96(2)	90(2)	141(2)	-1(2)	-15(2)	30(2)
Cl(2G)	153(3)	105(2)	160(3)	-60(2)	-10(2)	-3(2)
Cl(3G)	76(2)	162(4)	205(4)	-78(3)	-2(2)	13(2)

Table V (Appendix). Hydrogen coordinates (x 10^4) and isotropic displacement parameters ($Å^2$ x 10^3) for *bis*-[*N*-pyrrolidyl-*N'*-(2,2-dimethylpropanoyl)thioureato]rhodium(III).

	x	y	z	U(eq)
H(2A1)	2382	8698	5608	201
H(2A2)	2380	7796	4993	201
H(2A3)	3637	8206	5126	201
H(2A4)	1453	7827	6776	157
H(2A5)	2190	6796	7271	157
H(2A6)	1550	6818	6292	157
H(2A7)	3311	6083	5565	201
H(2A8)	3776	5861	6606	201
H(2A9)	4650	6276	5851	201
H(4A1)	4224	10501	9108	63
H(4A2)	3672	9673	9745	63
H(4A3)	2441	11521	9562	85
H(4A4)	1684	10621	9691	85
H(4A5)	845	11425	8285	91
H(4A6)	2163	11695	7967	91
H(4A7)	2248	10313	7206	69
H(4A8)	1412	9815	7950	69
H(2B1)	9434	3905	5640	142
H(2B2)	8384	4893	5466	142
H(2B3)	8040	3905	5977	142
H(2B4)	9735	3937	7997	133
H(2B5)	10361	3434	7127	133
H(2B6)	8998	3282	7434	133
H(2B7)	10169	5611	7113	142
H(2B8)	9554	5873	6114	142
H(2B9)	10697	4954	6303	142
H(4B1)	3425	4971	8401	62
H(4B2)	4159	4335	9276	62
H(4B3)	3020	3184	8939	104
H(4B4)	2869	3603	7880	104
H(4B5)	4308	2209	7768	111
H(4B6)	4929	2272	8745	111
H(4B7)	6374	2913	7866	79
H(4B8)	5387	3325	7043	79
H(2C1)	8652	9741	6109	88
H(2C2)	9651	9718	6907	88
H(2C3)	8841	10759	6488	88
H(2C4)	7935	11269	7944	87
H(2C5)	8884	10324	8414	87
H(2C6)	7429	10480	8642	87
H(2C7)	5886	10286	7399	82
H(2C8)	6402	9958	6433	82
H(2C9)	6450	11050	6710	82
H(4C1)	10608	5758	9446	63
H(4C2)	10134	6267	10361	63
H(4C3)	12222	6069	10682	97
H(4C4)	12594	6020	9627	97
H(4C5)	12924	7532	9807	118...

Table V (Appendix). Hydrogen coordinates (x 10^4) and isotropic displacement parameters ($Å^2$ x 10^3) for *bis*-[*N*-pyrrolidyl-*N'*-(2,2-dimethylpropanoyl)thioureato]rhodium(III).

	x	y	z	U(eq)
H(4C6)	11878	7717	10577	118
H(4C7)	10713	8635	9412	69
H(4C8)	11505	8025	8649	69
H(1G)	7070	7701	5666	98

Table VI (Appendix). Torsion angles (degrees) for *bis*-[*N*-pyrrolidyl-*N'*-(2,2-dimethylpropanoyl)-thioureato]rhodium(III).

O(1B)-Rh(1)-O(1A)-C(2A)	157.6(5)
O(1C)-Rh(1)-O(1A)-C(2A)	-114.5(5)
S(5B)-Rh(1)-O(1A)-C(2A)	61.7(5)
S(5C)-Rh(1)-O(1A)-C(2A)	141.0(9)
S(5A) Rh(1)-O(1A)-C(2A)	-26.0(5)
Rh(1)-O(1A)-C(2A)-N(3A)	34.8(9)
Rh(1)-O(1A)-C(2A)-C(2A1)	-146.4(5)
O(1A)-C(2A)-N(3A)-C(4A)	-8.2(11)
C(2A1)-C(2A)-N(3A)-C4A)	173.0(6)
C(2A)-N(3A)-C(4A)-N(4A1)	160.5(6)
C(2A)-N(3A)-C(4A)-S(5A)	-23.4(10)
N(3A)-C(4A)-S(5A)-Rh(1)	19.5(6)
N(4A1)-C(4A)-S(5A)-Rh(1)	-164.5(4)
O(1A)-Rh(1)-S(5A)-C(4A)	2.0(2)
O(1B)-Rh(1)-S(5A)-C(4A)	110.4(18)
O(1C)-Rh(1)-S(5A)-C(4A)	88.6(2)
S(5B)-Rh(1)-S(5A)-C(4A)	-87.24(19)
S(5C)-Rh(1)-S(5A)-C(4A)	-176.59(19)
O(1A)-C(2A)-C(2A1)-C(2A2)	-97.1(10)
N(3A)-C(2A)-C(2A1)-C(2A2)	81.9(11)
O(1A)-C(2A)-C(2A1)-C(2A4)	32.1(11)
N(3A)-C(2A)-C(2A1)-C(2A4)	-148.9(9)
O(1A)-C(2A)-C(2A1)-C(2A3)	141.7(8)
N(3A)-C(2A)-C(2A1)-C(2A3)	-39.3(10)
N(3A)-C(4A)-N(4A1)-C(4A2)	170.8(6)
S(5A)-C(4A)-N(4A1)-C(4A2)	-5.9(8)
N(3A)-C(4A)-N(4A1)-C(4A5)	-5.7(9)
S(5A)-C(4A)-N(4A1)-C(4A5)	177.7(5)
C(4A)-N(4A1)-C(4A2)-C(4A3)	-165.6(6)
C(4A5)-N(4A1)-C(4A2)-C(4A3)	11.1(8)
N(4A1)-C(4A2)-C(4A3)-C(4A4)	-28.8(8)
C(4A2)-C(4A3)-C(4A4)-C(4A5)	36.9(8)
C(4A3)-C(4A4)-C(4A5)-N(4A1)	-29.4(8)
C(4A)-N(4A1)-C(4A5)-C(4A4)	-171.2(6)
C(4A2)-N(4A1)-C(4A5)-C(4A4)	11.9(8)
O(1A)-Rh(1)-O(1B)-C(2B)	-102.0(5)
O(1C)-Rh(1)-O(1B)-C(2B)	171.1(5)
S(5B)-Rh(1)-O(1B)-C(2B)	-13.0(5)
S(5C)-Rh(1)-O(1B)-C(2B)	76.2(5)
S(5A)-Rh(1)-O(1B)-C(2B)	149.3(16)
Rh(1)-O(1B)-C(2B)-N(3B)	25.8(9)
Rh(1)-O(1B)-C(2B)-C(2B1)	-157.8(4)
O(1B)-C(2B)-N(3B)-C(4B)	-10.1(11_
C(2B1)-C(2B)-N(3B)-C(4B)	173.4(6)
C(2B)-N(3B)-C(4B)-N(4B1)	165.0(6)
C(2B)-N(3B)-C(4B)-S(5B)	-19.7(9)
N(4B1)-C(4B)-S(5B)-Rh(1)	-161.3(4)
N(3B)-C(4B)-S(5B)-Rh(1)	23.5(6)
O(1A)-Rh(1)-S(5B)-C(4B)	78.5(2)
O(1B)-Rh(1)-S(5B)-C(4B)	-7.4(2)...

Table VI (Appendix). Torsion angles (degrees) for *bis*-[*N*-pyrrolidyl-*N'*-(2,2-dimethylpropanoyl)-thioureato]rhodium(III).

O(1C)-Rh(1)-S(5B)-C(4B)	123.9(12)
S(5C)-Rh(1)-S(5B)-C(4B)	-95.2(2)
S(5A)-Rh(1)-S(5B)-C(4B)	173.8(2)
O(1B)-C(2B)-C(2B1)-C(2B3)	139.6(8)
N(3B)-C(2B)-C(2B1)-C(2B3)	-43.4(9)
O(1B)-C(2B)-C(2B1)-C(2B2)	-101.2(8)
N(3B)-C(2B)-C(2B1)-C(2B2)	75.8(8)
O(1B)-C(2B)-C(2B1)-C(2B4)	11.9(9)
N(3B)-C(2B)-C(2B1)-C(2B4)	-171.2(7)
N(3B)-C(4B)-N(4B1)-C(4B5)	-0.19(9)
S(5B)-C(4B)-N(4B1)-C(4B5)	-176.0(6)
N(3B)-C(4B)-N(4B1)-C(4B2)	177.1(6)
S(5B)-C(4B)-N(4B1)-C(4B2)	1.1(8)
C(4B)-N(4B1)-C(4B2)-C(4B3)	173.9(7)
C(4B5)-N(4B1)-C(4B2)-C(4B3)	-8.7(9)
N(4B1)-C(4B2)-C(4B3)-C(4B4)	25.5(10)
C(4B2)-C(4B3)-C(4B4)-C(4B5)	-32.9(11)
C(4B)-N(4B1)-C(4B5)-C(4B4)	166.7(7)
C(4B2)-N(4B1)-C(4B5)-C(4B4)	-10.8(10)
C(4B3)-C(4B4)-C(4B5)-N(4B1)	26.9(11)
O(1A)-Rh(1)-O(1C)-C(2C)	157.0(4)
O(1B)-Rh(1)-O(1C)-C(2C)	-117.0(4)
S(5B)-Rh(1)-O(1C)-C(2C)	111.5(11)
S(5C)-Rh(1)-O(1C)-C(2C)	-29.2(4)
S(5A)-Rh(1)-O(1C)-C(2C)	61.6(4)
Rh(1)-O(1C)-C(2C)-N(3C)	39.7(8)
Rh(1)-O(1C)-C(2C)-C(2C1)	-143.8(4)
O(1C)-C(2C)-N(3C)-C(4C)	-8.7(10)
C(2C1)-C(2C)-N(3C)-C(4C)	174.8(6)
C(2C)-N(3C)-C(4C)-N(4C1)	157.2(6)
C(2C)-N(3C)-C(4C)-S(5C)	-28.9(9)
N(3C)-C(4C)-S(5C)-Rh(1)	24.3(6)
N(4C1)-C(4C)-S(5C)-Rh(1)	-161.8(4)
O(1A)-Rh(1)-S(5C)-C(4C)	105.3(11)
O(1B)-Rh(1)-S(5C)-C(4C)	88.8(2)
O(1C)-Rh(1)-S(5C)-C(4C)	1.2(2)
S(5B)-Rh(1)-S(5C)-C(4C)	-175.4(2)
S(5A)-Rh(1)-S(5C)-C(4C)	-87.7(2)
O(1C)-C(2C)-C(2C1)-C(2C4)	28.4(8)
N(3C)-C(2C)-C(2C1)-C(2C4)	-154.7(6)
O(1C)-C(2C)-C(2C1)-C(2C2)	-91.4(6)
N(3C)-C(2C)-C(2C1)-C(2C2)	85.6(7)
O(1C)-C(2C)-C(2C1)-C(2C3)	150.5(6)
N(3C)-C(2C)-C(2C1)-C(2C3)	-32.5(8)
N(3C)-C(4C)-N(4C1)-C(4C2)	178.7(6)
S(5C)-C(4C)-N(4C1)-C(4C2)	4.1(8)
N(3C)-C(4C)-N(4C1)-C(4C5)	2.8(9)
S(5C)-C(4C)-N(4C1)-C(4C5)	-171.8(5)
C(4C)-N(4C1)-C(4C2)-C(4C3)	176.6(7)
C(4C5)-N(4C1)-C(4C2)-C(4C3)	-7.1(8)...

Table VI (Appendix). Torsion angles (degrees) for *bis*-[*N*-pyrrolidyl-*N'*-(2,2-dimethylpropanoyl)-thioureato]rhodium(III).

N(4C1)-C(4C2)-C(4C3)-C(4C4)	22.8(10)
C(4C2)-C(4C3)-C(4C4)-C(4C5)	-29.9(12)
C(4C)-N(4C1)-C(4C5)-C(4C4)	166.1(7)
C(4C2)-N(4C1)-C(4C5)-C(4C4)	-10.3(9)
C(4C3)-C(4C4)-C(4C5)-N(4C1)	24.8(11)

Appendix IX

UV spectra of all ligands and their Pt(II), Pd(II) and Rh(III) complexes

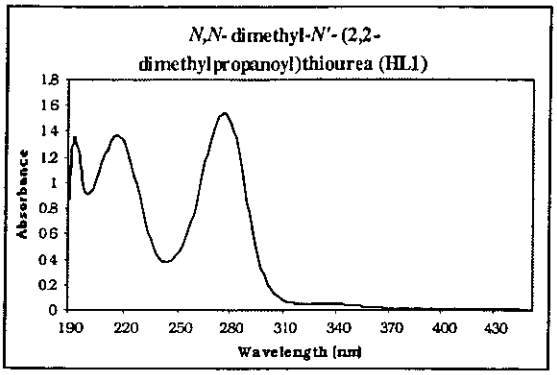

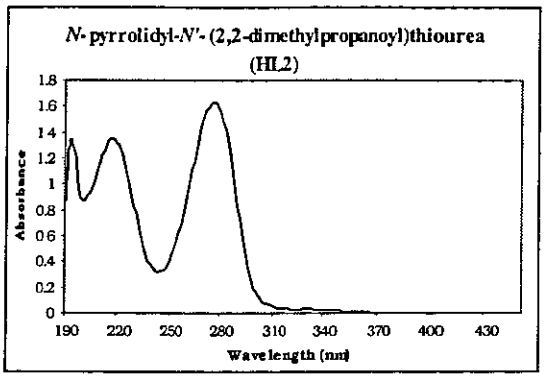

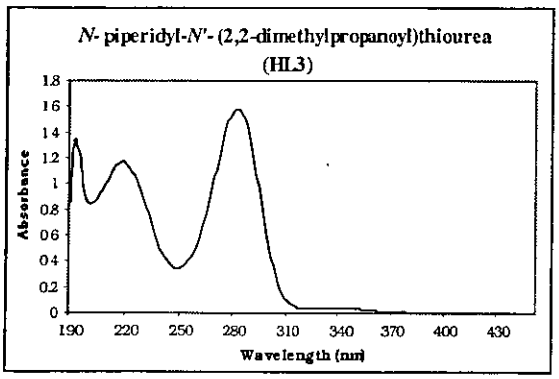

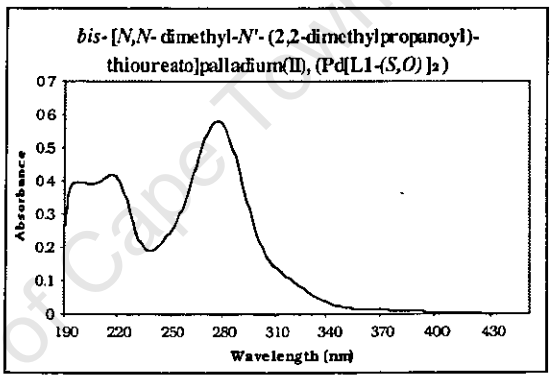

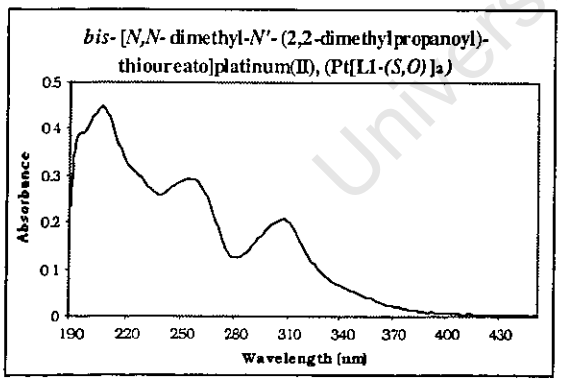

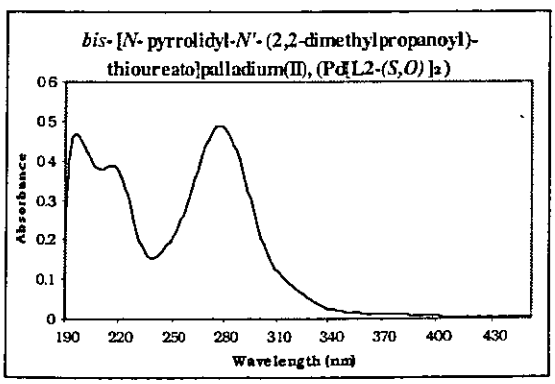

...continued.

Appendix IX
(...continued).

UV spectra of all ligands and their Pt(II), Pd(II) and Rh(III) complexes

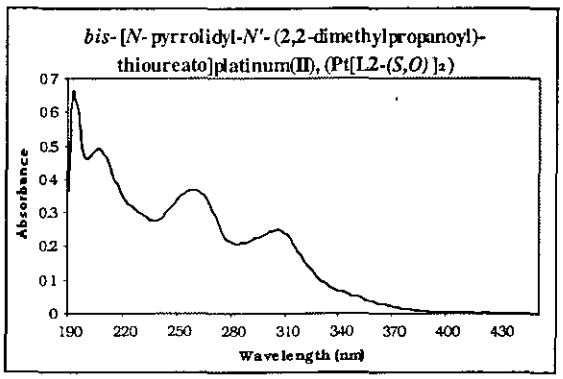

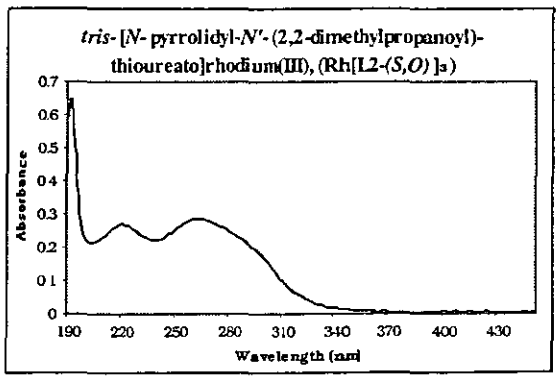

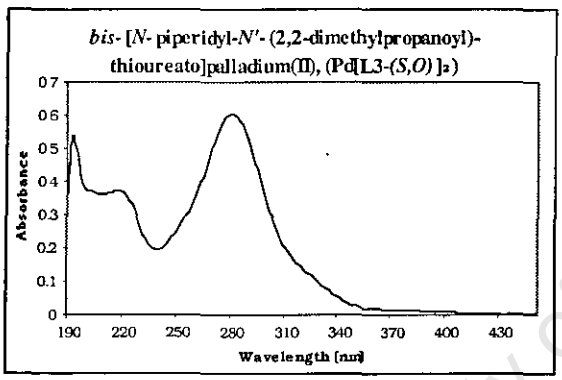

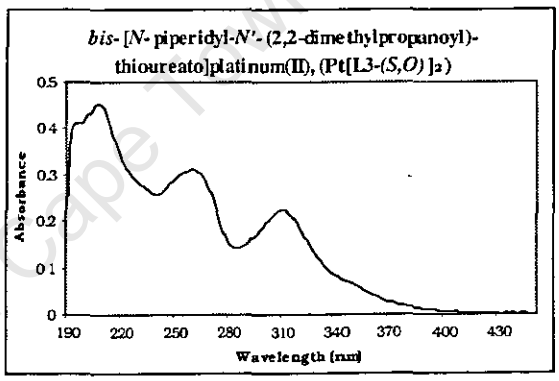

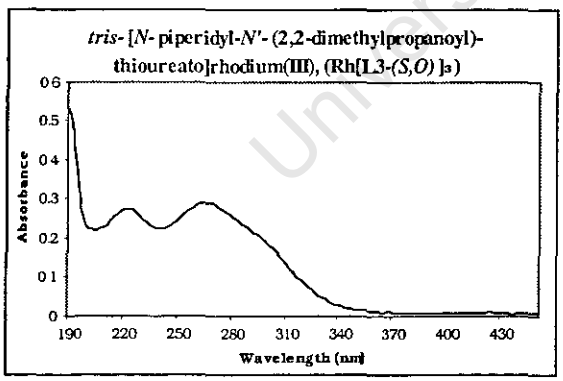

Statistical formulae and tables for evaluation of error

To comprehensively asses the present RP-HPLC method using statistical methods, one needs to note a few basic points. Any limited set of replicate measurements (called *sample*) is a small fraction of an infinite number of measurements that could in theory be made. This set is a part of the universe of data which, in principle, exists. Strictly speaking, laws of statistics apply only to a universe of data (called *population*).

In order to distinguish between the average (or mean) of a *sample* and that of a *population*, different symbols are used namely $\bar{x}$ and μ, respectively. The symbols s and σ are used for the standard deviations of the *sample* and the *population*, respectively. The parameters, $\bar{x}$ and s, can be determined according to the equations shown below while the determination of μ and σ is practically impossible as infinite number of measurements are required.

$$\bar{x} = [(x_1 + x_2 + x_3 + x_4 + \ldots x_n) / n]$$

$$s = [\{(x_1 - \bar{x})^2 + (x_2 - \bar{x})^2 + (x_3 - \bar{x})^2 + (x_4 - \bar{x})^2 + \ldots (x_n - \bar{x})^2\} / \{n - 1\}]^{1/2}$$

The distribution of error of a large number of replicate measurements has been found to take the shape of a bell as shown in Figure III, and is roughly symmetric about the mean. This curve satisfies a mathematical model called *Gaussian* distribution which is given by the equation:

$$y = [1 / \sigma(2\pi)^{1/2}]\, e^{-[(x-\mu)/2\sigma]^2}$$

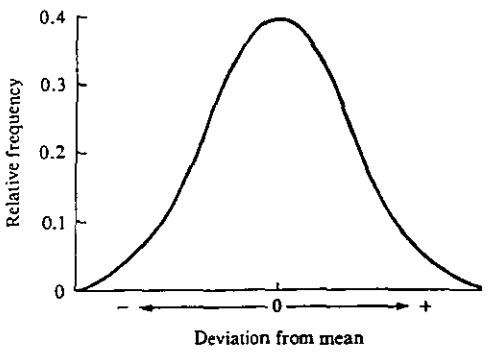

Figure III (Appendix): Distribution of error from a large number of replicate measurements[73].

Statistical formulae and tables for evaluation of error

It has been determined, with statistical formulae, that with this type of distribution, 68% of all values fall within ± 1σ, 96% within ± 2σ and 99.7% within ± 3σ. These limits (also referred to as confidence limits) are given in Table VII.

Table VII (Appendix). Table of confidence limits obtained in a normal error (or *Gaussian*) curve[73].

Confidence limit	Deviations from the mean
50%	0.67σ
68%	1.00σ
80%	1.29σ
90%	1.64σ
95%	1.96σ
96%	2.00σ
99%	2.58σ
99.7%	3.00σ
99.9%	3.29σ

It is possible using a given sample size, to estimate the confidence range within which μ may be found, by applying the following formula:

$$\mu = \bar{x} \pm [ts / (n)^{1/2}],$$

where t is a parameter that depends on the number of degrees of freedom, $\nu\,(n - 1)$

The value of t can be obtained from Table VIII, which is a tabulation of calculated values of t-distributions for various degrees of freedom using the following formula:

$$t = [(\bar{x} - \mu)n^{1/2}] / s$$

Table VIII (Appendix). Values of the parameter, t, at various confidence levels[69].

	Confidence limits				
ν	80%	90%	95%	99%	99.9%
1	3.078	6.314	12.706	63.657	636.62
2	1.886	2.920	4.303	9.925	31.598
3	1.638	2.353	3.182	5.841	12.924
4	1.533	2.132	2.776	4.604	78.610
5	1.476	2.015	2.571	4.032	6.869
6	1.440	1.943	2.447	3.707	5.959